2013

Stabilization and Reactivity of Low Oxidation State Indium Compounds

Christopher Allan
Universty of Windsor

STABILIZATION AND REACTIVITY OF LOW OXIDATION STATE INDIUM COMPOUNDS

By
Christopher J. Allan

A Dissertation
Submitted to the Faculty of Graduate Studies
Through Chemistry and Biochemistry
In Partial Fulfillment of the Requirements for
The Degree of Doctor of Philosophy at the
University of Windsor

Windsor, Ontario, Canada
2013

Stabilization and Reactivity of Low Oxidation State Indium Compounds

by

Christopher Allan

APPROVED BY:

M. Hill, External Examiner
University of Bath

M. Cioppa
Earth and Environmental Science

J. Green
Department of Chemistry & Biochemistry

J. Rawson
Department of Chemistry & Biochemistry

C. Macdonald, Advisor
Department of Chemistry & Biochemistry

September 17, 2013

Declaration of Co-Authorship / Previous Publications

I. Declaration of Co-Authorship

This thesis incorporates the outcome of joint research undertaken in collaboration with Hugh Cowley under the supervision of Jeremy Rawson. The collaborative work is present in Chapter 4 of the thesis. In all cases, primary contributions, experimental designs, data analysis, and interpretation were performed by the author and the contribution of the co-authors was primarily through the provision of electron paramagnetic resonance spectroscopy.

I am aware of the University of Windsor Senate Policy on Authorship and I certify that I have properly acknowledged the contribution of the other researchers in my thesis, and have obtained written permission from each of the co-author(s) to include the above material(s) in my thesis.

I certify that, with the above qualification, this thesis, and the research to which it refers, is the product of my own work

II. Declaration of Previous Publications

This thesis includes a summarized version of a book chapter as well as an original manuscript that have been previously submitted for publication in peer reviewed journals, as summarized below:

	Citation	Status
Chapter 1	Christopher J. Allan, Charles, L B. Macdonald; Low Coordinate Main Group Centers - Group 13 in *Comprehensive Inorganic Chemistry II*; Jan Reedijk, Kenneth Poeppelmeier, **2013**.	Accepted
Chapter 4	Non-Innocent Ligand Effects on Low Oxidation State Indium Complexes; Christopher J. Allan, Benjamin F. T. Cooper, Hugh J. Cowley, Jeremy M. Rawson, and Charles L. B. Macdonald. *Chemistry - A European Journal,* **2013**.	Accepted

I certify that I have obtained written permission from the aforementioned publishers to include said work in this dissertation. I certify that the work contained in this document was completed during my registration as a graduate student at the University of Windsor.

I declare that, to the best of my knowledge, my thesis does not infringe upon anyone's copyright nor violate any proprietary rights and that any ideas, techniques, quotations, or any other material from the work of other people included in my thesis, published or otherwise, are fully acknowledged in accordance with the standard referencing practices. Furthermore, to the extent that I have included copyrighted material that surpasses the bounds of fair dealing within the meaning of the Canada Copyright Act, I certify that I have obtained a written permission from the copyright owner(s) to include such material(s) in my thesis.

I declare that this is a true copy of my thesis, including any final revisions, as approved by my thesis committee and the Graduate Studies office, and that this thesis has not been submitted for a higher degree to any other University or Institution.

Abstract

The work described herein focuses on the chemistry of low oxidation state indium salts. Indium in its +1 oxidation state is electron rich, as it possesses a "lone pair" of electrons which are capable of undergoing further chemistry, such as oxidative addition and transition metal ligation. One of the main benefits of In(I) compounds is that they are amphoteric and thus capable of acting as both a Lewis acid as well as a Lewis base.

One of the major drawbacks in the field of In(I) chemistry, however, is a lack of convenient starting materials. The In(I) halides have very poor solubility in non-donor solvents and readily decompose in the presence of strong donor molecules. The addition of acyclic polyethers to a series of In(I) (and III) salts very rarely resulted in decomposition. Their effect on solubility is investigated and reported.

A more soluble indium(I) salt is indium trifluoromethanesulfonate (indium triflate, InOTf). This salt is significantly more stable than its halide counterparts, however it is sometimes too inert and does not react at all. It has been previously reported that the addition of crown ether ligands increase the reactivity of the metal centre and can cause oxidative addition into carbon-chlorine bonds. The effects of various destabilizing ligands is discussed and a computational investigation provides insight into the electronic stability of these ligated systems.

The reactivity with InOTf with "non-innocent" α-diimine (DAB) ligands is also investigated. These ligands are capable of undergoing redox chemistry and generating ambiguous metal oxidation states. Substitution patterns on DAB ligands were found to play a major role in the reactivity of InOTf as shown by X-ray crystallography, EPR spectroscopy, cyclic voltammetry and computational analysis.

Acknowledgements

First and foremost, I would like to extend my gratitude towards my supervisor, Chuck Macdonald. He has been an excellent source of information, advice, and guidance and has always been more than willing to share his wisdom (both in and outside of chemistry). Thank you for four great years.

There have been many students who have come and gone over the years who have made the time spent here memorable. I would like to thank Jill, Heather, Ben, Greg, Meghan, Raj, Steph, Jenn, and "Shmala". The fun we had with wheely chairs, practical jokes involving bubble wrap, sprinkles, and the starfish, have all made the "MacJohnson" office a fun place to work. I would also like to thank Martin for his volunteer work in the lab (although he never remembered to add a stir bar to the flask).

I would like to thank the faculty and staff in the chemistry department for their help and guidance along the way, including committee members Jim Green and Jeremy Rawson who have been more than willing to answer my burning questions. Special mention goes to Una for letting me borrow equipment/glassware from the undergraduate labs.

Thank you to my family for their support over the years. Even though they may not fully understand what I've accomplished, they can still give anyone who is curious a "Three Minute" summary.

Finally I would like to thank my external committee members Michael Hill and Maria Cioppa for reading my thesis, as well as the government of Ontario and the University of Windsor for funding.

Table of Contents

List of Tables

List of Figures

List of Schemes

Glossary of Terms

°	degrees
°C	degrees celcius
Å	angstroms
Ar	aryl
Ar*	terphenyl ligand
bp	bis(pyrazolyl)borates ligand
Bu	butyl
Ct	centroid
Cp	cyclopentadienyl
Cp'	substituted cyclopentadienyl
Cp*	pentamethylcyclopentadienyl
CSD	Cambridge Structural Database
CV	cyclic voltammetry
d	doublet
DAB	diazabutadiene ligand
DFT	density functional theory
BIAN	Bis(imino)acenaphthene
DIMPY	2,6-di(arylimino)pyridyl
Dipp	1,6-diisopropylpheyl
DMP	2,6-dimethylphenyl
DMPE	dimethylphosphinoethane
DMPU	dimethylpropyleneurea

DMPTU	dimethylpropylenethiourea
DPPE	diphenylphosphinoethane
E	group 13 element
EPR	electron paramagnetic resonance
Et	ethyl
eV	electron volt
g	gram
H	hartrees
HMPA	hexamethylphosphoramide
HMPAT	hexamethylphosphoramidethione
HOMO	highest occupied molecular orbital
^{i}Pr	iso-propyl
J_{ab}	couple between nuclei a and b
K	degrees kelvin
L	litres
LUMO	lowest unoccupied molecular orbital
Me	methyl
MeCN	acetonitrile
Mes	1,3,5-trimethylphenyl
mg	milligram
mL	millilitre
mmol	millimole
MO	molecular orbital

mol	mole
NacNac	β-diketiminate ligand
NBO	natural bond orbital
^{n}Bu	n-butyl
NHB	N-heterocyclic borylene
NHC	N-heterocyclic carbene
NHGa	*N*-heterocyclic gallylene
NIL	non-innocent ligand
NIR	near infrared
NMR	nuclear magnetic resonance
OTf	trifluoromethanesulfonate
Ph	phenyl
ppb	parts per billion
ppm	parts per million
pz	pyrazolyl
quin	quinuclidine
R	substituent
s	singlet
SCF	self consistent field
SOMO	semi-occupied molecular orbital
Stdev	standard deviation
t	triplet
TMIO	tetramethylimidazole-one

TMIT	tetramethylimidazolethione
^{t}Bu	tertiary butyl
TMEDA	tetramethylethylenediamine
Tp	tris(pyrazolyl) ligand
Trp	terphenyl
WBI	Wiberg Bond Index
X	halogen
α	alpha
β	beta
δ	chemical shift
λ	wavelength
π	pi
σ	sigma

Chapter 1: Introduction

1.1 Oxidation State vs Valence State vs Coordination Number

As a preface to the discussion of compounds that exhibit a lower than normal oxidation state, it is important to define some of the types of models employed to describe coordination chemistry, namely: oxidation state, valence state and coordination number. In its most simple formulation, an oxidation state is a model used to describe the number of electrons associated with a particular atom and often to infer the chemical behavior of the compound in which the element is found.[1] Formal oxidation states are typically assigned to an element on the basis of simple counting rules and axioms (e.g. oxygen is typically counted as having a (-2) charge). Although oxidation states are used extensively (and successfully) to rationalize the redox chemistry of transition metal complexes, there are significant deficiencies with such formal oxidation state models that become particularly apparent when such rules are applied to main group, p-block elements. For example, the following carbon-based compounds all feature a carbon atom with a formal 0 oxidation state: diamond, graphite, graphene, fullerenes, chlorocarbene (**C**HCl), formaldehyde (H_2**C**O), 2-butyne (H_3C-**C**≡**C**-CH_3) and dichloromethane (**C**H_2Cl_2). In spite of the identical formal oxidation state, the structures, stabilities and reactivities exhibited by each of these compounds differ substantially.

The valence state of an atom is a related, but distinct, model to assess the number of electrons associated with a particular element; it may be summarized succinctly as the number of electrons used for chemistry (either in the formation of bonds to other elements or as charges). In contrast to a formal oxidation state, which can often be

assigned on the basis of an empirical molecular formula, the valence state assigned to a particular atom usually requires knowledge of the actual distribution of the electrons within the molecule. As outlined by Parkin and others, oxidation states and valence states are often assumed incorrectly to be synonymous: there are certain instances in which the two numbers (or at least their magnitudes) coincide, however such cases are fortuitous.[2] While the identification of an unusual oxidation state may suggest that there is something unconventional about the chemistry of a given compound, because the valence state is more dependent on the electron distribution, it often provides significantly more insight into the structure, bonding and reactivity of the compound in which the element is found.

Most simply defined, the coordination number of an atom is simply the sum of the number of other atoms to which it is bonded in any way. Compounds in which an element has a lower-than-usual coordination number often exhibit chemical and physical properties that are considerably different than those in which the element has a higher coordination number. These differences often render such low coordinate compounds suitable for uses ranging from synthons and reagents, to catalysts and materials precursors. For uncomplexed neutral compounds of the lighter group 13 elements, the anticipated coordination number for the trivalent state elements is three, however the electron deficient nature of such elements means that coordination numbers of four, five, six and higher are often observed for both neutral and anionic species. In light of the foregoing, this chapter will concentrate on the description of compounds in which the group 13 element (also called a “triel”) exhibits an oxidation state of two or less. It should be emphasized that because of periodic trends (e.g. "inert s-pair",[3] weaker bond

energies[4-5] and relativistic effects[6-7]), thallium is usually more stable in a univalent state and may be anticipated to exist as mono-coordinate or zero coordinate (completely ionic) species.

To aid in the differentiation between these different models, several examples of compounds containing group 13 in low formal oxidation states are illustrated in Table 1.1.

Table 1.1: Diagram illustrating the differences between oxidation states, valence states and coordination numbers for a series of group 13 compounds.

	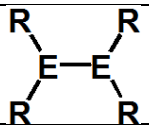		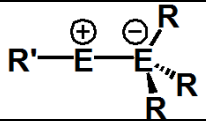		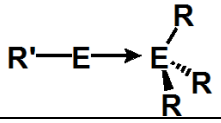			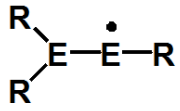	
Formal Oxidation State:	E (+2)	E(+2)	E(+2)	E(+2)	E(+1)	E(+3)	E(+1)	E(+2)	E(+1)
Valence State:	E^{III}	E^{III}	E^{III}	E^{III}	E^{III}	E^{III}	E^{I}	E^{III}	E^{II}
Coordination Number:	3	3	2	4	2	4	1	3	2

The work explored in this dissertation is concentrated exclusively on indium. As such, a depiction of the oxidation states of indium can be found in Table 1.2.

Table 1.2: Oxidation states, valence states and coordination numbers of indium.

	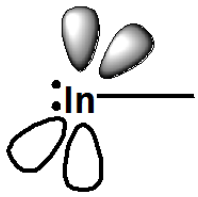	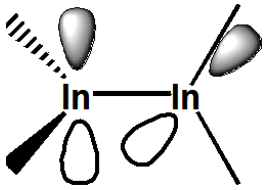	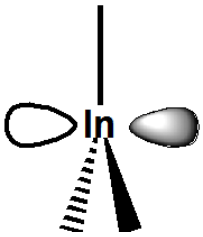
Oxidation State	E(+1)	E(+2)	E(+3)
Valence State	E^{I}	E^{III}	E^{III}
Coordination Number	1	3	3

Regardless of its oxidation state, indium possesses at least one empty p-orbital, making it acidic. Indium in its +1 oxidation state, however, also features a "lone pair" of electrons and can therefore act as both a Lewis acid as well as a Lewis base. Base-stabilization of indium(I) compounds entails coordination of ligands to the empty p-orbitals whilst still allowing the "lone pair" of electrons to react and undergo further chemistry. Unfortunately, in the presence of strong donor molecules (particularly multi-dentate ones), indium(I) compounds have a propensity to undergo disproportionation, producing metal as well as chelated higher oxidative species. While the indium(I) halides remain the primary starting materials for nearly all In(I) complexes, their inherent insolubility and instability is the primary hurdle in the field.[8] In spite of this, low oxidation state group 13 compounds make up an incredibly rich area of main group chemistry and, as discussed below, there exists many ways in which these compounds can be stabilized and further utilized.

1.2 - Nitrogen-based Ligands:

One of the richest and most well-investigated classes of compounds containing low-coordinate, low-valent group 13 compounds are those based on ligands that coordinate to the metal(loid) element through at least one nitrogen atom.[9]

β-diketimine ligands

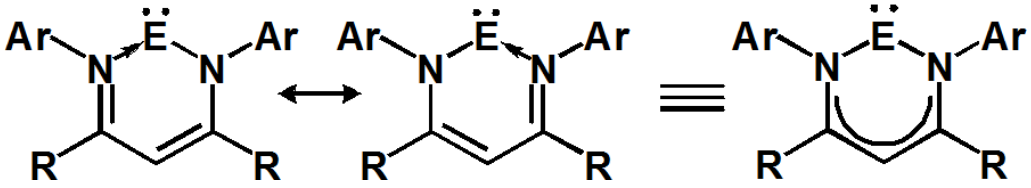

Scheme 1.1: General structure of β-diketiminate ligands.

β-diketiminate ligands are monoanionic bidentate nitrogen-based analogues of β-diketonate ligands; the most common β-diketonate ligand is acetylacetonate ("acac") and its β-diketiminate derivatives are often referred to as "NacNac" ligands, Scheme 1.1. One advantageous feature of β-diketiminate ligands, in comparison to their oxygen-based analogues, is the presence of substituents (R-groups in the diagram below, Figure 1.1) on the nitrogen atoms. These substituents impart an aspect of “tuneability” to the ligand in that the steric bulk and the electronic properties can be modified easily through the judicious selection of the R-groups on the nitrogen atoms.

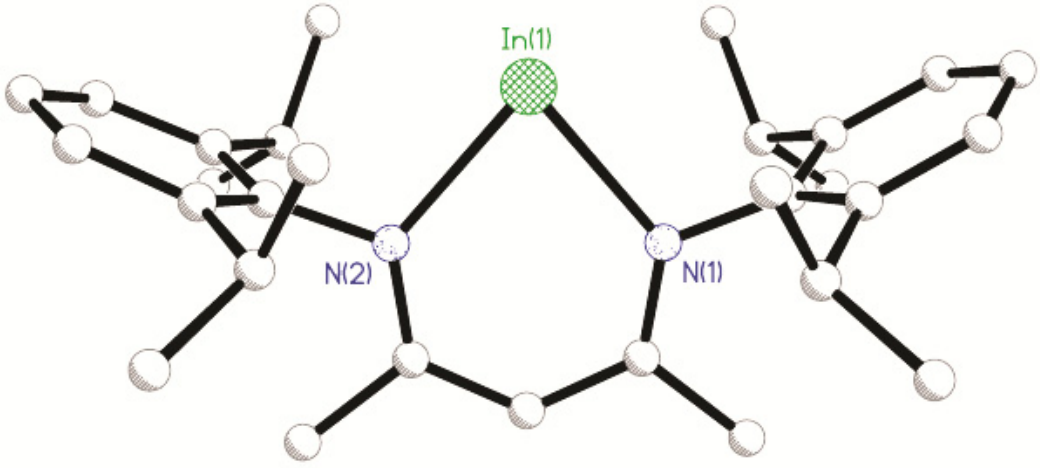

Figure 1.1: Solid state structure of [^{Dipp}NacNac^{Me}][In].[10] Analogous compounds have also been obtained for Al,[11] Ga,[12] and Tl.[13]

Moving down the periodic table, the nitrogen-metal bond length increases from Al to Tl in the manner that one would anticipate on the basis of the relative sizes of the metal atoms. Although most of the complexes that have been characterized crystallographically have Dipp (2,6-diisopropylphenyl) substituents on each nitrogen atom, changes in the properties of the aryl substituents on the nitrogen atoms can have a dramatic effect on the N-E bond distance for complexes of a given metal. For example, introduction of an electron-donating para-anisole group yields two very distinct nitrogen-indium bonds (2.277 & 2.557 Å).[14] Elongation of the nitrogen-indium bond is observed at both nitrogen centres; however, a more drastic elongation is seen at the nitrogen bearing the electron-rich arene ring. Likewise, when the aryl isopropyl groups on compound [^{Dipp}NacNac^{Me}][Tl] are replaced with smaller methyl groups, a shorter thallium-nitrogen bond is observed.[15]

Modifications to the R-groups on the carbon backbone of the β-diketiminate ligand can also lead to significant changes in the metrical parameters observed for analogous complexes of a single metal. Introduction of bulkier groups appear to have little to no effect on the system. Substitution of the methyl groups in [^{Dipp}NacNac^{Me}][Al] for ^{t}Bu groups results in a slightly longer Al-N bond (ca. +0.05 Å).[16] A more substantial difference is observed, however, when the backbone substituents are replaced with fragments that possess different electronic properties. For example, replacement of the methyl groups in compound [^{Dipp}NacNac^{Me}][In]with electron withdrawing CF_3 groups removes electron density from the ligand and thus results in an elongated N-In bond (+0.1 Å).[13]

Perhaps more importantly, Hill and co-workers found that when the N-Aryl groups used in such compounds are significantly less bulky, dimerization of the metal β-diketiminate complex can occur.[14] As illustrated in by the structure in Figure 1.2, when sterically-demanding aryl substituents, such as Dipp, are replaced with smaller DMP (2,6-dimethylphenyl) groups, enough room is created to allow for dimerization.

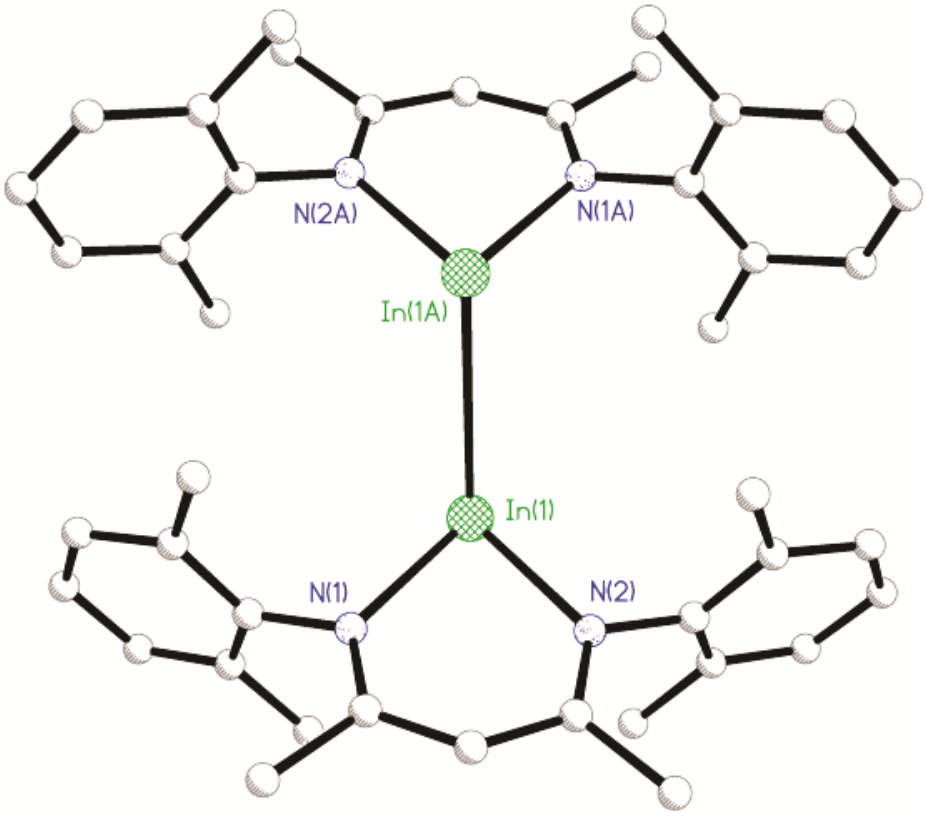

Figure 1.2: Crystal structure of dimerized In[((DMP)NCMe)$_2$CH].

This dimerized complex has shorter N-In bond lengths than the mononuclear complex depicted in Figure 1.1. This can be attributed to less steric hindrance around the metal centre allowing for closer contact to the nitrogen fragments.

As one would perhaps anticipate given the low-coordinate and low-valent nature of these species, much of the chemistry displayed by such compounds involves the formation of compounds in which the coordination number and/or valence state of the group 13 centre is increased. For the lighter analogues, common classes of reactions include: insertion into element-halogen bonds and other reactive element-element bonds;

the formation of coordination complexes with main group and transition metal acceptors; the coordination of unsaturated compounds; and small molecule activation. Reactivity of these β-diketiminates is a consequence of the reducing power of the E(I) metal. Univalent aluminum β-diketiminates tend to be considerably more reducing and more reactive overall than the heavier congeners, as one would anticipate on the basis of periodic trends. At the other end of the spectrum, the stability of the "lone pair" on thallium in its monovalent β-diketiminates appears to preclude donor or oxidation chemistry and such species have only been used as metathesis reagents to introduce the β-diketiminate ligand onto other elements. Whilst a rich array of reactivity is observed for the lighter aluminum and gallium analogues, the reactivity of the indium β-diketiminate complexes is limited exclusively to formal oxidative addition reactions that result in the insertion of the indium atom into carbon-halogen bonds (either Br or I).[17]

Pyrazolyl-based ligands

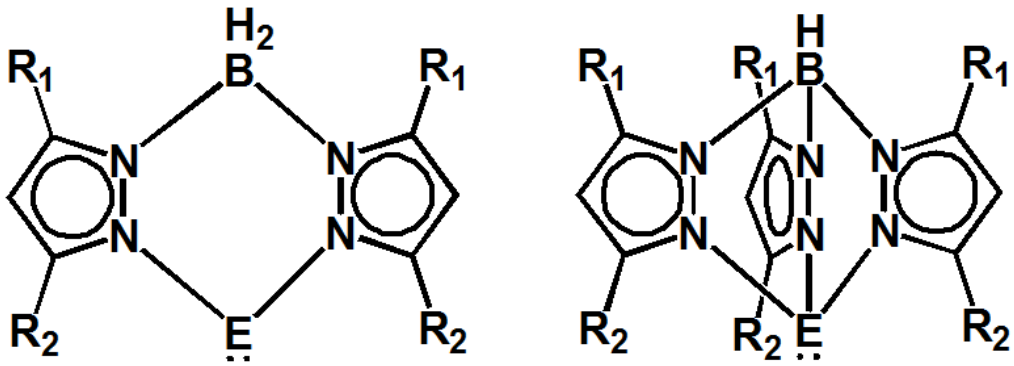

Scheme 1.2: General structure of Bis- and Tris(pyrazolyl borate) salts.

As free fragments, pyrazoles are aromatic heterocyclic diazoles, in which the 5-membered ring contains two nitrogen atoms in adjacent positions. In contrast to the superficially-similar cylcopentadienide ligands, pyrazoles and the corresponding pyrazolate anions tend to function as σ-type ligands via the nitrogen atoms rather than as π-donors using the π-system of the heterocycle (Scheme 1.2).

In the context of low valent group 13 chemistry, the two major classes of pyrazolyl-based ligands that have been used to prepare compounds containing low-coordinate triel centres are the monoanionic bis(pyrazolyl)borates (Bp) of the general form $[H_2B(pz)_2]^{1-}$, sometimes called "scorpionate" ligands, and the tris(pyrazolyl)borates (Tp) of the general form $[HB(pz)_3]^{1-}$; the tetrakis(pyrazolyl)borates $[B(pz)_4]^{1-}$ often behave similarly to the Tp ligands but are not used as frequently.[18-20] Although it is obvious that the bis(pyrazolyl)borate ligands, which are analogous to the β-diketiminate described above, can support a di-coordinate metal fragment, the case for including complexes featuring tris(pyrazolyl)borate ligands perhaps requires some further clarification. As noted by Trofimenko, tris(pyrazolyl)borate ligands are isolobal with cyclopentadienyl ligands and can function as 6-electron ligands that can donate to both σ- and π-type orbitals.[19] One final note regarding the various pyrazolyl-based ligands is that the steric properties of these ligands are readily modified by changing the substitutents on the carbon atoms of the heterocycle, typically those at the 3 and 5 positions, and the resultant ligands – particularly the roughly cylindrical Tp variants – have sufficient bulk to allow for the isolation of some types of reactive species that remain elusive for the related Cp-type substituents. The vast majority of pyrazolate complexes are thallium(I) salts. In fact, the bis(pyrazolyl) salts exclusively feature

coordinated thallium. It is only with the more sterically-demanding and electron-donating tris(pyrazolyl)borate ligand system that low valent complexes of the lighter group 13 elements have proven amenable to isolation.

There are only a handful of *pseudo*-monocoordinate complexes of the lighter group 13 elements. While compounds of $[HB(pz)_3][Ga]$[21] and $[HB(pz)_3][In]$,[22-24] are known, analogous aluminum salts have yet to be reported in the literature. Predictably, the E-N bond distances elongate as one moves down the periodic table on the basis of periodic trends. As seen for the β-diketiminate ligands, functionalization with electron withdrawing CF_3 groups (Figure 1.3) renders a more electron poor ligand, resulting in elongated In-N bonds.

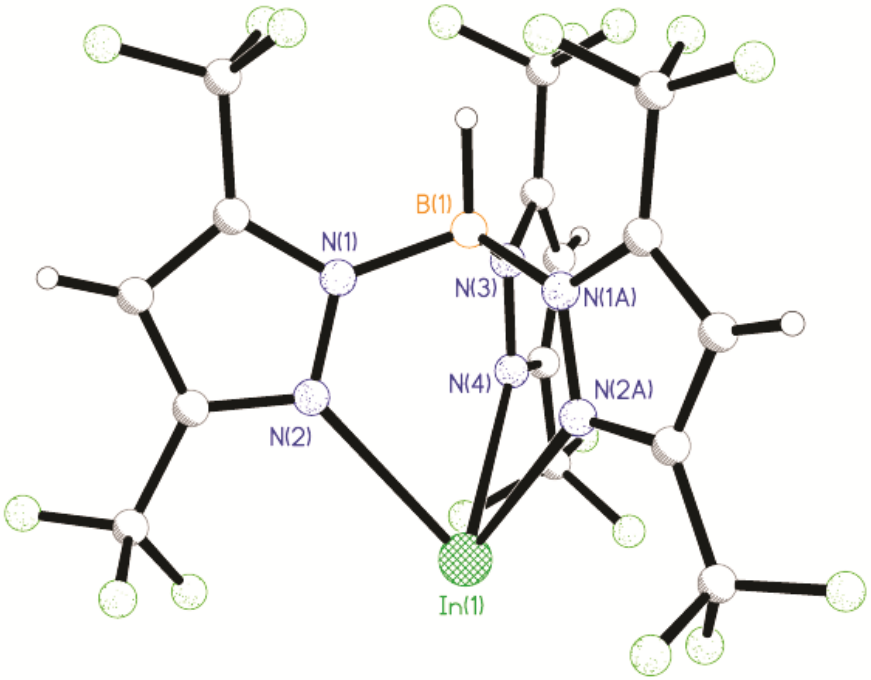

Figure 1.3: Solid state structure of $[HB(pz^{CF3})_3][In]$.

The large number of thallium(I) Bp and Tp complexes highlights the importance of such compounds as metathesis reagents that are soluble in many organic solvents. Thus, in many cases, such thallium compounds are employed to introduce the pyrazole-based ligands to other metals, including some of the lighter group 13 metals described above. In contrast, the chemistry demonstrated by the monovalent gallium and indium Tp complexes is considerably more varied. While some of the reactivity exhibited by these TpE complexes is similar to that described previously for the low valent β-diketiminates, such as functioning as 2-electron ligands to transition metal complexes[25-26] and main group Lewis acids[27-30] or undergoing oxidative addition/insertion reactions,[31] the steric bulk of substituted Tp groups also allows for some unique chemistry. For example, the oxidation of some TpE species with chalcogens results in the formation of complexes of the general form TpE=Ch (Ch = S, Se, Te; E = Ga, In);[32-34] in contrast to the β-diketiminate analogues, these tris(pyrazolyl)borate complexes do not dimerize and thus feature multiple bonds between the group 13 element and the chalcogen. As one would expect, the effect of oxidation of the triel centre with chalcogens is a sharp decrease in the E-N bond distance (ca. 0.2 Å) as the metal goes from a formal +1 to +3 charge.

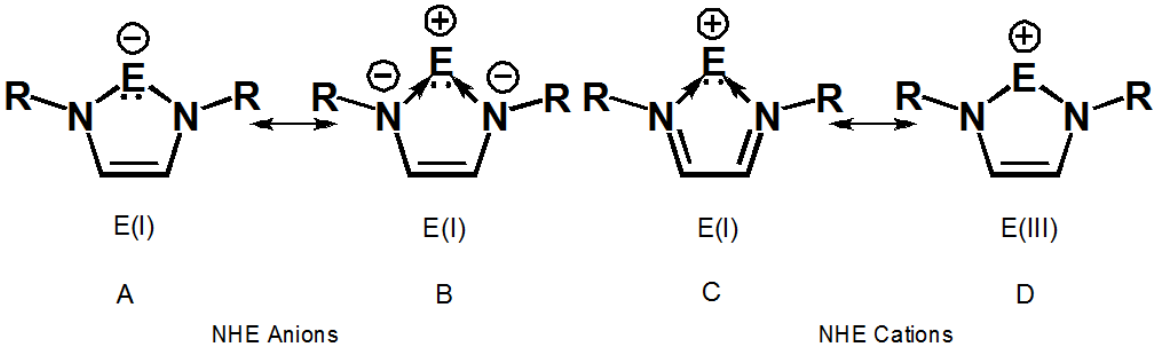

Scheme 1.3: Anionic and cationic *N*-Heterocyclic groups 13 compounds.

The chemistry of p-block analogues of *N*-heterocyclic carbenes (NHCs), in which the main group element is di-coordinate and formally has a total of 6 valence electrons, has been a focus of investigation in inorganic chemistry for several decades.[9, 35-36] It is only relatively recently, however, that examples featuring group 13 have been prepared and studied. A computational study by Schoeller *et al.* provided insight into the electronic structure of group 13 NHC analogues and suggested that such compounds should be amenable to isolation.[35] More recently, an investigation by Tuononen *et al.* examined the electronic properties of all of the p-block NHC analogues from groups 13-16.[36] One of the most important observations they reported is that there is significant covalent bonding and π-delocalization between the diamido ligand and the lighter group 13 atoms, B and Ga (Scheme 1.3 A). For heavier elements such as indium, the nature of the ligand-metal interaction appears to be best-described as primarily ionic with no significant π-delocalization (Scheme 1.3 B). Interestingly, to date the only examples of salts containing such anions that have been isolated contain either boron (NHB salts)[37-40] or

gallium (NHGa salts),[41-45] which are the two most electronegative of the group 13 elements.

The first isolated example of any group 13 NHC analogues, namely the salt [K([18]crown-6)·2 THF][Ga($N^tBuCH)_2$], was generated by the treatment of the dilithiated α-diimine with $GaCl_3$ and resulted in the formation of a dimeric tricyclic structural isomer. However, reduction of this trivalent halogallane with potassium did indeed produce the target NHGa salt.[41]

The non-innocence of DAB ligands in regard to redox chemistry is well known and some univalent gallyl anions have been generated from paramagnetic precursors in which the unpaired electron resides primarily on the organic ligand. For example, salts containing NHGa anions have been prepared by the reduction of paramagnetic gallium(III) precursors of the type $DABGaI_2$ and gallium(II) dimers of the general form $(DABGaI)_2$.[42] An alternative but similar method that has been demonstrated to generate salts of monovalent gallium anions of the related delocalized bis(imino)acenaphthene (BIAN) system begins with the direct treatment of the diimine with gallium metal. This produces the digallane BIANGa-GaBIAN, which can be reduced with alkali or alkaline earth metals to yield the desired salts.[45]

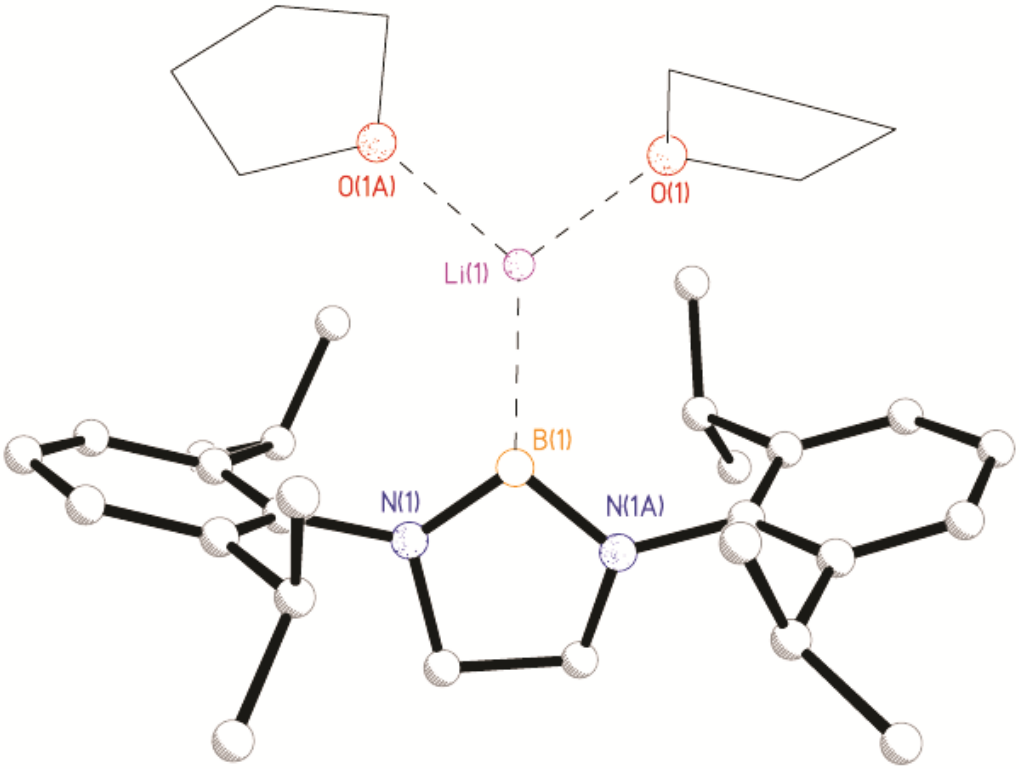

Figure 1.4: Solid state structure of $[Li(THF)_2][B((Dipp)NCH_2)_2]$.[38]

The electron-rich nature of the univalent group 13 element allows the resultant anionic diimine complexes to function as donors and, in the absence of superior ligands, these associate with the cations in the solid state, as illustrated for an NHB salt in Figure 1.4. However, if superior ligands are employed, the absence of cation-anion contacts results in longer N-E bonds.[44-45] This is as one would anticipate on the basis of the formal reduction of electron density at the triel centre upon coordination to an acceptor. In any event, the perturbations of the nominally di-coordinate group 13 anions are relatively minor and, regardless of the solid state structures, the reactivity exhibited by these salts is consistent with the ions being adequately separated in solution.

As one would anticipate on the basis of their isovalent relationship with NHCs in addition to the negative charge they possess, these anionic group 13 complexes are potent electron donors and nucleophiles. NHB anions can attack aldehydes,[37-39] esters,[38] and other unsaturated compounds.[38, 46] Furthermore, the presence of the s-block metal counter cations renders such salts particularly effective for reactions with halogenated reagents;[37-38] the products derived from such reactions are typically those that one would anticipate for a salt metathesis process. Given the importance of cross-coupling reactions using boryl reagents in organic synthesis, the convenient preparation of organoboryls demonstrated by this class of ligands has the potential to be of great practical importance.

Although, the products derived from NHGa salts may not appear to be as immediately useful as those of the corresponding boryl anions, the investigation of the reactivity of such species, in particular salts of the anion [$^{Dipp}DAB^{H}$][Ga], has revealed a phenomenal amount of interesting chemistry. As one would anticipate, NHGa anions have proven to be excellent donors to metals and acceptors from the s-, p-, d- and f-blocks.[9, 47] One notable observation is that the NHGa anion proves to be a stronger donor than analogous heavier group 14 carbenoids and thus it functions as a donor in the adducts that are formed.[48] Furthermore, the NHGa anions are observed to insert in a formal manner into element-hydrogen bonds such as those of imidazolium ions and those of water.[49] It has also proven possible to oxidize NHGa anions to generate species with Ga-Ga bonds, in effect accomplishing the reverse of the reductive process that may be used to prepare NHGa.[48-51] Finally, as seen previously for the similar β-diketiminate species, oxidation of the Ga centre with chalcogens[52] or azides[53-54] results in the formation of σ-bonded dimers rather than multiply-bonded compounds.

The chemistry of *N*-Heterocyclic group 13 cations (Scheme 1.3 C & D) will be discussed in detail in Chapter 4.

NCN Ligands: Amidinates and Guanidinates

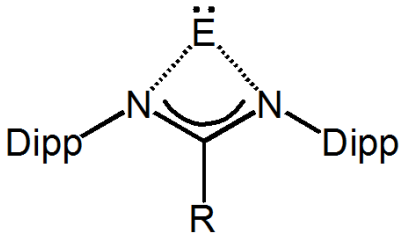

Figure 1.5: Lewis structure of guanidinate and amidinate, "NCN" ligands. When R is amino-based it is a guanidinate analogue, otherwise it is an amidinate analogue (even when the substituent is another pnictogen, such as P).

Amidinate and guanidinate ligands, collectively termed "NCN ligands", are similar in nature to the β-diketiminate family of ligands presented above in that they each contain two nitrogen donor atoms, bear a single negative charge, and feature a delocalized organic backbone (Figure 1.5). Furthermore, both classes of ligand employ bulky aryl groups that allow for kinetic stabilization of the dicoordinate triel site and provide tuneability to the ligand properties. The most obvious differences between the classes of ligands is that NCN ligands only have a single bridging carbon between the two nitrogen donor sites and thus produce a 4 membered ring when the ligand functions as an *N*,*N*-chelate (Figure 1.5).

In the guanidinates, the presence of an amino substituent on the backbone carbon atom renders the ligands more electron rich than the corresponding amidinates. A perhaps less obvious, but very important, consequence of the smaller bite angle of these types of ligands is the effect on their steric properties: the geometrical constraints of the 4-membered ring orient the substituents on the nitrogen atoms further away from the di-coordinate centre (in comparison to the 6- and 5-membered ring systems described above) resulting in diminished kinetic shielding. These properties do have a significant effect on the complexes that such ligands can stabilize and, in contrast to the 6-membered ring complexes described above, no examples of stable complexes for boron or aluminum have been reported for these classes of chelating nitrogen ligands.[55]

Interestingly, only bulky guanidinate ligands have allowed for the isolation of univalent gallium ($R=N(Cy)_2$)[56] and indium ($R=N(Cy)_2$[56] or DMP[57]) complexes that contain dicoordinate metal centres in the 4-membered ring that one would anticipate.[58] However, when the same guanidinate ligand is employed for thallium, a considerably different structure is obtained.[57-58] Instead of the normal *N,N'*-chelate structure, the metal is bound by one of the nitrogen and binds η^3 with one of the Dipp ligands (analogous to Figure 1.6 B). The adoption of such a "coordination isomer" structure is attributable to the larger size of the thallium(I) cation: the adoption of a *pseudo*-5-membered ring allows for a considerably less strained complex and the greater electron density and geometric properties of the arene ring allow the ligand to more effectively satisfy the coordination requirements of the larger cation. Similar behavior is also observed for the univalent complexes of indium when the NCN ligand employed is less electron rich or less stercially-demanding than the guanidinate.[56] In particular, when

ligand features substituents such as R=^{t}Bu or R=P(Cy)$_2$ (a phosphaguanidinate complex)[57] on the carbon atom of the backbone, the arene-bound isomer is obtained in lieu of the 4-membered ring (Figure 1.6 B). As one would expect, the N-,*π-aryl*-chelate is still observed for Tl amidinates.[56-57]

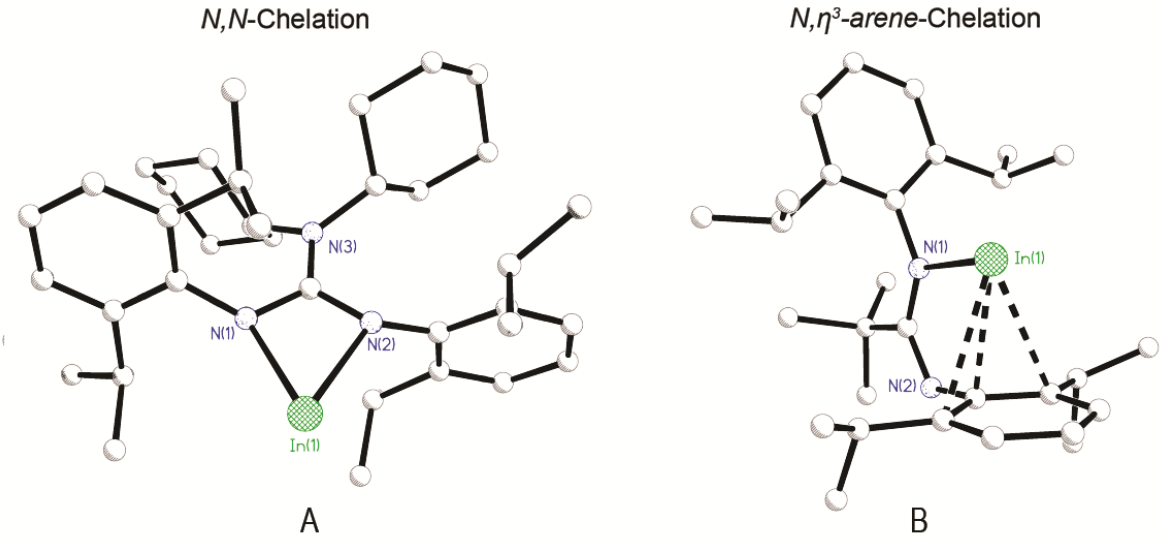

Figure 1.6: A: In N(Cy)$_2$-guanidinate complex; B: In ^{t}Bu-amidinate complex. The gallium N(Cy)$_2$-guanidinate analogue binds in the same fashion as the structure on the left.

Although only a small sample size is available for the guanidinate ligands, changing the amino substitution the backbone from DMP to N(Cy)$_2$ yields no change in In-N bond length.[58] As expected for such 4-membered rings, N-E-N angles are all very acute and are less than 60° for both the DMP and N(Cy)$_2$ of the indium(I) complexes and less than 64° for the N(Cy)$_2$ gallium(I) complex.

Computational investigations suggest that such univalent complexes should be excellent σ-donors but relatively poor π-acceptors and that bonding between the ligand and metal is highly ionic in nature[58-59] and, as such, have been used as ligands for transition metals, primarily group 10.[60-62] The gallium analogue has also been shown to insert into I_2 and Me_3Si-I.[56-57]

Amido-based ligands

Extremely bulky amido ligands have also allowed for the isolation of mono-coordinate compounds of gallium and thallium. Whereas the reactions of salts of most amido substituents with low-valent group 13 synthons typically yield oligomeric group 13 amides or related cluster compounds,[63-64] the treatment of the very bulky lithium amide Li[(2,6-$Mes_2C_6H_3$)(Me_3Si)N] with "GaI" results in the formation of the monomeric univalent gallium amide (2,6-$Mes_2C_6H_3$)(Me_3Si)NGa.[65] The structure, illustrated in Figure 1.7, features a mono-coordinate gallium atom with a Ga-N distance of 1.980 Å; not surprisingly, there appears to be a relatively close contact between the most proximate aryl group and the gallium centre with a C_{ipso}-Ga distance of 2.65 Å. The treatment of the gallium amide with the bulky aryl azide 2,6-$Mes_2C_6H_3N_3$ results in the elimination of N_2 and the formation of the amidoimidogallium compound (2,6-$Mes_2C_6H_3$)(Me_3Si)NGa=N(2,6-$Mes_2C_6H_3$) which features a Ga-N double bond.

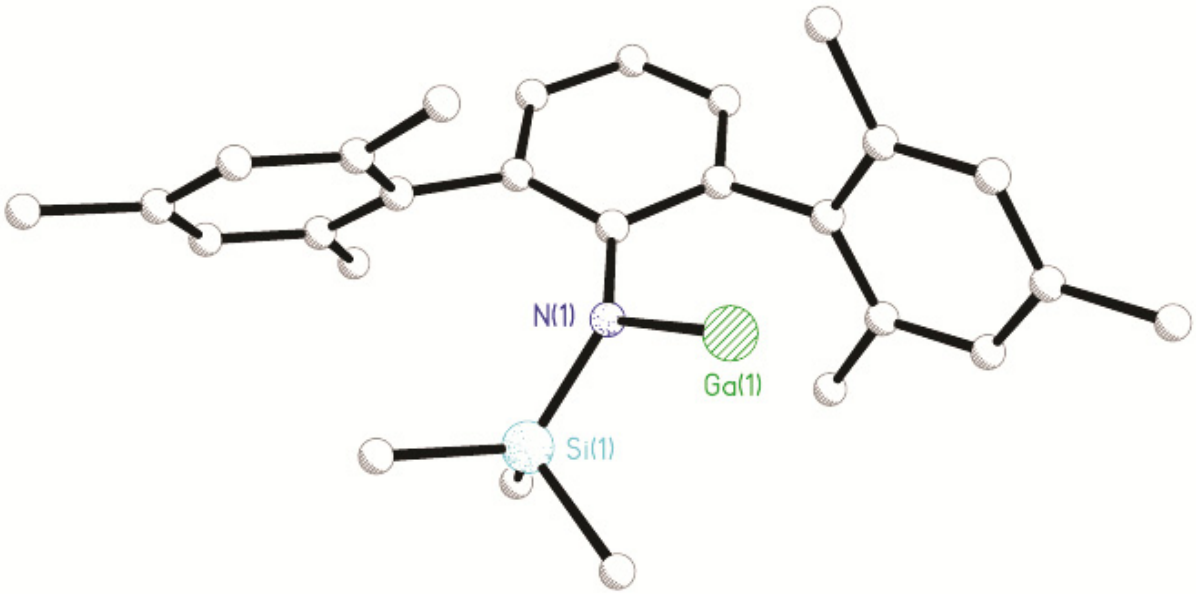

Figure 1.7: Solid state structure of (2,6-$Mes_2C_6H_3$)(Me_3Si)NGa.

Not surprisingly, bulky amides have also proven suitable for the isolation of monomeric univalent thallium compounds, of which one, (Dipp)(Me_3Si)NTl, was isolated as early as 1994.[66] This compound features long intermolecular interactions between the arene group on one molecule and the thallium centre of an adjacent molecule. The other crystallographically characterized example of such a monomeric thallium amide, (2,6-$Mes_2C_6H_3$)(Me)NTl, was reported more recently by Power and co-workers.[67] Perhaps surprisingly, the TlN(Me)C_{ipso} moiety is roughly co-planar with the central arene of the terphenyl group – this unusual orientation allows each thallium centre to engage in an intramolecular contact with an *ortho*-arene from the ligand. It should also be noted that attempts to generate univalent aluminum amides analogous to those mentioned above have yielded only oligomeric (usually tetrameric) clusters.[68-69]

Similarly, the use of smaller amide ligands also results in the formation of tetrameric gallium(I) amides rather than monomeric species.[70]

One final class of nitrogen-based complexes that should be mentioned are the cationic indium(I) 2,6-di(arylimino)pyridyl (DIMPY) complexes of Richeson and co-workers. Whereas the reaction of indium(I) halides with DIMPY ligands results in disproportionation and the generation of chelated indium(III) products, the treatment of the more stable InOTf with the same ligands provides salts of the coordination complexes of the general form [(DIMPY)In][OTf].[71] The structure of one such salt is illustrated in Figure 1.8 and exhibits an In-N_{pyr} distance of 2.495 Å and considerably longer contacts of 2.689 and 2.747 Å to the nitrogen atoms of the imino groups. On the basis of structural, computational and solid-state NMR investigations, the authors conclude that the cations in these salts are best considered as weakly-interacting coordination complexes.[72-73] Attempts to prepare similar complexes of univalent gallium using "GaI" were unsuccessful and resulted primarily in the formation of radical species.[74]

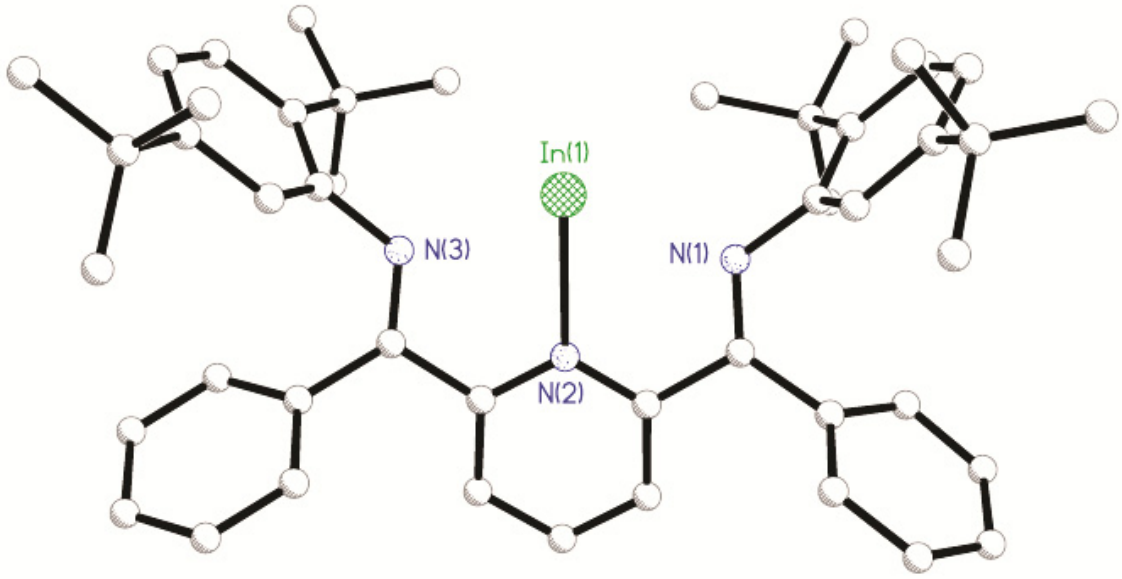

Figure 1.8: Solid state structure of [(2,6-[(2,5-^{t}Bu$_2$C$_6$H$_3$)NC(Ph)]C$_5$H$_3$N)In][OTf]. Counterion OTf$^-$ not shown for clarity.

1.3 - Carbon-based Ligands:

Although there are fewer distinct *classes* of carbon-based ligands in comparison to nitrogen-based ligands that have been employed to prepare and isolate compounds containing low-coordinate group 13 centres, some of the families of ligands that have proven to be successful have yielded many individual examples. In the following subsections, complexes derived from σ-bonded carbon-based ligands are presented first followed by those featuring π-bonded carbocyclic ligands.

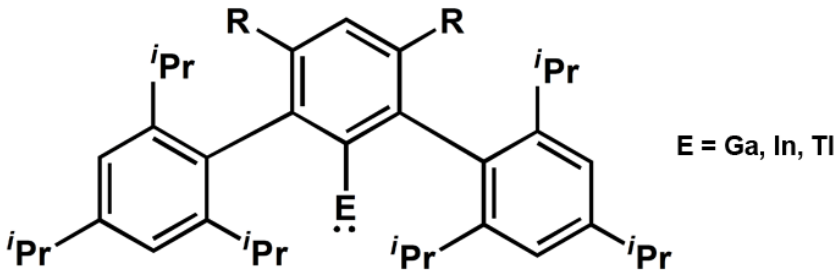

Figure 1.9: Coordinated terphenyl ligand with the heavier triels.

Large, sterically-demanding substituents have proven to be absolutely essential for the isolation of low-coordinate group 13 compounds because of the inherently high reactivity of such species and their propensity for oligomerization. The most effective class of σ-bonded substituents are the bulky terphenyl ligands (Ar*)[75] that have even allowed for the isolation of mono-coordinate group 13 centres of Ga,[76] In,[77-78] and Tl[79] (Figure 1.9).

The particularly bulky terphenyl substituents bearing ^{i}Pr groups at the 2- and 6-positions of the *ortho*-arene fragments have proven capable of supporting monocoordinate univalent group 13 centres for gallium, indium and thallium.

The metrical parameters and other features of the the univalent complexes are perhaps predictable, with E^{I}-C_{arene} bonds that tend to be somewhat longer than those of comparable E^{III}-C_{arene} bonds because of the differences in ionic radii (the more electron rich E^{I} centre is larger than the E^{III} centre). The most notable aspect of the structures, an example of which is illustrated in Figure 1.10 A, is that they are often unambiguously

monomeric even in the solid state. This should prove useful in the future for fine tuning the reactivity of low oxidation state indium complexes.

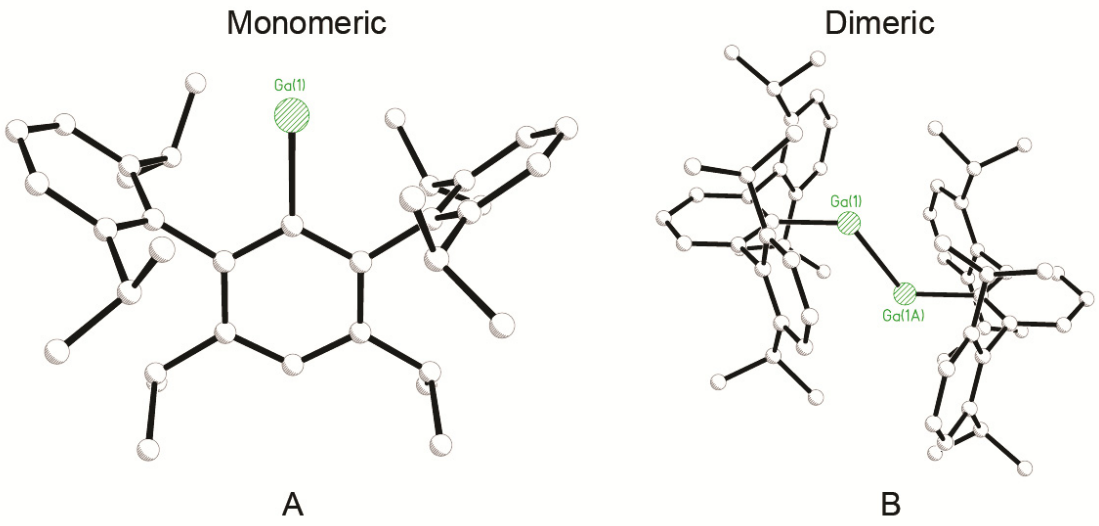

Figure 1.10: Solid state structures of A: GaTrp and B: TrpGa-GaTrp.

It must be noted that the use of these ligands does not always yield monomeric products: some bulky terphenyls do not preclude the formation of possible metal-metal bonds and dimeric structures are observed in the solid state (Figure 1.10 B) for Ga,[76, 80] In,[81] and Tl.[82] Small modifications to the central phenyl ring allow for two molecules to come in close enough proximity to dimerize and is most likely a consequence of hindered rotation of the Dipp rings.

Each of these dimeric compounds feature very long element-element bonds (Ga: 2.43-2.63 Å; In: 2.98 Å; Tl: 3.09 Å) and distinctly bent environments about the dicoordinate group 13 metal centres. In fact, the strength of the bonding in these "dimers" is very weak (< 9 kcal mol^{-1} for the strongest) and computational studies suggest that it is comparable in strength to those of closed shell interactions.[76]

Consequently, these compounds readily dissociate in solution and serve as effective sources of Ar*E species.

Univalent group 13 terphenyl compounds have demonstrated a considerable range of reactivity and, as one would anticipate for a uni-coordinate metal compound, the coordination number of the metal is increased in every instance. The thallium terphenyl compounds, as usual, are typically used as agents to transfer the organic ligand to other elements. However, the products observed in the reaction of Ar*Tl with P_4 are interesting multiply-bonded polyphosphorus species (Ar*-PH-P=P-PH-Ar*).[83] Most of the lighter Ar*E compounds have been observed to undergo a variety of oxidation and oxidative addition/insertion reactions and they have been used extensively as 2-electron donors. In spite of the steric bulk of the terphenyl substituents, they have proven useful as 2-electron donors for transition metals and Lewis acids. Thus the treatment of the univalent group 13 terphenyl compound with either transition metal complexes[77, 84] featuring a labile ligand or with the strong Lewis acid $B(C_6F_5)_3$ results in the formation of the anticipated complexes.[81-82, 85] The oxidation of Ar*E (E = Ga, In) complexes with chalcogen sources produces σ-bonded dimeric Ar*E(μ^2-Ch)$_2$EAr* heterocycles rather than multiply-bonded species.[86] In contrast, the related oxidation reaction with bulky organo-azides yields monomeric multiply-bonded compounds, Ar*-E=N-Ar (E = Ga, In).[87] Low valent gallium terphenyl compounds are found to insert into a variety of bonds including the N-H bond in ammonia and the H-H bond in molecular hydrogen.[88]

All of the donor-acceptor adducts feature essentially linear geometries at the di-coordinate group 13 site with bond distances that are consistent with the different sizes of the group 13 elements. It is worth noting that the E-C distance decreases markedly upon

complexation – this behavior is somewhat counterintuitive given that bond distances are often correlated with coordination number – however the observation is as one would anticipate given that the formation of the donor-acceptor complex effectively removes electron density from the group 13 centre. Furthermore, as discussed below for related systems, the molecular orbital associated with the lone pair of electrons on the group 13 element in the (putative) monovalent donor often has a considerable σ-antibonding C-E component; the depopulation of this MO via electron donation to an acceptor results in the shortening of the C-E bond.[76] Although the nature of such a correlation is not necessarily direct because of differences in the steric interactions between the donors and the acceptors, the sum of the C-B-C angles in the $B(C_6F_5)_3$ complexes suggest that the univalent group 13 terphenyl compounds are comparable donors to trialkyl (*ca*. 337-338°) and triaryl phosphines (*ca*. 340°), with the gallium compounds being better donors than the indium or thallium congeners.

Although they were not prepared from isolated Ar*E reagents, the metallocene complexes where two EAr* are coordinated can be generated from the one-pot simultaneous reduction of Ar^*ECl_2 *and* Cp_2MCl_2 (E = Ga, In; M = Ti, Zr, Hf) using either sodium or magnesium as the reductant provides the metallocene complexes (Ar^*E-$M(Cp)_2$-EAr^*).[89-91] The metrical parameters for each of the metallocene complexes are as one would anticipate. Each of the group 13 centres features an almost linear geometry with C-E distances that are comparable to those of the corresponding "free" ligand. The examination of MOs generated by computational investigations suggest that the bonding between the Ar*E fragment and the transition metal features components of both ligand-

metal σ-bonding and metal-ligand π-backbonding; such arguments will be examined in more detail below.

Whereas the bulky terphenyl aromatic groups are sufficiently bulky to stabilize unambiguously monomeric compounds that feature a σ-bond to a carbon atom, the situation for bulky aliphatics is somewhat more complicated. It is clear that large, bulky protecting groups are required for kinetic and thermodynamic stabilization to prevent oligomerization for these types of compounds. However, at least in the solid state, sterically-demanding aliphatic substituents have not yet proven able to provide monomeric species. However, there are several examples of σ-bound complexes that effectively behave as if they are monomeric R-E species in solution. For example, Uhl's tetrameric compound $[TlC(SiMe_3)_3]_4$ illustrated in Figure 1.11, which features bulky $C(SiMe_3)_3$ ("trisyl") ligands, exhibits a very distorted tetrahedral geometry in the solid state. Although this compound is clearly not low coordinate in the solid state, the reactivity observed by the reagent suggests that it dissociates from this tetrahedral arrangement in solution and serves as a source of R-Tl.[92]

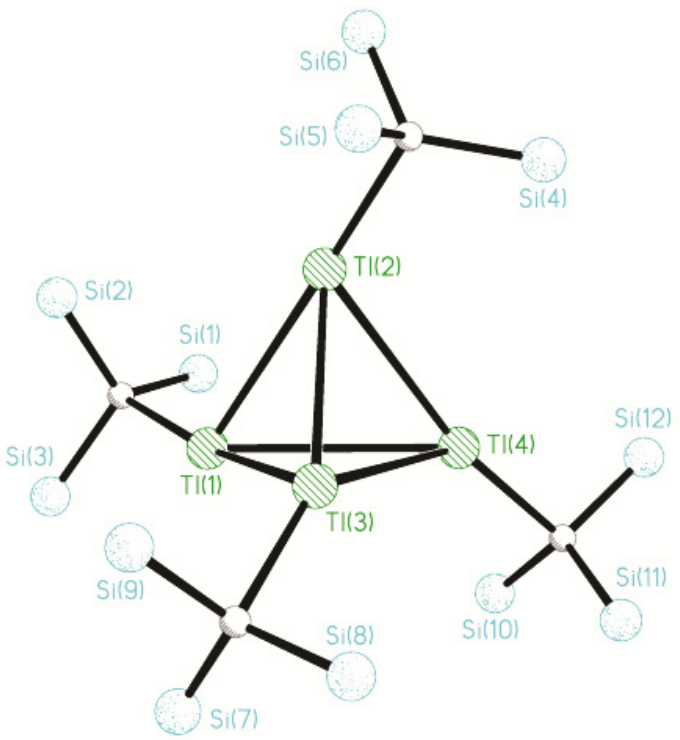

Figure 1.11: Solid state structure of $[TlC(SiMe_3)_3]_4$. Select bond distances Tl-C: 2.333 – 2.383 Å; Tl-Tl: 3.322 – 3.638 Å. Methyl groups have been omitted for clarity.

The other examples of lighter group 13 compounds with $C(SiMe_3)_3$ and related trisilyl ligands are also observed as tetramers with E-E bonds in the solid state.[92-98] However, although such clusters are more strongly bound than those of thallium, these lighter congeners also have been used as sources of neutral, two electron donors of the general form R-E for transition metal complexes. The transition metal complexes that result from the ligation of these putative mono-coordinate univalent ligands contain di-coordinate group 13 centres. For the trisyl group 13 ligands, prominent examples include Uhl's homoleptic nickel complexes, $Ni(EC(SiMe_3)_3)_4$ (E = Ga[99]; In[100]), each of which features four ER fragments around the metal centre. The complexes each exibit the

anticipated undistorted tetrahedral structure, as illustrated for the gallium analogue in Figure 1.12. The Ni-E bond distances (Ni-Ga: 2.170 Å; Ni-In: 2.304 Å) are considerably shorter than other comparable bonds (*vide infra*) and are consistent with the presence of metal-ligand π-back-bonding in each case. Uhl and co-workers also synthesized a platinum analogue, $Pt(InC(SiMe_3)_3)_4$. The In-Pt distance in the complex of 2.441 Å is, again, much shorter than those observed for other In-Pt bonds.[101] It is also worth noting that the E-C bonds in these coordination complexes are all comparable to or longer than those in the starting tetrameric precursors, as one would anticipate for a situation in which the E-C σ*-orbital is populated by metal-ligand π-backbonding.

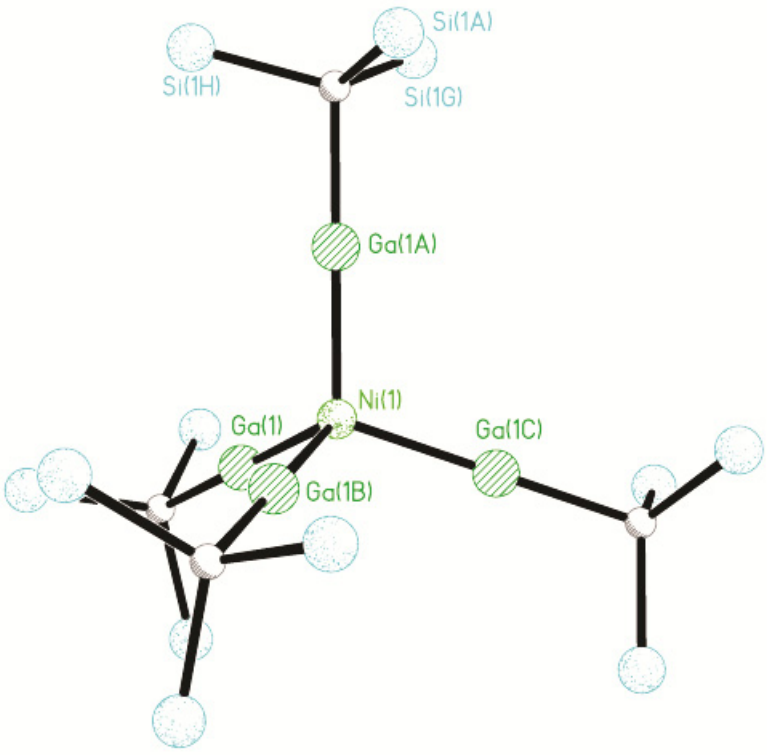

Figure 1.12: Solid state structure of $Ni[GaC(SiMe_3)_3]_4$. Methyl groups on Si have been omitted for clarity. Si-Ga-Ni: 180.00°.

One final interesting and unique compound that should be noted in this section is Lappert's $[Li]_2[Tl(CHSiMe_3SiMe(OMe)_2)]_2$, which is a lithium salt of a univalent thallate anion in which each thallium centre is σ-bonded to two carbon fragments that bear silyl groups.[102] The relative stability of thallium(I) is sufficient to allow for the formation of such an electron-rich anion, for which there are no analogous lighter congeners. As illustrated in Figure 1.13, the structure of the salt, which occurs in two different polymorphic forms, consists of a bent di-coordinate thallium centre with Tl-C distances ranging from 2.512 to 2.580 Å, and C-Tl-C angles of 89.6 to 91.1°. The lithium counter cation is situated in close proximity to the methoxy groups on the silane moieties and, as a result, the compound dimerizes in the solid state, bridging through the cations.

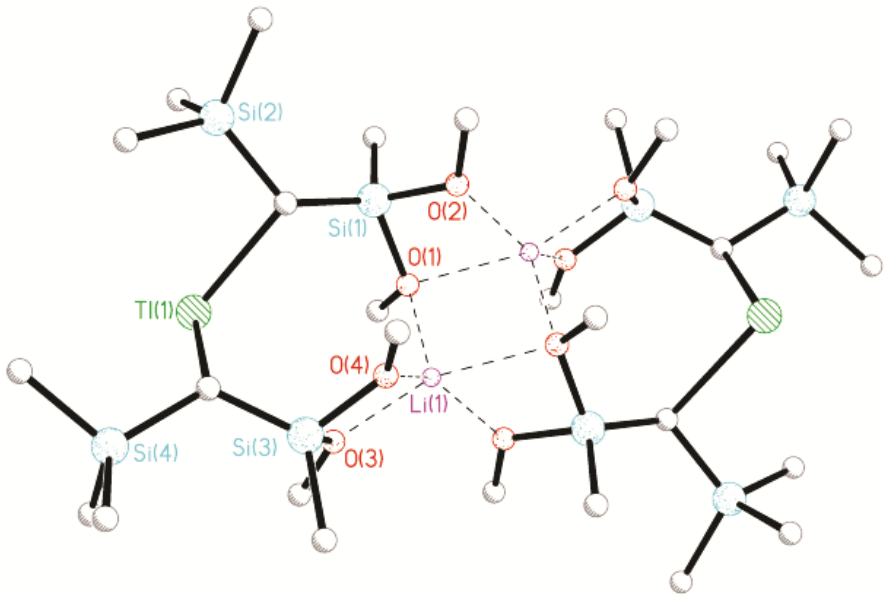

Figure 1.13: Solid state structure of $[Li]_2[Tl(CHSiMe_3SiMe(OMe)_2)]_2$.

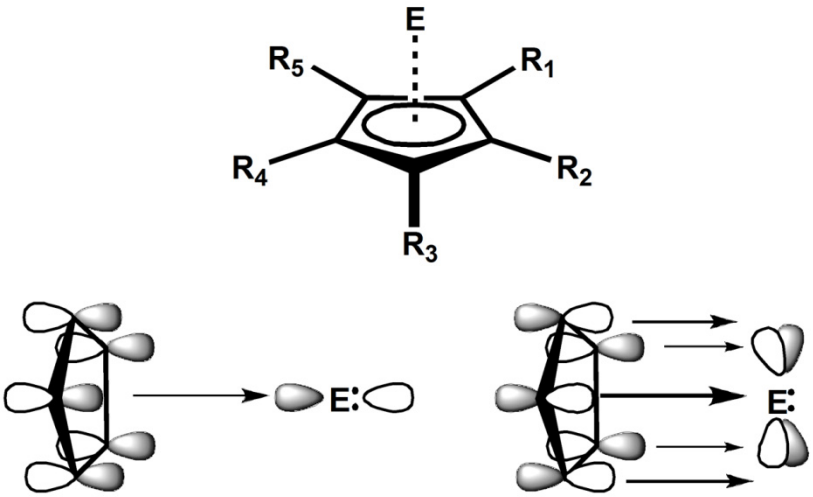

Scheme 1.4: Top: General structure of CpE species. Bottom: Molecular orbital diagrams of CpE bonding.

Cyclopentadienyl ligands (Cp') (Scheme 1.4) have the ability to function as ligands ranging from 2-electron σ-donors to 6-electron donors that provide both σ- and π-electron density. Furthermore, the substituents about the C_5 ring may be chosen to modify the steric and electronic properties of the ligands; such steric and electronic flexibility has been exploited to prepare complexes of Cp' groups with elements from all blocks of the periodic table. Main group cyclopentadienyl complexes have been investigated for many decades and, because of their ability to act as steric shields and to function as σ- and π-donors, such ligands have proven particularly suitable for the stabilization of E(I) species. Major reviews by Jutzi in 1999 and 2000 described the preparation and chemistry of such main group Cp' compounds including: synthesis, reactivity, and molecular orbital treatments of the bonding for a variety of ECp

compounds.[103-104] Interestingly, aluminum analogues of ECp compounds do not form monomeric units in the solid state, but rather tetramize to form tetrahedral complexes (Figure 1.14).[105-106] Much like the trisyl ligand mentioned above, $(AlCp)_4$ dissociates in solution and acts as a source for AlCp. With the heavier CpE complexes, if the R groups on the Cp ring are sufficiently bulky, they form octahedral structures with very long E-E contact distances (Ga-Ga: *ca*. 4.2 Å; In-In: *ca*. 3.9 Å).[107-109] If the R groups are small, like hydrogen or even persubstituted rings, they form a sandwich polymer with alternating E and Cp groups.[110-113] Arene complexes[114] have a very extensive history and their chemistry has been reviewed recently.[115-116]

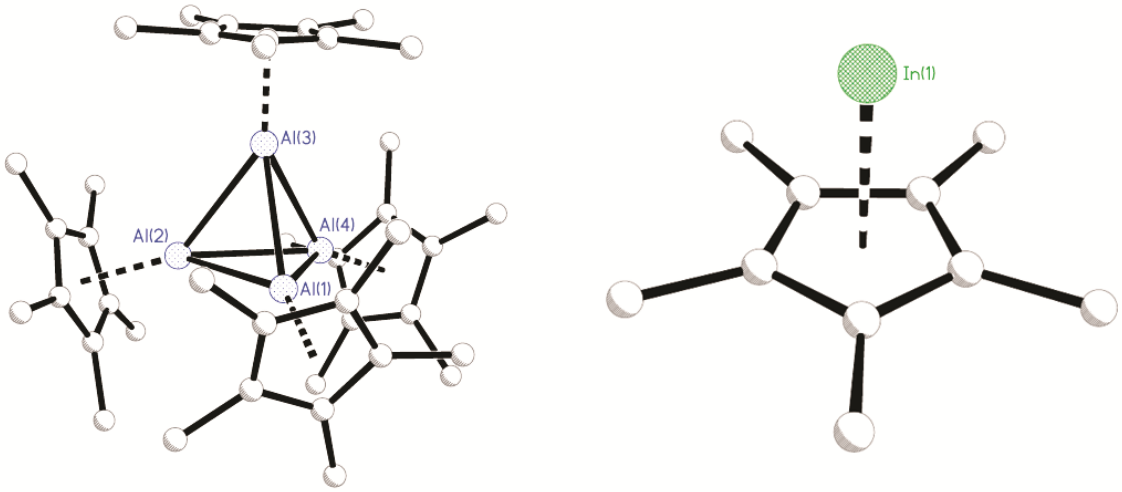

Figure 1.14: Left: Solid state structure of AlCp*. Right: Solid state structure of InCp*

Computational examination of the bonding and electronic structures of model complexes for several univalent group 13 compounds including the half-sandwich compounds CpE, Cp*E (E = B, Al, Ga, In).[117] More recently, Frenking and Rayón have

published an in-depth study, including comprehensive energy decomposition analyses, of several classes of main group cyclopentadienyl complexes, including those of the general form ECp' (E = B, Al, Ga, In, Tl) which provide details regarding the structures, bonding energies, orbital contributions and other fundamental aspects of these complexes.[118] Overall, these calculations confirm that although much of the interaction between the Cp groups and the metal in such complexes is electrostatic, there is a sizeable covalent component. Furthermore, the HOMO in most cases is the orbital attributable to the "lone pair" on the metal and corroborates the use of such compounds as ligands.

In addition to the ligand chemistry displayed by Cp'E molecules, there is also a vast amount of oxidation, oxidative addition and cycloaddition chemistry similar to that described above for the analogous β-diketiminate univalent group 13 compounds. Furthermore, because of their volatility, many of these cyclopentadienides have also proven to be useful precursors for the formation of materials containing group 13 elements and have been reviewed extensively.[103-104, 119-120]

A large variety of related sandwich and half-sandwich compounds of formally low-coordinate univalent group 13 elements bonded to cyclopentadienyl and/or arenes have also been isolated (Figure 1.15).[112, 121-127] The preparative routes to many of these compounds often involve the protonolytic cleavage of a small volatile molecule – e.g. Cp'H from Cp'E precursors – to afford the desired products. Arene-complexed group 13 cations are often observed when such reactions are performed in aromatic solvents.

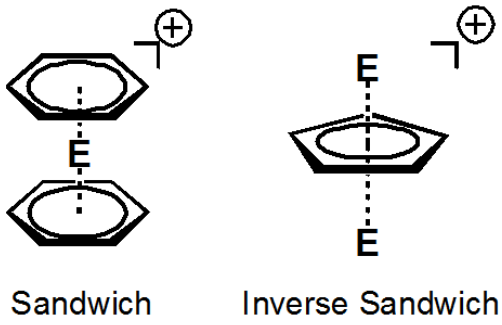

Figure 1.15: Generic structures of sandwich and inverse sandwich E-Aryl structures.

All of the complexes feature η^5-bonded cyclopentadienyl groups and/or η^6-bonded arenes to the univalent group 13 element. Almost all of the sandwich complexes also feature "bent" arrangements of the π-donors rather than parallel arrangements. Such geometries are often attributed to the presence of a stereochemically-active pair of electrons on the metal centre, however the presence of relatively close contacts between the cations and corresponding anions also contributes to the observed structures.[114-115] The distances between a given metal and the corresponding π-donor ligand follow the anticipated trends: inverse sandwich compounds in which one ligand interacts with two metals exhibit longer distances than those of the corresponding Cp'E;[128] anionic cyclopentadienyl ligands form shorter bonds than do neutral arene donors; and, more electron-rich donors tend to form shorter bonds than less electron-rich ligands.

It is noteworthy that only for thallium(I) has it proven possible to generate anionic bent-metallocene complexes such as $[Tl_3Cp'_2]^-$ through the reaction of a neutral Cp'Tl compound with a source of cyclopentadienyl anions.[129] Salts of the simplest such *pseudo*-dicoordinate complexes were first obtained by Wright and co-workers in the early

1990's.[129-130] Attempts to generate the lighter analogues often results in disproportionation or decomposition of the group 13 precursor. While the reactivity of most of the sandwich compounds has not been examined in great detail, compounds such as $[Cp^*_2Ga]^-$ and $[Tol_2Ga]^+$ have proven to be rarely useful sources of Ga^+ ions, in particular for transition metal complexes.[121, 123, 131]

Phospholyl ligands are a class of monoanionic ligands closely related to cyclopentadienyl ligands in which C-R fragments have been formally replaced by an isovalent P centre – in fact such groups are also often called "phospha-cyclopentadienyl" ligands and are prepared in a similar fashion to the Cp complexes.[132-134]

Only a small handful of phospholyl ligands have been characterized crystallographically. They typically employ bulky ^{t}Bu groups adjacent to the phosphorus centres to provide kinetic stabilization as well as to promote η^5-coordination rather than σ-coordination.[135] Although the presence of the multiple ^{t}Bu groups about the ligands also appears to decrease the degree of oligomerization of the group 13 complexes in the solid state, long range dimers and 1D-coordination polymer assemblies are observed. In spite of the foregoing, it should be noted that, when thallium binds to an unsubstituted phospholyl ligand, it binds in an η^5-fashion. Perhaps expectedly, the complex forms a 1D-coordination polymer in the solid state with alternating Tl cations and phospholyl ligands as illustrated in Figure 1.16.

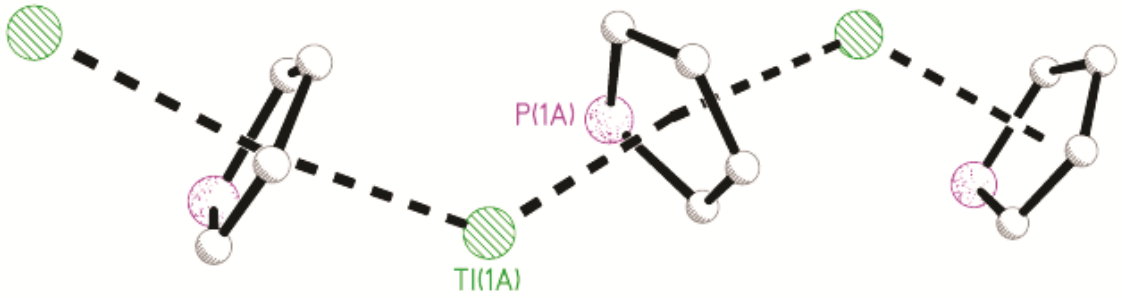

Figure 1.16: Solid state structure of $[PC_4H_4][Tl]$, showing the 1D-polymeric structure of alternating phospholyls and thalliums that occurs when crystallized.

The number of phosphorus atoms in the 5-membered ring ligand has a drastic effect on the distance between the centroid and the metal centre. For example, $[PC_2(C^tBu)_2]Ga$[136-137] and $[P_3(C^tBu)_2]Ga$[138] only differ in that there are two additional phosphorus atoms in the ring; however an increase in the ring centroid to gallium distance of over 0.12 Å is observed because of the alteration. Such elongations are attributed to the observation that the presence of the phosphorus atom has an overall electron-withdrawing effect in comparison to the CR fragments.[133] As with many of the trends mentioned above, going from Ga to Tl increases the E-Ct distance as one would expect on the basis of atomic size of the triel.[138-140]

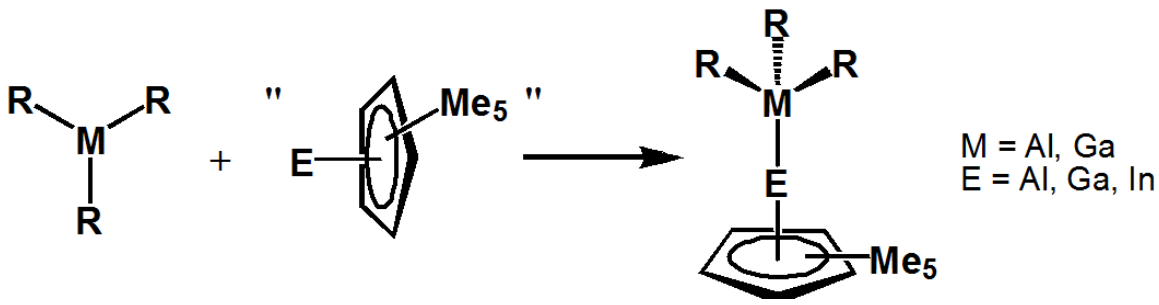

Scheme 1.5: Most general preparative route to triel-triel donor-acceptor complexes.

As with many of the low valent group 13 complexes described above, the presence of a "lone pair" on the triel centre in Cp'E complexes allows them to function as Lewis bases. In fact, the relative stability and convenient (and early) preparation of Cp'E compounds rendered them suitable to be used as donors in the first examples of such donor-acceptor complexes. Furthermore, because compounds of trivalent group 13 elements are the classic examples of Lewis acids, the development of group 13 donors allowed for the ready preparation of mixed valent group 13 donor-acceptor complexes. This class of complexes that feature elongated 'piano stool' arrangements has recently been reviewed by Cowley[141] and the bonding in such donor-acceptor complexes has been elucidated and reviewed by Frenking.[142] The preparation for many of the triel-triel donor-acceptor complexes is straight forward. Treatment of the appropriate Cp'E donor with the chosen MR_3 acceptor produces the target Cp'E-MR_3 complex rapidly and in quantitative yield (Scheme 1.5).[143-147] As suggested above, the Cp'E species need not be monomeric in the solid state (e.g. $Al_4Cp^*_4$) and examples with several different substitution patterns on the Cp' ligand have been obtained. However, not all group 13 Lewis acids are suitable for use. While tris(fluoroaryl)-substituted acceptors generally

appear to work, the attempted use of group 13 trihalides usually results in decomposition or redox reactions.

Each of the ER_3 fragments goes from being formally trigonal planar in the starting material to a tetrahedral geometry upon the formation of the dative bond from the Cp'E compound (Figure 1.17). As indicated previously, the magnitude of the deviation from planarity (as measured by the sum of the C-E-C angles in the acid fragment) has been used to assess the relative strength of the donor. Such analyses suggest that Cp*E donors are comparable to Ph_3P for E = Al and Ga and weaker donors than trialkylphosphines. The formation of the dative bond also has a pronounced effect on the other metrical parameters within the resultant complex. Compared to their respective starting materials, a considerable decrease in the average E-Cp* distance is observed in the univalent donor fragments. This change is attributable to the depopulation of the "lone pair" orbital, which has some Cp*-E antibonding character, and to the increased partial positive charge on the group 13 centre in the donor, which would also produce a closer contact to the Cp*-ring as the effective size of the element effectively decreases.[117] It is also worth emphasizing that although most of the donor-acceptor complexes feature nearly linear Ct-E_1-E_2 fragments, very significant deviations are observed for complexes that contain η^1-Cp* on the acceptor fragment, which appears to interact with the donor group 13 element.[145] Similar interactions of the donor triel with, for example, F atoms from the acceptor fragment, also result in non-linear arrangments.[148]

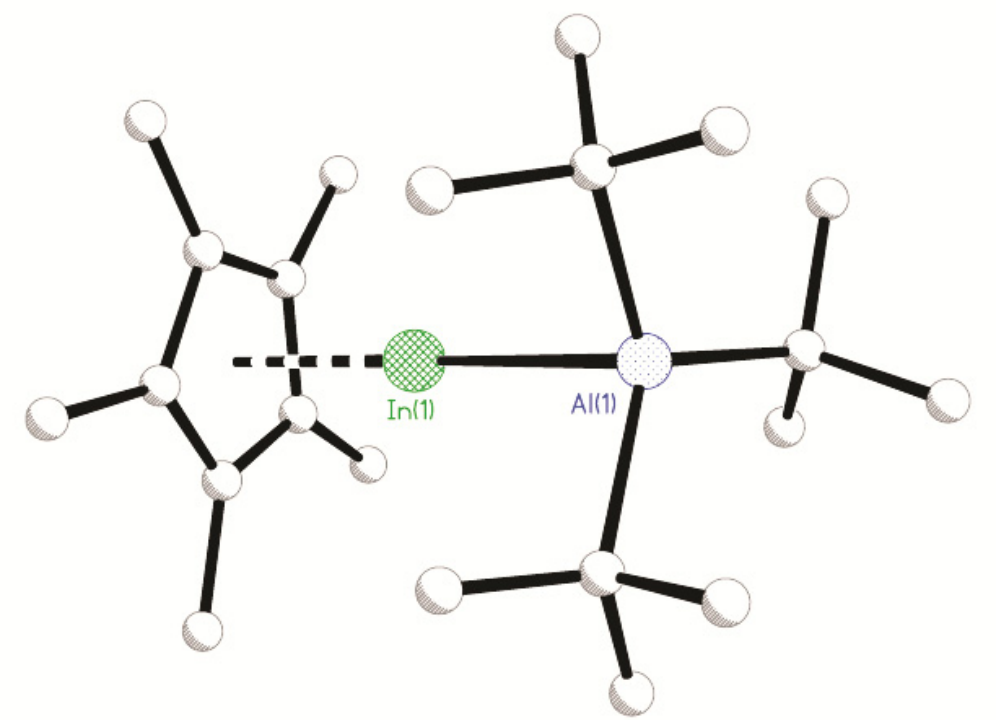

Figure 1.17: Solid state structure of the donor-acceptor complex, Cp*In-Al^{t}Bu$_3$.

Although there are no stable univalent boron cyclopentadienyl compounds of the type Cp'B, donor-acceptor complexes analogous to those described above have indeed been isolated. The compound Cp*B-BCl_3 is best prepared through the treatment of Cl_2BBCl_2 with one equivalent of Cp*-$SiMe_3$;[149] the rearrangement of the presumed intermediate Cp*$ClBBCl_2$ to the donor-acceptor isomeric form has been computed to be favourable[150] and the final product features a near linear geometry about the Ct-B-B bond (179.35°).

In light of the electron-rich nature of the univalent group 13 compounds previously described, it will come as no surprise that such compounds have been used extensively as ligands for transition metals. For some classes of group 13 donors, such as

the mono-coordinate terphenyl complexes, the resultant transition metal complexes still contain di-coordinate triel centres and were described within that section. There are, however dozens of transition metal complexes synthesized from Cp'E donors. The nature of the bonding between low-coordinate species of many types, including that of univalent group 13 donors, and transition metal fragments has been reviewed in detail.[151-152]

1.4 - Chalcogen-based ligands

Substituents based on chalcogen ligands are a mainstay in inorganic coordination chemistry and organometallic chemistry. There are, as one would anticipate, a considerable number of simple thallium(+1) salts of chalcogenide ligands that contain di-coordinate thallium centres.[153] For indium and the lighter group 13 elements, many chalcogen-based ligands produce compounds that undergo spontaneous disproportionation. There are, however, a few examples of stable chalcogenolato complexes featuring the lighter group 13 elements in low coordinate environments. Roesky and co-workers' 1989 compounds, $[E_2(\mu\text{-}O(2,4,6\text{-}(CF_3)_3C_6H_2))_2]$ (E = In, Tl), deserve special mention in that each exhibits a discrete dimeric structure in the solid state, consisting of a 4 membered ring with alternating triel and O atoms.[154-155] In fact, such a cyclic dimeric structure is even adopted by the parent indium(+1) compound InH, which was examined experimentally more than 10 years later by Pullumbi and co-workers using matrix isolation methods.[156] Interestingly, an analogous Tl_2O_2 motif is observed for the thallium(+1) complex of the tris(pyrazolyl)methanesulfonate anion $[(Pz^{tBu})_3CSO_3]^-$. Rather than binding the thallium cation via the nitrogen atoms in the manner described

above for the tris(pyrazolyl borates), the anion binds instead through one of the oxygen atoms on each sulfonate group to produce a dimeric structure of the form $Tl_2(\mu\text{-}OSO_2C(Pz^{tBu})_3)_2$.[157]

Macdonald and co-workers reported the structure of the relatively stable and soluble trifluoromethanesulfonate salt of indium(+1) that features a similar arrangement, as illustrated in Figure 1.18. Although the compound is probably best considered as an ionic species, two adjacent [In][OTf] fragments adopt a dimeric arrangement in the solid state remisiscent of the E_2O_2 moieties described.[158] The triflate group is, however, considerably more electron withdrawing than the 2,4,6-tris(trifluomethyl)phenyl group and the In-O bond distances within the $In_2(\mu\text{-}OTf)_2$ fragment are considerably longer and are at best consistent with being contact ion pairs. Such an assessment is corroborated by the metrical parameters within the triflate anion, which are consistent with those of a "free" anion. Furthermore, it should be noted that treatment of [In][OTf] with [18]crown-6 results in a monomeric contact ion pair of the form [In([18]crown-6)][OTf] in which the closest In-O distance is of 2.370 Å, thus the distances within "$In_2(\mu\text{-}OTf)_2$" are clearly exceptionally long.[159]

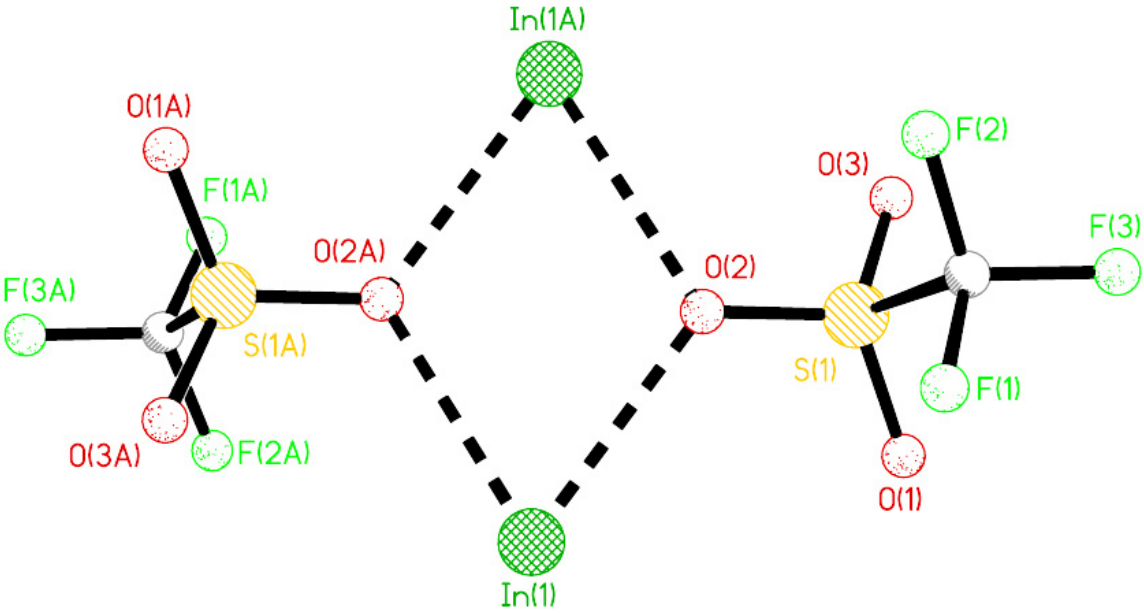

Figure 1.18: Solid state structure of [In][OTf] as a dimeric species.

As discussed above, β-diketiminate anions have proved to be suitable ligands for the isolation of many univalent group 13 compounds, including even examples for Al and Ga. In contrast, the corresponding acetylacetonate (acac) ligands (and other related β-diketonate ligands), which have been employed extensively in the classical coordination chemistry of many metals, are not effective for the stabilization of univalent group 13 elements other than thallium. However, even for thallium, the absences of steric bulk around the metal centre allows for the dimerization or oligomerization of these β-diketonate complexes. For thallium, there are only a handful of examples in which β-diketonate ligands are coordinated. In the solid state, the parent acac complex [Tl][$(OCMe)_2CH$] forms polymeric chains in which one of the oxygen atoms in the acac ligand also binds to a neighbouring chelated thallium centre.[160] Laguna and coworkers

also reported aurate salts of dimeric trinuclear or tetranuclear thallium acac cations, $[Tl]_n[(OCMe)_2CH]_2$ (n = 3 or 4), respectively (Figure 1.19).[160] Interestingly, in spite of the different number of thallium atoms bonded to each acac the average Tl-O bond distances for the tetracoordinate thallium ions remains relatively the same at *ca*. 2.71 Å. It should be noted that there are close contacts and strong interactions between the dicoordinate thallium centres and the gold atoms which give rise to materials with interesting luminescent properties.[161]

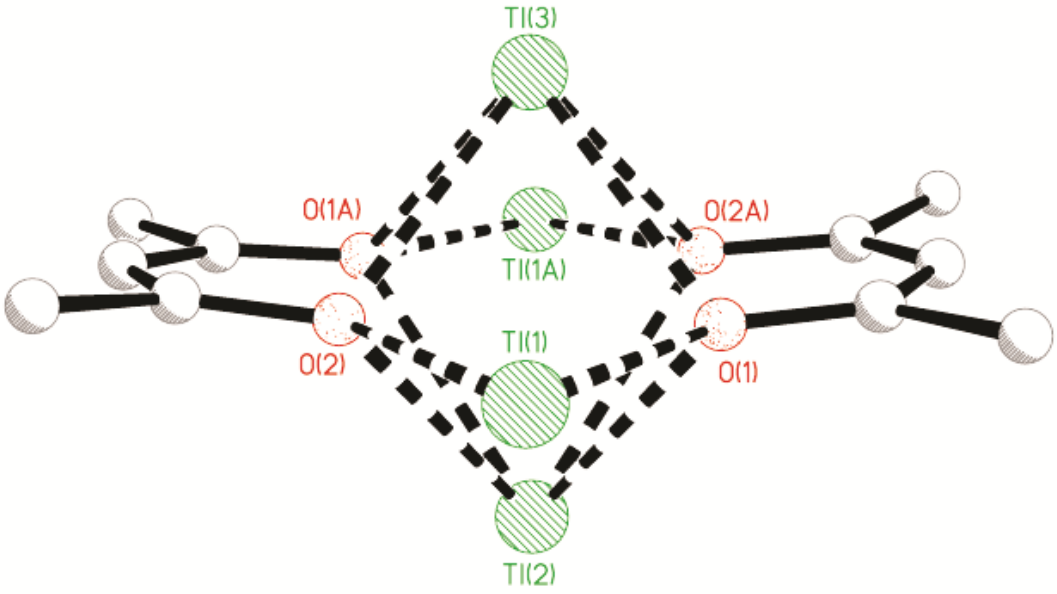

Figure 1.19: Solid state structure of $[Tl]_4[(OCMe)_2CH]_2^-$. Cocrystallized $Ag(C_6Cl_5)_2$ not shown.

1.5 - Conclusions:

There are a tremendous number of group 13 compounds in which the triel centres feature a low oxidation state. Such species feature many different types of substituents that provide the necessary steric and/or electronic stabilization that is required to prevent the triel centre from oxidation.

Predictably, the reactivity exhibited by all classes of low coordinate group 13 compounds almost universally results in an increase in the coordination number at that metal. For the electron-rich low valent species described at the start of this chapter, the increase in coordination number is achieved either through oxidative addition into suitable bonds or through the formation of coordination complexes with suitable acceptors. The great diversity of structural types and chemical properties engendered by the substituents employed to prepare low coordinate group 13 compounds provides for reagents with a vast number of applications, ranging from chemical synthesis and catalysis, to materials precursors. Given the rapid development of ligands and triel sources suitable for the preparation of low coordinate group 13 compounds since the late 1990's, the future bodes well for the generation of new compounds and new applications for such species.

The work described herein pertains to indium in its +1 oxidation state. As stated earlier, the indium(I) halides, although the primary source for all indium(I) species, are extremely insoluble in most organic solvents as well as unstable in the presence of donor molecules. Chapter 2 discusses a method to improve the solubility of such halides in both donor and non donor solvents. Chapter 3 examines insertion chemistry of carbon-halogen bonds into InOTf via *in situ* destabilization of the 5s orbital. Chapter 4 explores the

reactivity of redox active α-diimine ligands and how slight modifications impact the products obtained. Finally, Chapter 5 provides some overall conclusions as well as some insight into the outlook for these indium-based projects.

1.6 - References

[1] McNaught, A. D.; Wilkinson, A., *IUPAC. Compendium of Chemical Terminology, 2nd ed. (the "Gold Book")*. 2 ed.; Blackwell Scientific Publications: Oxford, UK, 1997.

[2] Parkin, G., *J. Chem. Educ.* **2006,** *83* (5), 791.

[3] Sidgwick, N. V., *The Covalent Link In Chemistry*. Cornell University Press: Ithaca, NY, 1933.

[4] Cotton, F. A.; Wilkinson, G.; Murillo, C. A.; Bochmann, M., *Advanced Inorganic Chemistry*. Sixth Edition ed.; John Wiley & Sons, Inc.: Chichester, 1999; p 1355.

[5] Schwerdtfeger, P.; Heath, G. A.; Dolg, M.; Bennett, M. A., *J. Am. Chem. Soc.* **1992,** *114* (19), 7518.

[6] Pyykko, P.; Desclaux, J. P., *Acc. Chem. Res.* **1979,** *12* (8), 276.

[7] Pyykko, P., *Chem. Rev.* **1988,** *88* (3), 563.

[8] Pardoe, J. A. J.; Downs, A. J., *Chem. Rev.* **2007,** *107* (1), 2.

[9] Asay, M.; Jones, C.; Driess, M., *Chem. Rev.* **2011,** *111* (2), 354.

[10] Hill, M. S.; Hitchcock, P. B., *Chem Commun* **2004,** (16), 1818.

[11] Cui, C. M.; Roesky, H. W.; Schmidt, H. G.; Noltemeyer, M.; Hao, H. J.; Cimpoesu, F., *Angew. Chem. Int. Ed. Engl.* **2000,** *39* (23), 4274.

[12] Hardman, N. J.; Eichler, B. E.; Power, P. P., *Chem Commun* **2000,** (20), 1991.

[13] Hill, M. S.; Hitchcock, P. B.; Pongtavornpinyo, R., *Dalton Trans.* **2005,** (2), 273.

[14] Hill, M. S.; Hitchcock, P. B.; Pongtavornpinyo, R., *Angew. Chem. Int. Ed.* **2005,** *44* (27), 4231.

[15] Hill, M. S.; Pongtavornpinyo, R.; Hitchcock, P. B., *Chem Commun* **2006,** (35), 3720.

[16] Li, X. F.; Cheng, X. Y.; Song, H. B.; Cui, C. M., *Organometallics* **2007,** *26* (4), 1039.

[17] Hill, M. S.; Hitchcock, P. B.; Pongtavornpinyo, R., *Inorg. Chem.* **2007,** *46*, 3783.

[18] Trofimenko, S., *J. Chem. Educ.* **2005,** *82* (11), 1715.

[19] Trofimenko, S., *Chem. Rev.* **1993,** *93* (3), 943.

[20] Reger, D. L., *Coord. Chem. Rev.* **1996,** *147*, 571.

[21] Kuchta, M. C.; Bonanno, J. B.; Parkin, G., *J. Am. Chem. Soc.* **1996,** *118*, 10914.

[22] Kuchta, M. C.; Das, H. V. R.; Bott, S. G.; Parkin, G., *Inorg. Chem.* **1996,** *35*, 943.

[23] Dias, H. V. R.; Jin, W., *Inorg. Chem.* **1996,** *35*, 267.

[24] Frazer, A.; Piggott, B.; Hursthouse, M. B.; Mazid, M., *J. Am. Chem. Soc.* **1994,** *116*, 4127.

[25] Reger, D. L.; Garza, D. G.; Rheingold, A. L.; Yap, G. P. A., *Organometallics* **1998,** *17* (16), 3624.

[26] Reger, D. L.; Mason, S. S.; Rheingold, A. L.; Haggerty, B. S.; Arnold, F. P., *Organometallics* **1994,** *13* (12), 5049.

[27] Kuchta, M. C.; Bonanno, J. B.; Parkin, G., *J. Am. Chem. Soc.* **1996,** *118* (44), 10914.

[28] Dias, H. V. R.; Jin, W. C., *Inorg. Chem.* **2000,** *39* (4), 815.

[29] Frazer, A.; Hodge, P.; Piggott, B., *Chem Commun* **1996,** (15), 1727.

[30] Yurkerwich, K.; Parkin, G., *J. Clust. Sci.* **2010,** *21* (3), 225.

[31] Kuchta, M. C.; Parkin, G., *Main Group Chem.* **1996,** *1* (3), 291.

[32] Kuchta, M. C.; Parkin, G., *Inorg. Chem.* **1997,** *36* (12), 2492.

[33] Kuchta, M. C.; Parkin, G., *J. Chem. Soc., Dalton Trans.* **1998,** (14), 2279.

[34] Kuchta, M. C.; Parkin, G., *J. Am. Chem. Soc.* **1995,** *117* (50), 12651.

[35] Sundermann, A.; Reiher, M.; Schoeller, W. W., *Eur. J. Inorg. Chem.* **1998,** (3), 305.

[36] Tuononen, H. M.; Roesler, R.; Dutton, J. L.; Ragogna, P. J., *Inorg. Chem.* **2007,** *46*, 10693.

[37] Segawa, Y.; Yamashita, M.; Nozaki, K., *Science* **2006,** *314*, 113.

[38] Segawa, Y.; Suzuki, Y.; Yamasaki, T.; Nozaki, K., *J. Am. Chem. Soc.* **2008,** *130*, 16069.

[39] Yamashita, M.; Suzuki, Y.; Segawa, Y.; Nozaki, K., *J. Am. Chem. Soc.* **2007,** *129*, 9570.

[40] Yamashita, M.; Suzuki, Y.; Segawa, Y.; Nozaki, K., *Chem. Lett.* **2008,** *37*, 802.
[41] Schmidt, E. S.; Jockisch, A.; Schmidbaur, H., *J. Am. Chem. Soc.* **1999,** *121*, 9758.
[42] Baker, R. J.; Farley, R. D.; Jones, C.; Kloth, M.; Murphy, D. M., *J. Chem. Soc., Dalton Trans.* **2002,** (20), 3844.
[43] Jones, C.; Mills, D. P.; Platts, J. A.; Rose, R. P., *Inorg. Chem.* **2006,** *45*, 3146.
[44] Fedushkin, I. L.; Lukoyanov, A. N.; Fukin, G. K.; Ketkov, S. Y.; Hummert, M.; Schumann, H., *Chem. Eur. J.* **2008,** *14*, 8465.
[45] Fedushkin, I. L.; Lukoyanov, A. N.; Tishkina, A. N.; Fukin, G. K.; Lyssenko, K. A.; Hummert, M., *Chem. Eur. J.* **2010,** *16*, 7563.
[46] Okuno, Y.; Yamashita, M.; Nozaki, K., *Angew. Chem. Int. Ed. Engl.* **2011,** *50*, 920.
[47] Baker, R. J.; Jones, C., *Coord. Chem. Rev.* **2005,** *249* (17-18), 1857.
[48] Green, S. P.; Jones, C.; Lippert, K. A.; Mills, D. P.; Stasch, A., *Inorg. Chem.* **2006,** *45* (18), 7242.
[49] Jones, C.; Mills, D. P.; Rose, R. P., *J. Organomet. Chem.* **2006,** *691* (13), 3060.
[50] Baker, R. J.; Jones, C.; Mills, D. P.; Kloth, M.; Murphy, D. M., *Chem. Eur. J.* **2005,** *11*, 2972.
[51] Baker, R. J.; Jones, C.; Kloth, M.; Platts, J. A., *Angew. Chem. Int. Ed. Engl.* **2003,** *42*, 2660.
[52] Baker, R. J.; Jones, C.; Kloth, M., *Dalton Trans.* **2005**, 2106.
[53] Jones, C.; Mills, D. P.; Rivard, E.; Stasch, A.; Woodul, W. D., *J. Chem. Crystallogr.* **2010,** *40*, 965.
[54] Baker, R. J.; Jones, C.; Mills, D. P.; Murphy, D. M.; Hey-Hawkins, E.; Wolf, R., *Dalton Trans.* **2006**, 64.
[55] Jones, C., *Coord. Chem. Rev.* **2010,** *254* (11-12), 1273.
[56] Jones, C.; Junk, P. C.; Platts, J. A.; Rathmann, D.; Stasch, A., *Dalton Trans.* **2005,** (15), 2497.
[57] Jin, G. X.; Jones, C.; Junk, P. C.; Stasch, A.; Woodul, W. D., *New J. Chem.* **2008,** *32* (5), 835.
[58] Jones, C.; Junk, P. C.; Platts, J. A.; Stascht, A., *J. Am. Chem. Soc.* **2006,** *128* (7), 2206.
[59] Overgaard, J.; Jones, C.; Dange, D.; Patts, J. A., *Inorg. Chem.* **2011,** *50* (17), 8418.
[60] Jones, C.; Stasch, A.; Moxey, G. J.; Junk, P. C.; Deacon, G. B., *Eur. J. Inorg. Chem.* **2009**, 3593.
[61] Green, S. P.; Jones, C.; Stasch, A., *Inorg Chem Commun* **2007,** *46*, 11.
[62] Moxey, G. J.; Jones, C.; Stasch, A.; Junk, P. C.; Deacon, G. B.; Woodul, W. D.; Drago, P. R., *Dalton Trans.* **2009**, 2630.
[63] Schnepf, A.; Schnockel, H., *Angew. Chem. Int. Ed.* **2002,** *41* (19), 3533.
[64] Schnockel, H.; Schnepf, A., Aluminium and Gallium Clusters: Metalloid Clusters and their Relationship to the Bulk Phases, to Naked Clusters and to Nanoscaled Materials. In *The Group 13 Metals Aluminium, Gallium, Indium and Thallium. Chemical Patterns and Peculiarities*, Aldridge, S.; Downs, A. J., Eds. John Wiley and Sons: Chichester, UK, 2011; pp 402.
[65] Wright, R. J.; Brynda, M.; Fettinger, J. C.; Betzer, A. R.; Power, P. P., *J. Am. Chem. Soc.* **2006,** *128*, 12498.
[66] Waezsada, S. D.; Belgardt, T.; Noltemeyer, M.; Roesky, H. W., *Angew. Chem. Int. Ed. Engl.* **1994,** *33* (13), 1351.
[67] Wright, R. J.; Brynda, M.; Power, P. P., *Inorg. Chem.* **2005,** *44* (10), 3368.
[68] Schiefer, M.; Reddy, N. D.; Roesky, H. W.; Vidovic, D., *Organometallics* **2003,** *22* (18), 3637.
[69] Sitzmann, H.; Lappert, M. F.; Dohmeier, C.; Uffing, C.; Schnockel, H., *J. Organomet. Chem.* **1998,** *561* (1-2), 203.
[70] Seifert, A.; Linti, G., *Eur. J. Inorg. Chem.* **2007,** (32), 5080.

[71] Jurca, T.; Lummiss, J.; Burchell, T. J.; Gorelsky, S. I.; Richeson, D. S., *J. Am. Chem. Soc.* **2009,** *131* (13), 4608.
[72] Jurca, T.; Korobkov, I.; Yap, G. P. A.; Gorelsky, S. I.; Richeson, D. S., *Inorg. Chem.* **2010,** *49* (22), 10635.
[73] Lo, A. Y. H.; Jurca, T.; Richeson, D. S.; Bryce, D. L., *J. Phys. Chem. Lett.* **2010,** *1* (20), 3078.
[74] Jurca, T.; Dawson, K.; Mallov, I.; Burchell, T.; Yap, G. P. A.; Richeson, D. S., *Dalton Trans.* **2010,** *39* (5), 1266.
[75] Clyburne, J. A. C.; McMullen, N., *Coord. Chem. Rev.* **2000,** *210*, 73.
[76] Zhu, Z. L.; Fischer, R. C.; Ellis, B. D.; Rivard, E.; Merrill, W. A.; Olmstead, M. M.; Power, P. P.; Guo, J. D.; Nagase, S.; Pu, L. H., *Chem. Eur. J.* **2009,** *15* (21), 5263.
[77] Haubrich, S. T.; Power, P. P., *J. Am. Chem. Soc.* **1998,** *120*, 2202.
[78] Marsh, R. E.; Clemente, D. A., *Inorg. Chim. Acta.* **2007,** *360*, 4017.
[79] Niemeyer, M.; Power, P. P., *Angew. Chem. Int. Ed. Engl.* **1998,** *37*, 1277.
[80] Hardman, N. J.; Wright, R. J.; Philips, A. D.; Power, P. P., *Angew. Chem. Int. Ed. Engl.* **2002,** *41*, 2842.
[81] Wright, R. J.; Philips, A. D.; Hardman, N. J.; Power, P. P., *J. Am. Chem. Soc.* **2002,** *124*, 8538.
[82] Wright, R. J.; Philips, A. D.; Hino, S.; Power, P. P., *J. Am. Chem. Soc.* **2005,** *127*, 4794.
[83] Fox, A. R.; Wright, R. J.; Rivard, E.; Power, P. P., *Angew. Chem. Int. Ed. Engl.* **2005,** *44*, 7729.
[84] Su, J.; Li, X.; Crittendon, R. C.; Campana, C. F.; Robinson, G. H., *Organometallics* **1997,** *16*, 4511.
[85] Hardman, N. J.; Wright, R. J.; Philips, A. D.; Power, P. P., *J. Am. Chem. Soc.* **2003,** *125*, 2667.
[86] Zhu, Z. L.; Wright, R. J.; Brown, Z. D.; Fox, A. R.; Phillips, A. D.; Richards, A. F.; Olmstead, M. M.; Power, P. P., *Organometallics* **2009,** *28*, 2512.
[87] Wright, R. J.; Philips, A. D.; Allen, T. L.; Fink, W. H.; Power, P. P., *J. Am. Chem. Soc.* **2003,** *125*, 1694.
[88] Zhu, Z. L.; Wang, X.; Peng, Y.; Lei, H.; Fettinger, J. C.; Rivard, E.; Power, P. P., *Angew. Chem. Int. Ed. Engl.* **2009,** *48*, 2031.
[89] Quillian, B.; Wang, Y.; Wei, P.; Robinson, G. H., *New J. Chem.* **2008,** *32*, 774.
[90] Yang, X.; Quillian, B.; Wang, Y.; Wei, P.; Robinson, G. H., *Organometallics* **2004,** *25*, 5119.
[91] Yang, X.; Wang, Y.; Quillian, B.; Wei, P.; Chen, Z.; Schleyer, P. V. R.; Robinson, G. H., *Organometallics* **2006,** *25*, 925.
[92] Uhl, W.; Keimling, S. U.; Klinkhammer, K. W.; Schwarz, W., *Angew. Chem. Int. Ed. Engl.* **1997,** *36*, 64.
[93] Schnitter, C.; Roesky, H. W.; Ropken, C.; Herbst-Irmer, R.; Schmidt, H. G.; Noltemeyer, M., *Angew. Chem. Int. Ed.* **1998,** *37* (13-14), 1952.
[94] Uhl, W.; Hiller, W.; Layh, M.; Schwarz, W., *Angew. Chem. Int. Ed. Engl.* **1992,** *31* (10), 1364.
[95] Uhl, W.; Jantschak, A., *J. Organomet. Chem.* **1998,** *555* (2), 263.
[96] Schluter, R. D.; Cowley, A. H.; Atwood, D. A.; Jones, R. A.; Atwood, J. L., *J. Coord. Chem.* **1993,** *30* (1), 25.
[97] Uhl, W.; Graupner, R.; Layh, M.; Schutz, U., *J. Organomet. Chem.* **1995,** *493* (1-2), C1.
[98] Uhl, W.; Jantschak, A.; Saak, W.; Kaupp, M.; Wartchow, R., *Organometallics* **1998,** *17* (23), 5009.
[99] Uhl, W.; Benter, M.; Melle, S.; Saak, W.; Frenking, G.; Uddin, J., *Organometallics* **1999,** *18*, 3778.
[100] Uhl, W.; Pohlmann, M.; Wartchow, R., *Angew. Chem. Int. Ed. Engl.* **1998,** *37*, 961.

[101] Uhl, W.; Melle, S., *Z. Anorg. Allg. Chem.* **2000,** *626*, 2043.
[102] Hitchcock, P. B.; Huang, Q.; Lappert, M. F.; Zhou, M., *Dalton Trans.* **2005**, 2988.
[103] Jutzi, P.; Burford, N., *Chem. Rev.* **1999,** *99* (4), 969.
[104] Jutzi, P.; Reumann, G., *J. Chem. Soc., Dalton Trans.* **2000,** (14), 2237.
[105] Dohmeier, C.; Robl, C.; Tacke, M.; Schnockel, H., *Angew. Chem. Int. Ed. Engl.* **1991,** *30*, 564.
[106] Yu, Q.; Purath, A.; Donchev, A.; Schnockel, H., *J. Organomet. Chem.* **1999,** *584*, 94.
[107] Loos, D.; Baum, E.; Ecker, A.; Schnockel, H.; Downs, A. J., *Angew. Chem. Int. Ed. Engl.* **1997,** *36*, 860.
[108] Beachley Jr., O. T.; Churchill, M. R.; Fettinger, J. C.; Pazik, J. C.; Victoriano, L., *J. Am. Chem. Soc.* **1986,** *108*, 4666.
[109] Beachley Jr., O. T.; Blom, R.; Churchill, M. R.; Faegri Jr., K.; Fettinger, J. C.; Pazik, J. C.; Victoriano, L., *Organometallics* **1989,** *8*, 346.
[110] Frasson, E.; Menegus, F.; Panattoni, C., *Nature (London)* **1963,** *199*, 1087.
[111] Beachley Jr., O. T.; Pazik, J. C.; Glassman, T. E.; Churchill, M. R.; Fettinger, J. C.; Blom, R., *Organometallics* **1988,** *7*, 1051.
[112] Dashti-Mommertz, A.; Neumuller, B.; Melle, S.; Haase, D.; Uhl, W., *Z. Anorg. Allg. Chem.* **1999,** *625*, 1828.
[113] Olbrich, F.; Behrens, U., *Z. Kristallogr.* **1997,** *212* (1), 47.
[114] Schmidbaur, H., *Angew. Chem. Int. Ed.* **1985,** *24*, 893.
[115] Schmidbaur, H.; Schier, A., *Organometallics* **2008,** *27*, 2361.
[116] Gorlov, M.; Kloo, L., *Coord. Chem. Rev.* **2008,** *252* (15-17), 1564.
[117] Macdonald, C. L. B.; Cowley, A. H., *J. Am. Chem. Soc.* **1999,** *121* (51), 12113.
[118] Frenking, G.; Rayon, V. M., *Chem. Eur. J.* **2002,** *8*.
[119] Roesky, H. W., Aluminum(I) Chemistry. In *Inorganic Chemistry in Focus II*, Meyer, G.; Naumann, D.; Wesemann, L., Eds. Wiley-VCH: Weinheim, 2005; pp 89.
[120] Roesky, H. W.; Kumar, S. S., *Chem Commun* **2005,** (32), 4027.
[121] Buchin, B.; Gemel, C.; Cadenbach, T.; Schmid, R.; Fischer, A., *Angew. Chem. Int. Ed. Engl.* **2006,** *45*, 1074.
[122] Linti, G.; Seifert, A., *Z. Anorg. Allg. Chem.* **2008,** *634* (8), 1312.
[123] Slattery, J. M.; Higelin, A.; Bayer, T.; Krossing, I., *Angew. Chem. Int. Ed. Engl.* **2010,** *49*, 3228.
[124] Cowley, A. H.; Macdonald, C. L. B.; Silverman, J. S.; Gorden, J. D.; Voigt, A., *Chem Commun* **2001,** (2), 175.
[125] Jones, J. N.; Macdonald, C. L. B.; Gorden, J. D.; Cowley, A. H., *J. Organomet. Chem.* **2003,** *666* (1-2), 3.
[126] Andrews, C. G.; Macdonald, C. L. B., *J. Organomet. Chem.* **2005,** *690*, 5090.
[127] Welsch, S.; Bodensteiner, M.; Dusek, M.; Sierka, M.; Scheer, M., *Chem. Eur. J.* **2010,** *16*, 13041.
[128] Fernandez, I.; Cerpa, E.; Merino, G.; Frenking, G., *Organometallics* **2008,** *27* (6), 1106.
[129] Armstrong, D. R.; Edwards, A. J.; Moncrieff, D.; Paver, M. A.; Raithby, P. R.; Rennie, M. A.; Russell, C. A.; Wright, D. S., *Chem. Commun.* **1995**, 927.
[130] Armstrong, D. R.; Herbstirmer, R.; Kuhn, A.; Moncrieff, D.; Paver, M. A.; Russell, C. A.; Stalke, D.; Steiner, A.; Wright, D. S., *Angew. Chem. Int. Ed. Engl.* **1993,** *32* (12), 1774.
[131] Aldridge, S., *Angew. Chem. Int. Ed.* **2006,** *45* (48), 8097.
[132] Nixon, J. F., *Chem. Rev.* **1988,** *88* (7), 1327.
[133] Nixon, J. F., *Coord. Chem. Rev.* **1995,** *145*, 201.
[134] Dillon, K. B.; Mathey, F.; Nixon, J. F., *Phosphorus: The Carbon Copy: From Organophosphorus to Phospha-organic Chemistry*. John Wiley & Sons: Chichester, 1998; p 366.

[135] Carmichael, D.; Richard, L.; Mathey, F., *J. Chem. Soc., Chem. Commun.* **1994**, 1167.
[136] Schnepf, A.; Stosser, G.; Carmichael, D.; Mathey, F.; Schnockel, H., *Angew. Chem. Int. Ed.* **1999,** *38* (11), 1646.
[137] Chojnacki, J.; Baum, E.; Krossing, I.; Carmichael, D.; Mathey, F.; Schnockel, H., *Z. Anorg. Allg. Chem.* **2001,** *627* (6), 1209.
[138] Francis, M. D.; Hitchcock, P. B.; Nixon, J. F.; Schnockel, H.; Steiner, J., *J. Organomet. Chem.* **2002,** *646*, 191.
[139] Clentsmith, G. K. B.; Cloke, F. G. N.; Francis, M. D.; Green, J. C.; Hitchcock, P. B.; Nixon, J. F.; Suter, J. L.; Vickers, D. M., *J. Chem. Soc., Dalton Trans.* **2000,** *11*, 1715.
[140] Callaghan, C.; Clentsmith, G. K. B.; Cloke, F. G. N.; Hitchcock, P. B.; Nixon, J. F.; Vickers, D. M., *Organometallics* **1999,** *18*, 793.
[141] Cowley, A. H., *Chem. Commun.* **2004**, 2369.
[142] Frenking, G.; Wichmann, K.; Frohlich, N.; Loschen, C.; Lein, M.; Frunzke, J.; Rayon, V. M., *Coord. Chem. Rev.* **2003,** *238*, 55.
[143] Gorden, J. D.; Voigt, A.; Macdonald, C. L. B.; Silverman, J. S.; Cowley, A. H., *J. Am. Chem. Soc.* **2000,** *122* (5), 950.
[144] Gorden, J. D.; Macdonald, C. L. B.; Cowley, A. H., *Chem Commun* **2001,** (01), 75.
[145] Jutzi, P.; Neumann, B.; Reumann, G.; Schebaum, L. O.; Stammler, H. G., *Organometallics* **2001,** *20* (13), 2854.
[146] Gorden, J. D.; Macdonald, C. L. B.; Cowley, A. H., *Main Group Chem.* **2005,** *4*, 33.
[147] Schulz, S.; Kuczkowski, A.; Schuchmann, D.; Florke, U.; Nieger, M., *Organometallics* **2006,** *25* (22), 5487.
[148] Romero, P. E.; Piers, W. E.; Decker, S. A.; Chau, D.; Woo, T. K.; Parvez, M., *Organometallics* **2003,** *22* (6), 1266.
[149] Greiwe, P.; Bethauser, A.; Pritzkow, H.; Kuhler, T.; Jutzi, P.; Siebert, A., *Eur. J. Inorg. Chem.* **2000,** (9), 1927.
[150] Timoshkin, A. Y.; Frenking, G., *J. Am. Chem. Soc.* **2002,** *124* (24), 7240.
[151] Frenking, G.; Frohlich, N., *Chem. Rev.* **2000,** *100* (2), 717.
[152] Frenking, G.; Wichmann, K.; Frohlich, N.; Loschen, C.; Lein, M.; Frunzke, J.; Rayon, V. M., *Coord. Chem. Rev.* **2003,** *238*, 55.
[153] Jones, C.; Stasch, A., The Chemistry of Group 13 Metals in the +1 Oxidation State. In *The Group 13 Metals Aluminium, Gallium, Indium and Thallium. Chemical Patterns and Peculiarities*, Aldridge, S.; Downs, A. J., Eds. John Wiley and Sons: Chichester, UK, 2011; pp 285.
[154] Scholz, M.; Noltemeyer, M.; Roesky, H. W., *Angew. Chem. Int. Ed. Engl.* **1989,** *28* (10), 1383.
[155] Roesky, H. W.; Scholz, M.; Noltemeyer, M.; Edelmann, F. T., *Inorg. Chem.* **1989,** *28* (20), 3829.
[156] Himmel, H.; Manceron, L.; Downs, A. J.; Pullumbi, P., *J. Am. Chem. Soc.* **2002,** *124*, 4448.
[157] Klaui, W.; Berghahn, M.; Rheinwald, G.; Lang, H. R., *Angew. Chem. Int. Ed.* **2000,** *39* (14), 2464.
[158] Macdonald, C. L. B.; Corrente, A. M.; Andrews, C. G.; Taylor, A.; Ellis, B. D., *Chem Commun* **2004,** (2), 250.
[159] Andrews, C. G.; Macdonald, C. L. B., *Angew. Chem. Int. Ed.* **2005,** *44* (45), 7453.
[160] Fernandez, E. J.; Laguna, A.; Lopez-De-Luzuriaga, J. M.; Monge, M.; Montiel, M.; Olmos, M. E.; Perez, J., *Organometallics* **2004,** *23* (4), 774.
[161] Fernandez, E. J.; Laguna, A.; Lopez-De-Luzuriaga, J. M.; Mendizabal, F.; Monge, M.; Olmos, M. E.; Perez, J., *Chem. Eur. J.* **2003,** *9* (2), 456.

Chapter 2: Experimental and Theoretical Insight into the Chelation of In(I) Salts

2.1 - Introduction

Over the past two decades, the chemistry of low oxidation state indium centres has gained immense interest due to their unique and useful chemical properties.[1] The high energy of the 5s orbital makes indium(I) centres prone to oxidative addition/insertion reactions (discussed in Chapter 3), and the comparable stabilities of In(I) and In(III) can allow for reversibility. Furthermore, the amphoteric nature of indium(I) fragments renders them of particular interest for organic C-C bond formation reactions, where activation from both a Lewis acid and a Lewis base are sometimes required.[2] The field, however, is sometimes limited by the complications that arise from its starting materials. Many indium(I) compounds are most effectively generated directly from an indium(I) source, rather than through the reduction of a higher oxidation precursor. As such, the In(I) halides are typically regarded as the best starting material for many preparations, due to their commercial availability and relatively low cost.[1] Complications arise, however, with the starting material's insolubility in common organic solvents. Typically, ligands are used to increase the solubility of salts, however, the indium(I) halides are susceptible to decompose in the presence of many donor molecules (e.g. TMEDA, MeCN, THF, crown ethers, etc., Scheme 2.1)[3-4] and therefore advancement of the field is hindered at its source.

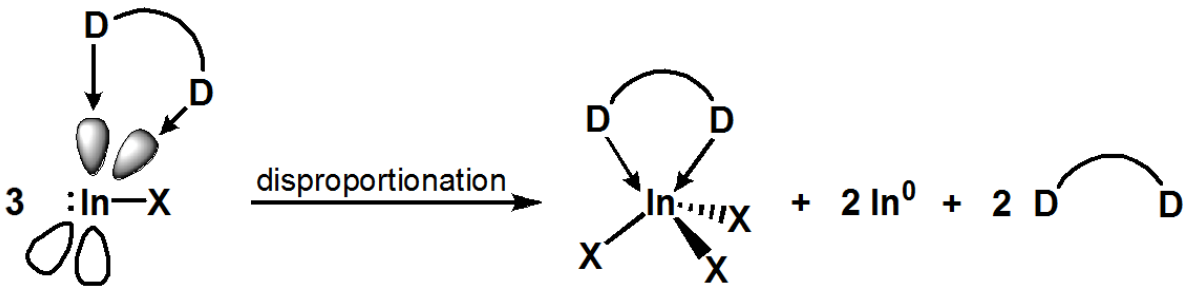

Scheme 2.1: Ligand-mediated disproportionation of In(I)X to In(III)X_3; only one possible decomposition product is illustrated.

Recently, Jones *et al.* found that TMEDA formed a base-stabilized complex with InBr in a 1:1 ratio.[5] Although this was the first example of a base-stabilized In(I) halide, the complex was only stable between -30 and -20˚C. At lower temperatures, the chelated species dimerizes and is insoluble. At higher temperatures, the complex disproportionates to yield the In(II)-In(II) species, In_2Br_4•2TMEDA and indium metal. Analogous attempts to isolate InI with TMEDA resulted in the formation of a mixed valent indium cluster, In_6I_8•4TMEDA,[6] which has an average oxidation state of indium of +1.33. A related compound is the quinuclidine-ligated cluster, $In_5X_8(quin)_4^-$ (X=Cl,[5] Br[7]), also synthesized by Jones, which has an average indium oxidation state of +1.4 (Figure 2.1). While these two clusters are considered to contain low oxidation state indium, it is clear that what species ends up being in solution is not necessarily what was originally intended.

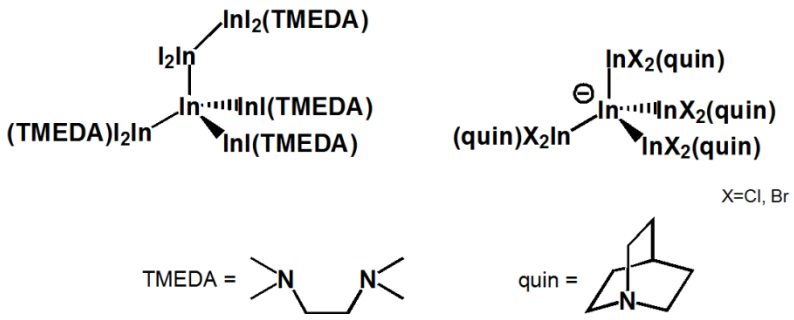

Figure 2.1: Structures of In_6I_8•4TMEDA and $In_5X_8(quin)_4^-$.

Other In(I) sources, which are more soluble than the halides are known, such as InCp,[8-9] $InBF_4$,[10] and InOTf[11], however their widespread use is again inhibited as they are often prepared from an insoluble indium(I) halide. It is worth noting that Macdonald *et al.* have shown that the more stable InOTf salt can be base-stabilized through the use of weak interactions between the indium centre and the donor atoms, as exemplified by the complex [In([18]crown-6)][OTf].[3] Unfortunately, the complexes obtained by incorporation of the indium(I) halides into [18]crown-6 appear to only be stable in the presence of Lewis acids; in fact, their absence causes rapid disproportionation to generate InX_3, which stabilizes the "crowned" InX fragment as a donor-acceptor complex.[12] More recently, our group has investigated the use of polyether ligands for the stabilization of tin(II) centres. Similar to the low oxidation state indium(I) triflate salt, $Sn(OTf)_2$ forms base-stabilized complexes with [18]crown-6, [15]crown-5 and [12]crown-4.[13-14] Not surprisingly, the acyclic polyether analogues of crown ethers (tetraglyme, triglyme, Figure 2.2) are also effective in the complexation of $Sn(OTf)_2$, forming 1:1 adducts. Both tetraglyme (MeO-$(CH_2CH_2O)_4$-Me) and triglyme (MeO-$(CH_2CH_2O)_3$-Me) were found to adopt structures very similar to that of [Sn[18]crown-6][OTf]$_2$ but did not destabilize the non-bonding electrons on Sn to the same extent.

Although cyclic crown ethers cause disproportionation of the indium(I) halides,[3] glymes are less constrained and have more degrees of freedom to adopt a geometry that is lower in energy, and thus provide the possibility of generating complexes that are more stable. Thus, in this chapter, we investigate the use of this strategy – treating a series of indium(I) (and III) salts with a selection of acyclic ether ligands with the goal of increasing solubility, whilst avoiding disproportionation.

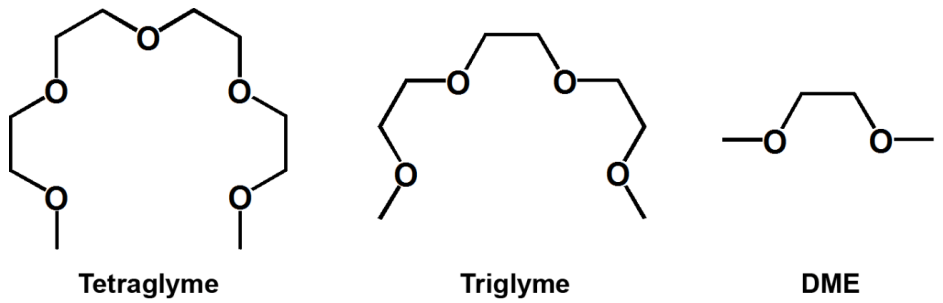

Figure 2.2: Structures of the acyclic polyether ligands used experimentally.

2.2 - Experimental Results and Discussion

Each of the indium(I) halides (X = Cl, Br, I) was treated with various stoichiometric amounts of the podands depicted in Figure 2.2 in order to evaluate changes in salt solubility and stability. Remarkably, the addition of InX to stoichiometric solutions of glymes only resulted in obvious disproportionation in a single case: namely, the reaction of InCl with tetraglyme in toluene. All samples were analyzed by Ion Coupled Plasma Mass Spectrometry at the Great Lakes Institute for Environmental Research (GLIER), located at the University of Windsor. Most samples were measured analyzing ^{115}In. At this mass, however, there is a ^{115}Sn contamination of 0.34%. To account for this, the mass quadrupole filter was set to ^{117}Sn. This isotope was chosen because no other

atoms possess an isotope of this mass. The tin values obtained from analyzing mass 117 were then subtracted from the 115 measurement and the difference obtained directly corresponded to the concentration of indium in the sample. Concurrently, measurements of ^{113}In were also run to compare to the results obtained from mass 115. Similarly as noted above, there is a ^{113}Cd overlap (12.22%) and therefore measurements of ^{111}Cd were recorded and subtracted from the 113 amu measurements. The majority of the results discussed in this chapter are those calculated from the ^{115}In measurements. A few samples (as noted in the supporting information) were calculated from the ^{113}In measurements due to low level of confidence in the 115 amu data. Instrumental drift was very small in the measurements; only 5 isotopes were run for each sample (^{111}Cd, ^{113}In, ^{115}In, ^{117}Sn, ^{205}Tl) and therefore the measurements were done in a short amount of time, limiting the drift.

Control experiments in which no ligand was added to solution give an idea for the solvents' inherent ability to bring the salt into solution (first two rows in Table 2.1). Diethyl ether was found to solubilize the halides more than toluene by a factor of about 2 and is possibly due to the ether's ability to donate into the empty p-orbitals on indium and its ability to interact (albeit weakly) with the halide anions too. Interestingly, the more stable triflate salt was found to be more soluble in the arene solvent, toluene, than in ether. This suggests that the π-donation from the aromatic ring on toluene is more favourable than the donation obtained from the oxygen in Et_2O.[15-16]

Table 2.1: Amounts of InX taken into ether or toluene solution as determined by ICP-MS. All values are given in %. All values reported represent the average of the triplicate trials. Missing values indicate disproportionation occurred. The complete set of data, including standard deviations, can be found in the supporting information.

Ligand	Solvent	Cl	Br	I	OTf	Cl_3
	Toluene	0.013	0.014	0.027	19.666	0.131
	Ether	0.059	0.027	0.056	13.276	46.792
DME[a]	Toluene	0.030	0.069	0.021	42.121	0.969
DME[a]	Ether	0.077	0.028	0.039	42.578	45.759
Triglyme	Toluene	0.256	0.079	0.048	39.182	1.277
Triglyme	Ether	0.172	0.019	0.013	39.350	3.611
Tetraglyme	Toluene		0.175	0.029	45.185	0.293
Tetraglyme	Ether	0.115	0.031	0.011	37.393	1.163
$DME_{(neat)}$			0.185	0.142	40.972	39.255
$Triglyme_{(neat)}$			0.821	0.218	38.336	39.098
$Tetraglyme_{(neat)}$			0.867	0.315	42.993	39.266

[a]Two equivalents of DME was used.

It is worth mentioning that InOTf completely dissolved into all solutions that had glyme present, regardless of chain size, and even dissolved into neat glyme. This observation, however, is in disagreement with the results obtained from ICP-MS, as the highest value reported for InOTf is 45%. While some loss is unavoidable by mechanical

manipulations it is more likely that all the data obtained by ICP-MS are undervalued, and perhaps they are all actually twice as large. Perhaps a better way of viewing these percentages is displayed in Table 2.2, where the values are related to the systems where no glymes were present.

Table 2.2: Percent change of indium salt taken into solution relative to systems without glyme. [t]Referenced to toluene. [e]Referenced to ether.

Ligand	Solvent	Cl	Br	I	OTf	Cl_3
DME[a]	Toluene	+135	+387	-19	+114	+642
DME[a]	Et_2O	+30	+5	-30	+221	-2
Triglyme	Toluene	+1877	+456	+81	+99	+878
Triglyme	Et_2O	+190	-29	-17	+196	-92
Tetraglyme	Toluene		+1134	+11	+130	+125
Tetraglyme	Et_2O	+93	+15	-81	+182	-98
$DME_{(neat)}$			$+1207^t$	$+436^t$	$+108^t$	$+29977^t$
			$+586^e$	$+154^e$	$+209^e$	-16^e
$Triglyme_{(neat)}$			$+5640^t$	$+720^t$	$+95^t$	$+29856^t$
			$+2913^e$	$+289^e$	$+189^e$	-16^e
$Tetraglyme_{(neat)}$			$+6030^t$	$+1087^t$	$+119^t$	$+29985^t$
			$+3117^e$	$+462^e$	$+224^e$	-16^e

[a]Two equivalents of DME were used.

The results from ICP-MS show that the presence of glymes greatly increases the solubility of indium(I) halides, especially when in toluene. This increase in solubility has the potential to improve yields in the synthesis of many indium(I) compounds. It is worthy to note that the presence of glyme also appeared to break up the crystal lattice of

these salts considerably. After 18 hours of stirring, flasks which contained glyme had a very fine suspension of the salt as opposed to those without. This drastic increase in surface area may also lead to improved synthetic routes to indium(I) compounds.

It may come as a surprise that the values obtained for $InCl_3$ are quite low. In ethereal solutions, the salt is less soluble when in the presence of glyme. Given the stronger attraction these ligands have to the formally charged +3 nucleus, it is possible that the ligand has encapsulated the indium centre, which caused a cleavage of one of the In-Cl bonds, which then coordinated to another molecule of $InCl_3$ to generate the salt $[InCl_2\bullet(glyme)][InCl_4]$. This was observed even in neat solutions of glyme, and is therefore not as effective of a solvent as diethyl ether when it comes to dissolving $InCl_3$.

Since only a small percentage of the acyclic polyether ligands end up being bound to the metal centre, attempts to monitor complexation using ^1H NMR spectroscopy proved to be unsuccessful. The vast amounts of uncomplexed ligand flood the spectra, which appear identical to those of the starting materials. Moreover, it is also likely that the complexed ligands are in rapid equilibrium (on the NMR time scale) with the uncomplexed ligands; because of the vast excess of the uncomplexed form, the average signals would be virtually identical to those of the free ligand.

The high boiling points for triglyme (216˚C) and tetraglyme (276˚C) and high melting points (ca. -30˚C) made crystallization of triglyme and tetraglyme adducts difficult. Upon standing for a duration of several weeks, a solution of Et_2O and InCl(tetraglyme) precipitated yellow crystals from solution. Rather than the expected ligated product, however, the crystals were confirmed to be InCl by single crystal X-ray diffraction. While this does not provide direct evident of a tetraglyme-InCl chelate, it

does suggest that there is indeed InCl being taken into solution. However, slow evaporation of the more volatile DME ligand and InCl afforded colourless crystals suitable for X-ray diffraction (Figure 2.3). In contrast to the InCl chelated structure one would anticipate, a DME-chelated $InCl_3$ structure was obtained instead. While no sign of the production of metal was observed during the reaction or crystallization process, it is possible that prolonged exposure to DME results in partial disproportionation and afforded the higher oxidation state species $InCl_3$•DME in the process.

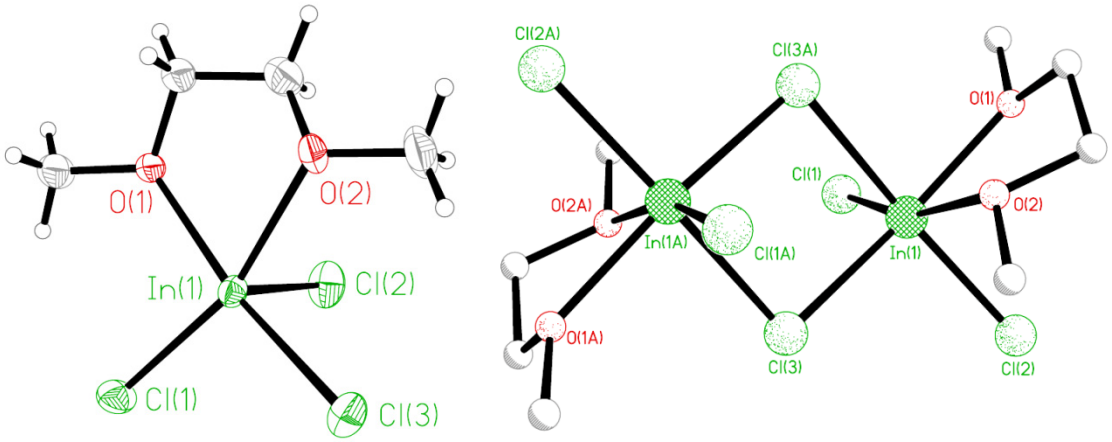

Figure 2.3: Crystal structure of $InCl_3$•DME. Left: Thermal ellipsoid plot (50%) of asymmetric unit. Right: ball and stick model of dimerized species (hydrogen atoms have been omitted for clarity). Selected bond lengths (Å) and angles (˚): In(1)-O(1): 2.242(3); In(1)-O(2): 2.278(3); In(1)-Cl(1): 2.3820(13); In(1)-Cl(2): 2.3845(13); In(1)-Cl(3): 2.5076(13); In(1)-Cl(3A): 2.5678(13); O(1)-In(1)-O(2): 72.62(12).

Although the isolation of an In(III)-chelated species was not the original intent, it provides some insight into the relative stability of these chelate systems. As disproportionation was not evident (no visible signs of metal being produced) with

tetraglyme and InCl (in Et_2O), it suggests that these complexes become increasingly stable with the greater number of oxygen atoms.

2.3 - Theoretical Calculations and Discussion

Given the lack of structural information for these chelated In(I)X species, a series of theoretical calculations were run to gain some insight into these systems. The structure of these complexes is as one would expect on the basis of a "lone pair" being present on the indium centre; the In-X fragment sits nearly perpendicular to the plane of the ligand (see, for example Figure 2.4). Graphical representations of all calculated structures are located in the supporting information. These are all very similar to the structure obtained crystallographically for [In([18]crown-6)][OTf].[3] Calculations were also run on InX•TMEDA so that comparisons between the oxygen-based ligands and the nitrogen-based ligand, which always result in rapid disproportionation at room temperature, could be made.

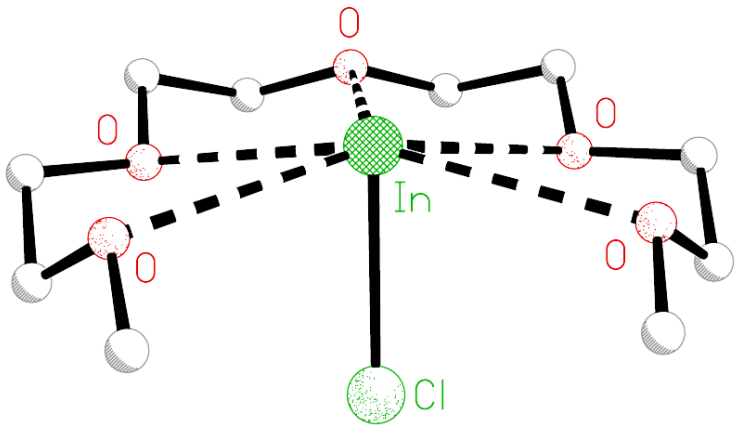

Figure 2.4: Optimized structure of InCl•Tetraglyme.

The stability of these In(I)X complexes is proposed to be directly correlated to the energy of the 5s orbital on indium.[14] Strong interactions between ligands and In(I) centres destabilize the "lone pair" of electrons and promote oxidation. Instead, ligands that have weak interactions with the metal centre appear to be more suitable for stabilization as they do not perturb the 5s electrons greatly.

Natural Bond Order analysis was done on optimized structures of InX•TMEDA and the InX•glyme complexes to gain insight into the electronic stability of the systems and compare the various energies of the systems (Table 2.3). Expectedly, the "lone pair" energy for the TMEDA complexes is higher in energy than the analogous DME complexes. This is consistent with the experimental observations, as disproportionation was not observed for any of the DME systems, and the heavier indium(I) halides were stable in neat DME solutions. However, examining only the "lone pair" energies suggests that complexation of tetraglyme should result in disproportionation. This, however, was only found to be true for InCl in solutions of toluene. Therefore, there must be other factors which dictate the stability, such as the HOMO-LUMO gap. While some "lone pair" energies for the glyme complexes are higher than some of the TMEDA complexes, the HOMO-LUMO gaps for the TMEDA complexes are considerably smaller and may make those complexes more reactive.

Table 2.3: Energies of optimized structures of InX•TMEDA and InX•Glymes.

Ligand	X	NBO Lone Pair Energy (eV)	SCF HOMO-LUMO gap (eV)	In-X Change (%)	NBO Wiberg Bond Index[#]
TMEDA	Cl	-7.01	4.83	+4.88	0.39 (-31)
	Br	-7.13	4.74	+4.50	0.42 (-26)
	I	-7.25	4.56	+5.05	0.50 (-26)
	OTf	-7.21	5.15	-4.06	0.13 (+21)
DME	Cl	-7.51	4.98	+5.86	0.42 (-25)
	Br	-7.56	4.80	+6.02	0.44 (-23)
	I	-7.70	4.55	+6.50	0.51 (-23)
	OTf	-7.57	5.66	+0.87	0.10 (-9.4)
Diglyme	Cl	-7.01	5.16	+5.80	0.35 (-37)
	Br	-7.09	5.04	+5.94	0.37 (-34)
	I	-7.27	4.63	+6.58	0.45 (-33)
	OTf	-7.03	5.57	-3.26	0.11 (-0.90)
Triglyme	Cl	-7.11	5.41	+3.80	0.35 (-38)
	Br	-7.17	5.28	+3.75	0.37 (-35)
	I	-7.32	5.07	+4.16	0.45 (-34)
	OTf	-7.21	5.82	-4.79	0.11 (+1.9)
Tetraglyme	Cl	-6.77	5.17	+6.19	0.32 (-43)
	Br	-6.89	5.06	+6.31	0.35 (-38)
	I	-7.04	4.88	+7.19	0.43 (-36)
	OTf	-6.85	5.55	-3.41	0.10 (-8.7)

[#]Number in brackets indicates the % change from WBI of optimized In-X structures: InCl: 0.56; InBr: 0.56; InI: 0.67; InOTf: 0.11.

The % elongation of the In-X bond upon complexation reveals a general trend of increasing bond length going from Cl to I. These values reflect how strongly the ligand

chelates to the metal centre from population of the In-X σ* orbital. InI, which contains the weakest of the In-X bonds, shows a more pronounced elongation than the rest of the halides and displays an increase of over 7% when complexed with tetraglyme. Naturally, with the increased number of donor atoms going from TMEDA to tetraglyme, population of the σ* antibonding orbital will be greater and result in longer In-X bonds. InOTf, however, is a more stable salt experimentally and the calculations suggest that it does indeed behave very differently than the halides. For the triflate salt, calculations show that the complexation often results in a shorter In-O distance. This, however, is perhaps an unrealistic depiction of how InOTf behaves in solution. In donor solvents such as MeCN, In^{+} and ^{-}OTf dissociate completely and therefore these calculations may not give as accurate of a result compared to the halides, which retain their covalent character. The computational results might be more indicative of the behaviour of the complex in non-polar, non-donor solvents.

Examination of the Wiberg Bond Index (WBI) provides insight into the covalent nature of the In-X bond. It should be noted that the WBI will always be a positive number, and as a result, differentiation between bonding and antibonding is not possible. The results obtained for InI seem to contradict the discussion above, regarding the bond strength. One thing to keep in mind is that the degree of covalency does not necessarily represent bond strength. Although InX (X=Cl, Br, I) all possess salt-like structures in the solid state, the ionic bonding character decreases with the heavier halides: InCl (26–28%); InBr (19–24%); InI (10–19%).[17] The WBI for the In-I bond indicates that it is the most covalent in nature out of the halides in the series. This higher WBI is consistent with the expectations of Hard-Soft Acid Base (HSAB) theory.[18-20] Comparing TMEDA to

DME, there is little change in the indices of the bond, however a decrease in the covalent character of the bond is observed for all the halides (again, complications can arise, in calculations containing the triflate anion as the dissociation cannot be measured properly).

Another way to measure how tightly these ligands bind to indium is to look at the snapping energies of these systems. Snapping energies are calculated by taking the optimized structures of InX•glyme and running single point calculation on the InX fragment and the glyme separately. Relaxation and decomplexation energies are then calculated by optimizing the "snapped" geometries of InX and glyme (Figure 2.5).

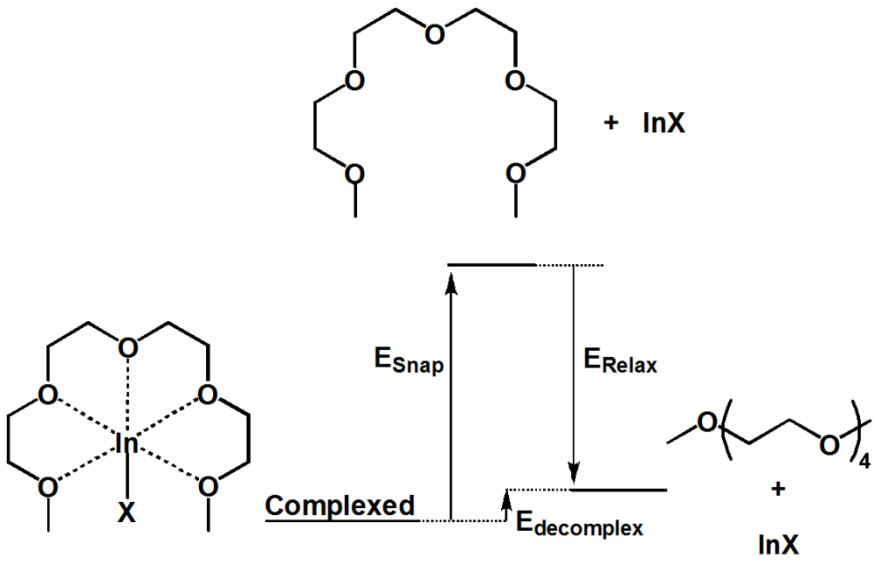

Figure 2.5: Snapping profile of InX with tetraglyme.

Table 2.4: Snapping, relaxing and decomplexation energies for InX•TMEDA and InX•Glyme complexes. All energies are given in kJ/mol.

Ligand	X	Snapping	Relax	Decomplex
TMEDA	Cl	94.90	-18.36	76.54
	Br	82.40	-15.95	66.45
	I	82.75	-16.99	65.76
	OTf	112.6	-50.11	62.47
1DME	Cl	55.94	-11.44	44.50
	Br	49.25	-10.88	38.37
	I	50.03	-10.87	39.16
	OTf	59.32	-15.36	43.96
2DME	Cl	71.39	-25.01	46.39
	Br	59.71	-24.70	35.01
	I	56.57	-21.90	34.66
	OTf	97.80	-61.29	36.51
Diglyme	Cl	75.56	-29.33	46.23
	Br	66.13	-29.09	37.04
	I	69.43	-31.06	38.37
	OTf	90.41	-52.42	37.99
Triglyme	Cl	73.72	-27.91	45.81
	Br	64.05	-25.01	39.04
	I	67.53	-25.68	41.85
	OTf	110.9	-59.40	51.48
Tetraglyme	Cl	72.47	-31.43	41.04
	Br	61.73	-29.62	32.11
	I	67.84	-31.80	36.03
	OTf	114.2	-68.44	45.79

Expectedly, the snapping energy for InOTf is the largest within all of the ligand sets because the contact between In and OTf is highly ionic in nature and therefore the indium has a higher affinity for the chelating ligands.

The snapping energy for TMEDA is significantly larger than for DME. This illustrates that the nitrogen-based ligand binds much more strongly to the indium centre than the oxygen-based ligand, and is a testament to nitrogen being a better electron donor than oxygen. Additionally, more energy is released by the relaxation of TMEDA than DME, which is most likely a consequence of the stronger "lone pair" repulsion on the nitrogen-based ligand. Expectedly, more energy is released when the longer polyether ligands are allowed to relax into a linear, trans-extended chain.

2.4 - Conclusions

The addition of acyclic polyether ligands (glymes) to solutions of indium(I) halides was found to increase the solubility of the salt and only resulted in disproportionation in a single case. With this, reactions that have previously not worked in the past may overcome solubility issues and now proceed. It is also worth noting that the presence of glymes broke up the crystal lattice of the InX salt, creating a fine suspension, and has the potential to increase overall kinetics due to the increased surface area and dissolved starting material. Reactions that would not benefit from the presence of glyme would be those that would require Lewis acid activation, as the glymes would compete for ligation.

Although the calculations performed reveal that complexation of InX with TMEDA doesn't raise the energy of the 5s orbital significantly, calculations of the snapping energies in these systems show that it forms a much stronger complex, and is more prone to cause disproportionation with metal centres.

2.5 - Experimental

2.5.1 General Methods

All manipulations were carried out using standard Schlenk techniques. Solvents were dried using a series of Grubbs'-type columns and degassed prior to use.[21] Samples were analyzed by ICP-MS at GLIER. Each sample was spiked with a 2 ppb thallium standard. The samples then were run on an X7-X1053 Thermoelemental ICP-MS. A complete dilution scheme of each sample is located in this chapter's supporting information.

2.5.2 General Synthetic Procedure for Glyme/Solvent InX

In a typical experiment, InCl (80 mg, 0.53 mmol), InBr (104 mg, 0.53 mmol), InI (129 mg, 0.53 mmol), InOTf (140 mg, 0.53 mmol) or $InCl_3$ (118 mg, 0.53 mmol) was added to a Schlenk flask, to which gylme/toluene (8 mL, 0.067M, 0.53 mmol), glyme/Et_2O(8 mL, 0.53 mmol), toluene (8 mL) or Et_2O (8 mL) was added. All samples were done in triplicate and the flasks were allowed to stir for 18 hours. Solutions were then centrifuged and, in a glove bag filled with argon gas, the liquid was decanted into vials. All volatile components were removed by evaporation and to the resulting oils, HNO_3 (10 mL, 2 M) was added and mixed thoroughly. The samples were diluted to the ppb range and then analyzed by ICP-MS.

2.5.4 General Synthetic Procedure for neat glyme InX

InBr, InI, InOTf and $InCl_3$ were added to neat glyme solutions (InCl resulted in disproportionation). To a flask of InBr (52 mg), InI (65 mg), InOTf (70 mg) or $InCl_3$ (59

mg), tetraglyme (4 mL, 0.018 mol), triglyme (3.3 mL, 0.018 mol) or DME (3.8 mL, 0.036 mol) was added. All samples were done in triplicate and the flasks were allowed to stir for 18 hours. Solutions were then centrifuged and, in a glove bag filled with argon gas, the liquid was decanted into vials. Due to the high boiling point of triglyme and tetraglyme, the neat samples were placed in a vacuum oven for 7 days at 160˚C and reduced pressure to remove the ligand. To the resulting oils, HNO_3 (10 mL, 2 M) was added and mixed thoroughly. The samples were diluted to the ppb range and sent away to be analyzed by ICP-MS.

2.5.5 Crystallography Methods

Crystals for investigation were covered in Nujol®, mounted into a goniometer head, then rapidly cooled under a stream of cold N_2 of the low-temperature apparatus (Oxford Cryostream Controller) attached to the diffractometer. The data were collected using the SMART software suite on a Bruker APEX CCD diffractometer using a graphite monochromator with MoKα radiation (λ=0.71073 Å). A hemisphere of data was collected using 10 seconds/frame at 173 K. SAINT-Plus[22] software was used for data reductions and SADABS[23] was used for absorption corrections (semi-empirical from equivalents). Structures were solved and refined using the SHELX[24] suite of programs as implemented in WinGX.[25]

2.5.6 Crystallographic Data for $InCl_3$•DME

Empirical formula	$C_4H_{10}Cl_3InO_2$	
Formula weight	311.29	
Temperature	150(2) K	
Wavelength	0.71073 Å	
Crystal system	Monoclinic	
Space group	$P2_1/n$	
Unit cell dimensions	a = 8.0572(13) Å	α= 90°.
	b = 12.395(2) Å	β= 94.861(2)°.
	c = 10.1547(17) Å	γ = 90°.
Volume	1010.5(3) $Å^3$	
Z	4	
Density (calculated)	2.046 Mg/m^3	
Absorption coefficient	3.080 mm^{-1}	
F(000)	600	
Theta range for data collection	2.60 to 28.45°.	
Index ranges	$-10 \leq h \leq 10$	
	$-16 \leq k \leq 16$	
	$-13 \leq l \leq 11$	
Reflections collected	8622	
Independent reflections	2390 [R(int) = 0.0547]	
Completeness to theta = 28.45°	93.5 %	
Refinement method	Full-matrix least-squares on F^2	
Data / restraints / parameters	2390 / 0 / 91	
Goodness-of-fit on F^2	0.907	
Final R indices [I>2sigma(I)]	R1 = 0.0394, wR2 = 0.0846	
R indices (all data)	R1 = 0.0532, wR2 = 0.0915	
Largest diff. peak and hole	1.071 and -0.699 $e.Å^{-3}$	

2.5.7 Computational Methods

All density functional theory (DFT) calculations were performed using the B3PW91 method[26-28] using the Gaussian 09[29] suites using the SHARCNET high-performance computing network (www.sharcnet.ca). Where applicable, the Stuttgart group (SDD) effective core potentials (ECP) and corresponding basis sets were used for indium and the halides, and the 6-31+G(d) basis set was used for all lighter atoms. Natural bond order (NBO) analyses[30] to determine orbital contributions, Wiberg Bond Indices and HOMO/LUMO energies were obtained using the routine included in the Gaussian distributions.[31] All stationary points were confirmed to be minima exhibiting no imaginary frequencies. Depictions of optimized geometries can be found in the supporting information. Output files from the optimizations are included in the digital media that accompanies this document.

2.6 Supporting Information

2.6.1 Pictures of Optimized Structures

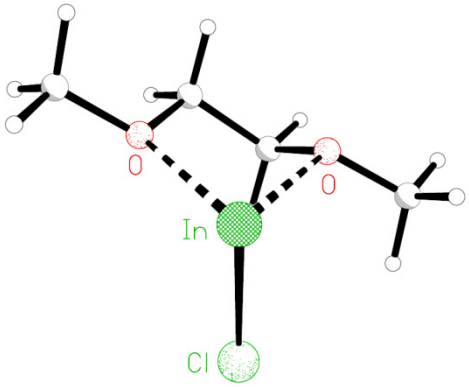

InCl•1DME

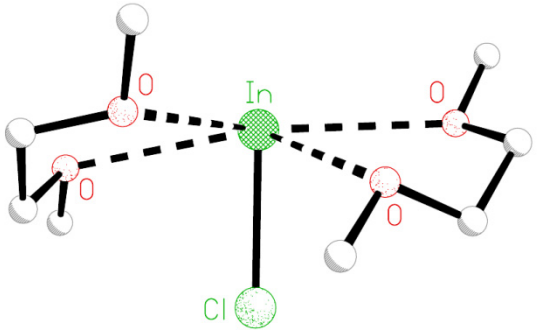

InCl•2DME

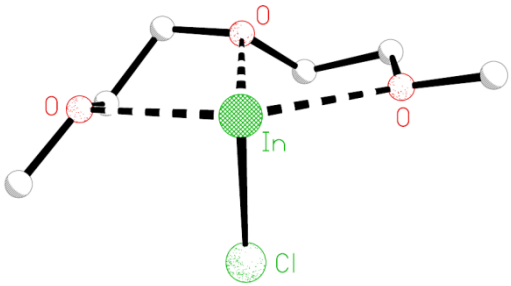

InCl•Diglyme

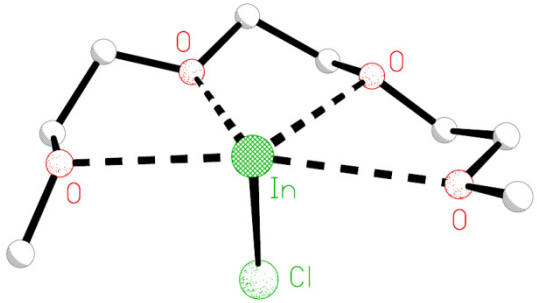

InCl•Triglyme

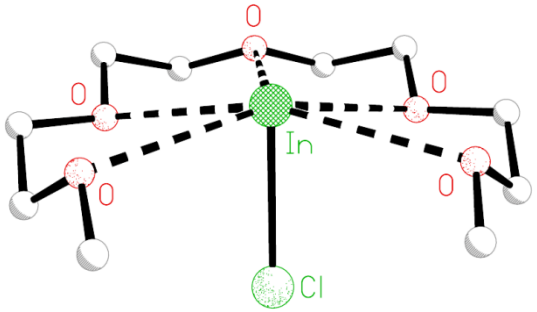

InCl•Tetraglyme

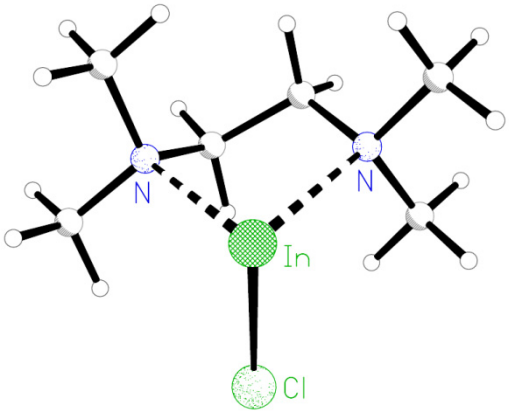

InCl•TMEDA

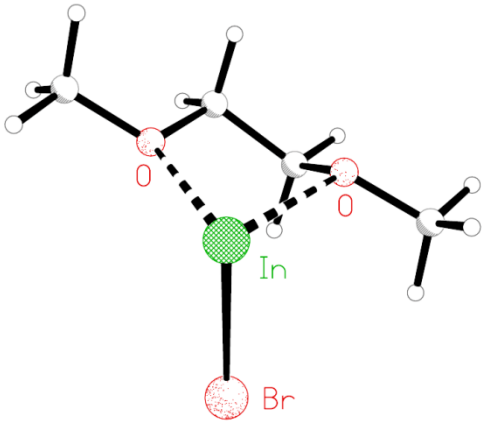

InBr•1DME

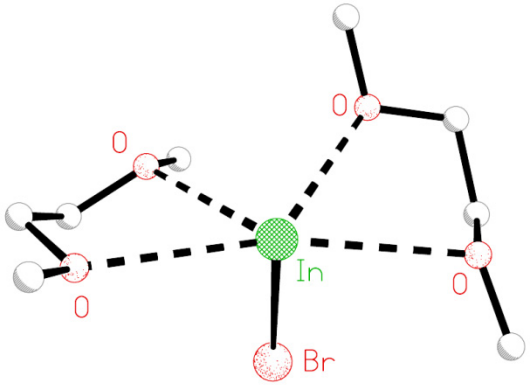

InBr•2DME

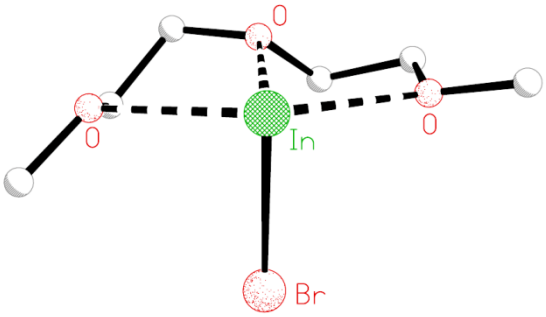

InBr•Diglyme

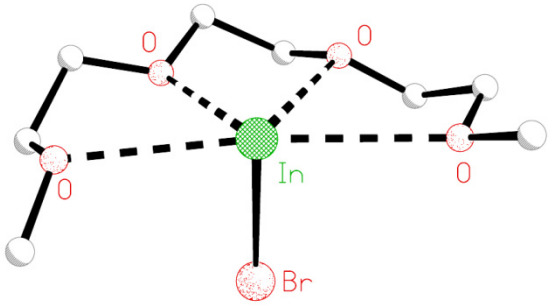

InBr•Triglyme

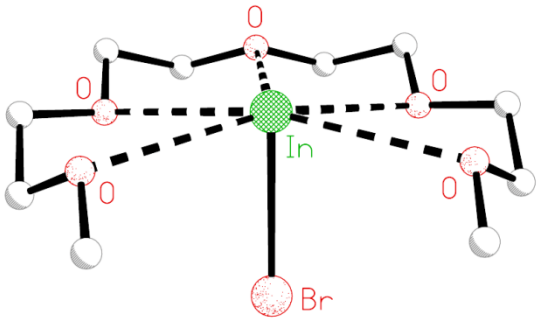

InBr•Tetraglyme

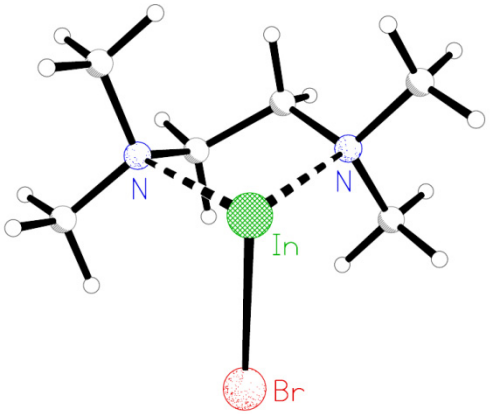

InBr•TMEDA

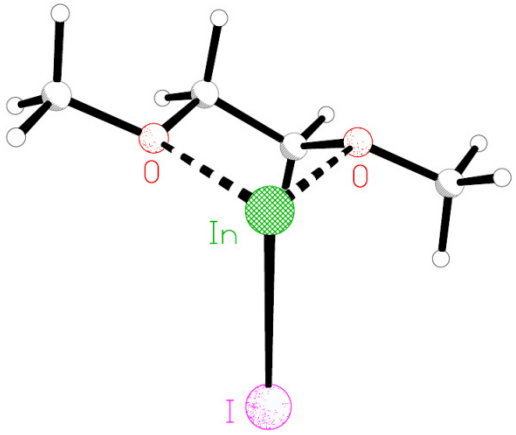

InI•1DME

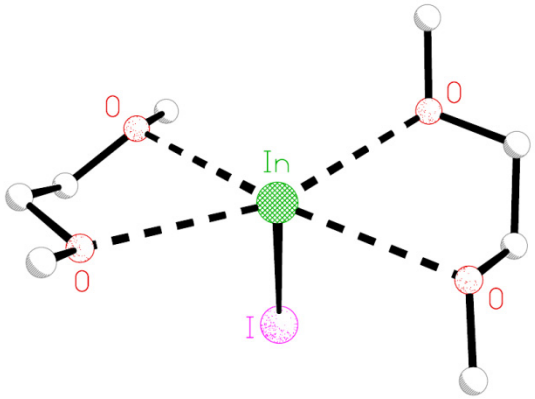

InI•2DME

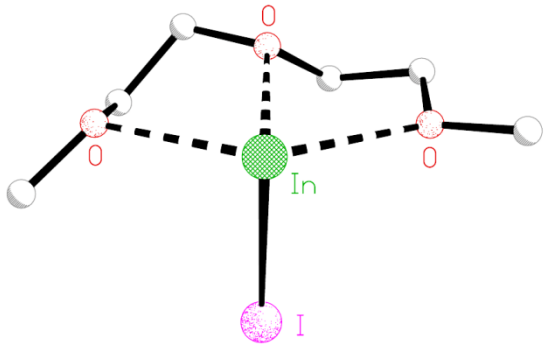

InI•Diglyme

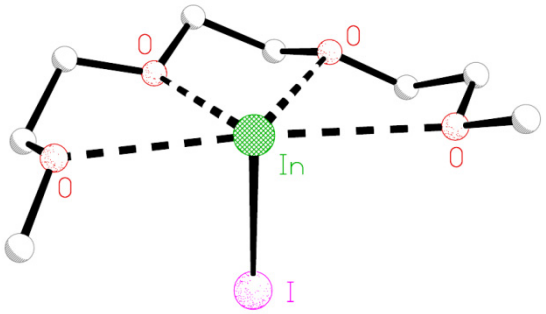

InI•Triglyme

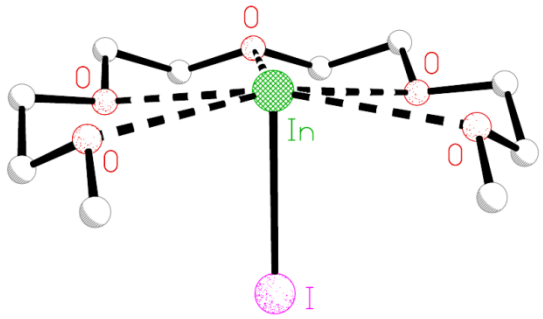

InI•Tetraglyme

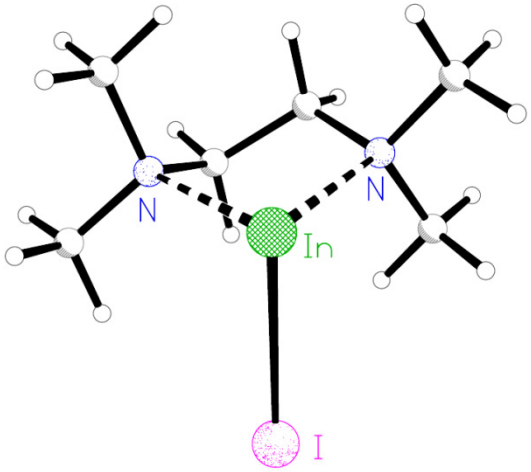

InI•TMEDA

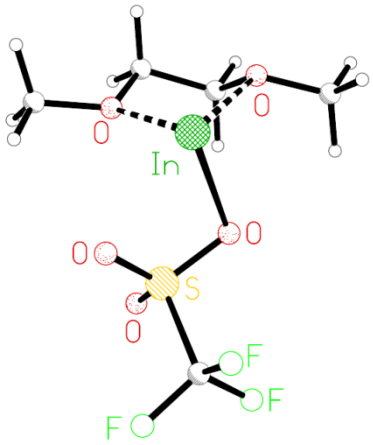

InOTf•1DME

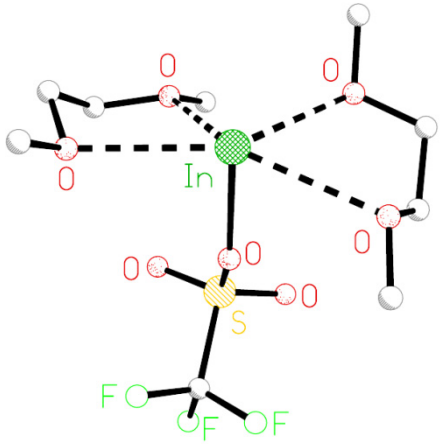

InOTf•2DME

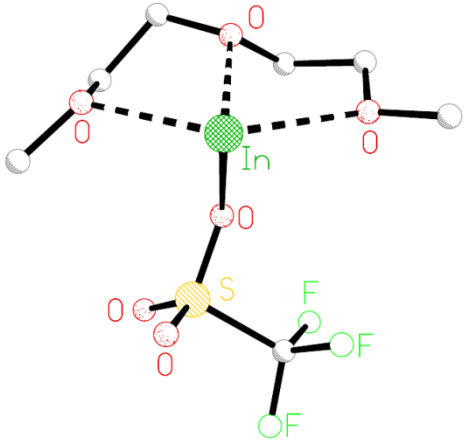

InOTf•Diglyme

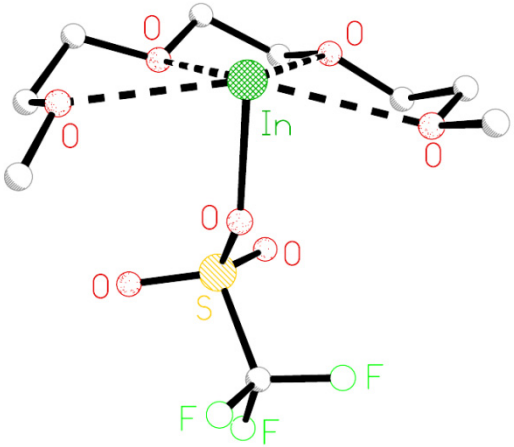

InOTf•Triglyme

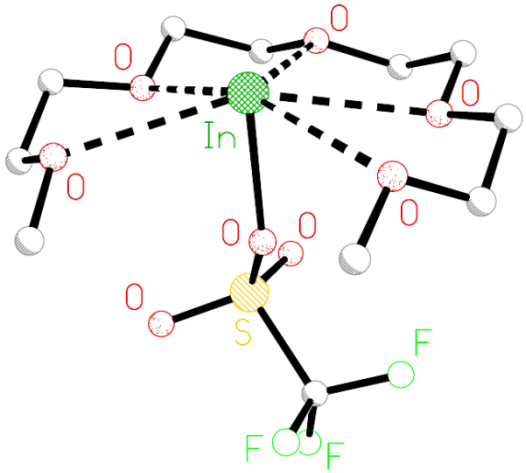

InOTf•Tetraglyme

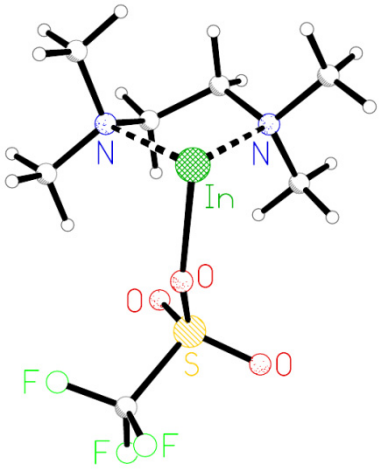

InOTf•TMEDA

2.6.2 Summary of Output Files from Optimized Structures

InX•TMEDA

X	Energy (H)	Complexation (KJ/mol)	HOMO (eV)	LUMO (eV)	Band Gap (eV)	In-X Length (Å)	In-X Change (%)	LP Energy (eV)	5s-Orbital Occupancy on In (e^-)	WBI	WBI Change (%)	s-character of "Lone Pair" (%)	Natural Charge on In (au)
Cl	-809.5	-76.54	-5.29	-0.45	4.83	2.59	4.88	-7.01	1.99	0.39	-30.70	94.64	0.65
Br	-362.8	-66.45	-5.28	-0.55	4.74	2.73	4.50	-7.13	1.99	0.42	-25.62	95.02	0.64
I	-360.8	-65.76	-5.24	-0.68	4.56	2.98	5.05	-7.25	1.99	0.50	-25.23	95.56	0.58
OTf	-1310	-62.47	-5.96	-0.81	5.15	2.26	-4.06	-7.21	1.97	0.13	+21.26	94.91	0.80

InX•DME

X	Energy (H)	Complexation (KJ/mol)	HOMO (eV)	LUMO (eV)	Band Gap (eV)	In-X Length (Å)	In-X Change (%)	LP Energy (eV)	5s-orbital occupancy on In (e^-)	WBI	WBI Change (%)	s-character of "Lone Pair" (%)	Natural Charge on In (au)
Cl	-770.7	-44.50	-5.78	-0.79	4.98	2.61	5.86	-7.51	1.99	0.42	-25.20	96.86	0.69
Br	-324.0	-38.37	-5.73	-0.93	4.80	2.77	6.02	-7.56	1.99	0.44	-22.89	97.15	0.69
I	-322.0	-39.16	-5.61	-1.06	4.55	3.02	6.50	-7.70	1.99	0.51	-23.43	97.63	0.64
OTf	-1272	-43.96	-6.46	-0.80	5.66	2.38	0.87	-7.57	1.98	0.10	-9.37	97.16	0.83

InX•2DME

X	Energy (H)	Complexation (KJ/mol)	HOMO (eV)	LUMO (eV)	Band Gap (eV)	In-X Length (Å)	In-X Change (%)	LP Energy (eV)	5s-orbital occupancy on In (e^-)	WBI	WBI Change (%)	s-character of "Lone Pair" (%)	Natural Charge on In (au)
Cl	-1079	-46.39	-5.31	-0.15	5.16	2.61	5.86	-7.01	1.98	0.33	-41.79	96.65	0.71
Br	-632.6	-35.01	-5.28	-0.24	5.03	2.77	6.02	-7.09	1.98	0.35	-37.46	97.13	0.70
I	-630.6	-34.66	-5.22	-0.58	4.63	3.02	6.50	-7.27	1.99	0.44	-35.19	97.83	0.64
OTf	-1580	-36.51	-6.00	-0.43	5.57	2.25	-4.54	-7.03	1.97	0.11	-4.23	98.89	0.83

InX•Diglyme

X	Energy (H)	Complexation (KJ/mol)	HOMO (eV)	LUMO (eV)	Band Gap (eV)	In-X Length (Å)	In-X Change %	LP Energy (eV)	5s-orbital occupancy on In (e^-)	WBI	WBI Change (%)	s-character of "Lone Pair" (%)	Natural Charge on In (au)
Cl	-924.4	-46.23	-5.47	-0.06	5.41	2.61	5.80	-7.11	1.98	0.35	-37.43	97.13	0.71
Br	-477.7	-37.04	-5.44	-0.16	5.28	2.77	5.94	-7.17	1.99	0.37	-33.96	96.07	0.69
I	-475.8	-38.37	-5.33	-0.26	5.07	3.03	6.58	-7.32	1.86	0.45	-33.51	83.81	0.65
OTf	-1425	-37.99	-6.21	-0.39	5.82	2.28	-3.26	-7.21	1.97	0.11	-0.90	96.41	0.83

InX•Triglyme

X	Energy (H)	Complexation (KJ/mol)	HOMO (eV)	LUMO (eV)	Band Gap (eV)	In-X Length (Å)	In-X Change (%)	LP Energy (eV)	5s-orbital occupancy on In (e^-)	WBI	WBI Change (%)	s-character of "Lone Pair" (%)	Natural Charge on In (au)
Cl	-1078	-45.81	-5.11	0.06	5.17	2.56	3.80	-6.77	1.95	0.35	-38.23	93.22	0.69
Br	-631.4	-39.04	-5.05	-0.06	5.06	2.71	3.75	-6.89	1.95	0.37	-34.70	93.98	0.68
I	-629.5	-41.85	-5.12	-0.17	4.88	2.96	4.16	-7.04	1.96	0.45	-33.61	94.29	0.63
OTf	-1579	-51.48	-5.88	-0.33	5.55	2.24	-4.79	-6.85	1.96	0.11	1.89	96.23	0.82

InX•Tetraglyme

X	Energy (H)	Complexation (KJ/mol)	HOMO (eV)	LUMO (eV)	Band Gap (eV)	In-X Length (Å)	In-X Change (%)	LP Energy (eV)	5s-orbital occupancy on In (e^-)	WBI	WBI Change (%)	s-character of "Lone Pair" (%)	Natural Charge on In (au)
Cl	-1232	-41.04	-5.04	0.31	5.34	2.62	6.19	-6.72	1.98	0.322	-42.89	97.61	0.69
Br	-785.1	-32.11	-5.00	0.20	5.20	2.78	6.31	-6.79	1.98	0.350	-38.08	97.55	0.67
I	-783.2	-36.03	-4.92	0.11	5.03	3.04	7.19	-6.92	1.98	0.430	-36.01	97.02	0.61
OTf	-1733	-45.79	-5.71	0.00081	5.71	2.27	-3.41	-6.73	1.94	0.101	-8.74	97.87	0.80

2.6.3 ICP-MS Dilution Scheme and Results

No Ligand

X	Solvent	Initial Mass (mg)	Dilution Factor 1	Dilution Factor 2	ICP-MS Raw Data (ppb)	Final Mass (mg)	% Uptake	Avg (%)	Stdev
Cl	Toluene	73	200	9.35	0.47990171	0.0095	0.0131		
Cl	Toluene	75	200	7.40	0.588120043	0.0092	0.0123		
Cl	Toluene	75	200	7.83	0.609035192	0.0101	0.0135	0.0130	0.0006
Br	Toluene	108	200	9.33	0.592341348	0.0117	0.0109		
Br	Toluene	103	200	7.76	0.507741431	0.0084	0.0081		
Br	Toluene	102	200	22.42	0.502625164	0.0239	0.0235	0.0141	0.0082
I	Toluene	125	200	20.21	0.540808932	0.0232	0.0186		
I	Toluene	123	200	19.93	0.43935043	0.0186	0.0151		
I	Toluene	123	200	20.04	1.328534224	0.0565	0.0460	0.0265	0.0169
OTf	Toluene	137	333	20.60	367.7986253	26.8136	19.5719		
OTf	Toluene	134	333	20.06	371.0959069	26.3495	19.6638		
OTf	Toluene	130	333	20.35	356.7248816	25.6924	19.7634	19.6664	0.0958
Cl_3	Toluene	124	1000	0.5089	0.731179933	0.1585	0.1278		
Cl_3	Toluene	123	1000	0.5095	0.739399719	0.1611	0.1309		
Cl_3	Toluene	116	1000	0.51	0.714332571	0.1540	0.1328	0.1305	0.0025
Cl	Et_2O	87	500	19.60	0.45541632	0.0474	0.0545		
Cl	Et_2O	82	500	20.48	0.197911116	0.0215	0.0262		
Cl	Et_2O	78	500	21.08	0.676167686	0.0757	0.0970	0.0592	0.0356
Br	Et_2O	103	500	20.38	0.220998804	0.0239	0.0232		
Br	Et_2O	103	500	19.84	0.397017439	0.0418	0.0406		
Br	Et_2O	99	500	20.48	0.155200041	0.0169	0.0170	0.0270	0.0122
I	Et_2O	132	500	20.44	1.16807011	0.1268	0.0960		
I	Et_2O	127	500	19.54	0.535810048	0.0556	0.0438		
$^{\#}$I	Et_2O	120	500	19.73	0.324230114	0.0340	0.0283	0.0560	0.0355
$^{\#}$OTf	Et_2O	145	1000	20.42	82.15973488	17.8160	12.2869		
$^{\#}$OTf	Et_2O	138	1000	20.78	85.73517071	18.9170	13.7080		
$^{\#}$OTf	Et_2O	134	1000	19.57	89.18068339	18.5356	13.8325	13.2758	0.8587
Cl_3	Et_2O	118	100000	20.54	2.236515477	48.7776	41.3370		
Cl_3	Et_2O	113	100000	20.14	2.718551717	58.1254	51.4384		
Cl_3	Et_2O	111	100000	19.91	2.499596208	52.8375	47.6013	46.7922	5.0991

$^{\#}$Analyzed from ^{113}In isotope

DME

X	Solvent	Initial Mass (mg)	Dilution Factor 1	Dilution Factor 2	ICP-MS Raw Data (ppb)	Final Mass (mg)	% Uptake	Avg (%)	Stdev
Cl	Toluene	79	1000	20.11	0.063690032	0.0136	0.0172		
Cl	Toluene	73	1000	19.96	0.08213385	0.0174	0.0238		
Cl	Toluene	72	1000	19.87	0.170970281	0.0361	0.0501	0.0304	0.0174
Br	Toluene	104	1000	19.69	0.495208064	0.1035	0.0996		
Br	Toluene	99	1000	20.31	0.220556058	0.0476	0.0480		
Br	Toluene	97	1000	19.99	0.270560215	0.0574	0.0592	0.0689	0.0271
I	Toluene	126	1000	19.80	0.091986125	0.0193	0.0153		
I	Toluene	126	1000	20.84	0.183904932	0.0407	0.0323		
I	Toluene	124	1000	20.90	0.092552306	0.0205	0.0166	0.0214	0.0095
OTf	Toluene	145	100000	20.00	3.167985622	67.2720	46.3945		
OTf	Toluene	138	100000	19.69	2.803338196	58.6118	42.4723		
OTf	Toluene	133	100000	19.74	2.379551254	49.8700	37.4962	42.1210	4.4595
Cl_3	Toluene	117	1000	19.05	5.369030462	1.0860	0.9282		
Cl_3	Toluene	117	1000	18.56	5.926317449	1.1680	0.9983		
Cl_3	Toluene	112	1000	19.33	5.34123691	1.0964	0.9790	0.9685	0.0362
Cl	Et_2O	76	1000	20.02	0.127814471	0.0272	0.0358		
Cl	Et_2O	74	1000	19.62	0.262209704	0.0546	0.0738		
Cl	Et_2O	73	1000	20.44	0.411522163	0.0893	0.1223	0.0773	0.0434
Br	Et_2O	104	1000	21.05	0.147682402	0.0330	0.0317		
Br	Et_2O	103	1000	20.68	0.126646527	0.0278	0.0270		
Br	Et_2O	98	1000	19.59	0.123566545	0.0257	0.0262	0.0283	0.0030
I	Et_2O	129	1000	20.34	0.108963824	0.0235	0.0182		
I	Et_2O	123	1000	19.70	0.505855818	0.1058	0.0860		
I	Et_2O	122	1000	19.77	0.077713913	0.0163	0.0134	0.0392	0.0406
OTf	Et_2O	140	100000	20.42	2.827626143	61.3033	43.7880		
OTf	Et_2O	139	100000	19.73	2.855015322	59.8176	43.0343		
OTf	Et_2O	138	100000	20.14	2.640007326	56.4576	40.9113	42.5779	1.4917
Cl_3	Et_2O	123	100000	18.94	2.221798186	44.6788	36.3242		
Cl_3	Et_2O	117	100000	19.67	2.746556404	57.3585	49.0244		
$^{\#}Cl_3$	Et_2O	113	100000	9.47	5.838407776	58.6793	51.9286	45.7591	8.2988

$^{\#}$Analyzed from ^{113}In isotope

Triglyme

X	Solvent	Initial Mass (mg)	Dilution Factor 1	Dilution Factor 2	ICP-MS Raw Data (ppb)	Final Mass (mg)	% Uptake	Avg (%)	Stdev
Cl	Toluene	80	1000	19.79	0.900344638	0.1892	0.2365		
Cl	Toluene	78	1000	20.51	0.990720669	0.2158	0.2766		
Cl	Toluene	74	1000	20.13	0.884210956	0.1890	0.2554	0.2562	0.0201
Br	Toluene	105	1000	20.20	0.419674946	0.0900	0.0857		
Br	Toluene	102	1000	20.22	0.485498991	0.1042	0.1022		
Br	Toluene	101	1000	19.71	0.231187717	0.0484	0.0479	0.0786	0.0278
I	Toluene	129	1000	20.22	0.26816622	0.0576	0.0446		
I	Toluene	128	1000	20.20	0.244717974	0.0525	0.0410		
I	Toluene	127	1000	20.25	0.345167141	0.0742	0.0584	0.0480	0.0092
OTf	Toluene	141	100000	19.74	2.833635104	59.3967	42.1253		
OTf	Toluene	132	100000	19.68	2.314364448	48.3694	36.6435		
OTf	Toluene	132	100000	19.71	2.446306166	51.1859	38.7772	39.1820	2.7632
Cl_3	Toluene	120	1000	20.31	6.975382188	1.5046	1.2538		
Cl_3	Toluene	118	1000	20.33	7.081151852	1.5282	1.2951		
Cl_3	Toluene	111	1000	19.84	6.756007231	1.4233	1.2822	1.2770	0.0211
Cl	Et_2O	82	1000	20.79	0.33505235	0.0740	0.0902		
Cl	Et_2O	82	1000	19.93	0.700241492	0.1482	0.1807		
Cl	Et_2O	73	1000	20.49	0.818223678	0.1780	0.2439	0.1716	0.0772
Br	Et_2O	106	1000	20.01	0.131859057	0.0280	0.0264		
Br	Et_2O	100	1000	20.45	0.060775565	0.0132	0.0132		
Br	Et_2O	96	1000	19.90	0.082435999	0.0174	0.0181	0.0193	0.0067
I	Et_2O	133	1000	19.86	0.150343081	0.0317	0.0238		
I	Et_2O	131	1000	19.88	0.054969971	0.0116	0.0089		
I	Et_2O	131	1000	19.57	0.041388368	0.0086	0.0066	0.0131	0.0094
OTf	Et_2O	139	100000	19.61	2.656673161	55.3307	39.8062		
OTf	Et_2O	136	100000	20.14	2.342005284	50.0933	36.8333		
OTf	Et_2O	132	100000	20.77	2.479038892	54.6626	41.4111	39.3502	2.3227
Cl_3	Et_2O	119	1000	19.45	21.45629649	4.4310	3.7235		
Cl_3	Et_2O	118	1000	18.59	19.8070977	3.9096	3.3132		
Cl_3	Et_2O	116	1000	19.17	21.62871237	4.4020	3.7948	3.6105	0.2599

Tetraglyme

X	Solvent	Initial Mass (mg)	Dilution Factor 1	Dilution Factor 2	ICP-MS Raw Data (ppb)	Final Mass	% Uptake	Avg (%)	Stdev
Br	Toluene	110	1000	19.69	0.413702221	0.0865	0.0786		
Br	Toluene	107	1000	20.29	0.787800638	0.1697	0.1586		
Br	Toluene	103	1000	19.60	1.418310645	0.2952	0.2866	0.1746	0.1049
I	Toluene	127	1000	19.99	0.280828361	0.0596	0.0469		
I	Toluene	125	1000	19.56	0.121138992	0.0252	0.0201		
I	Toluene	123	1000	20.68	0.118993042	0.0261	0.0212	0.0294	0.0152
OTf	Toluene	137	100000	19.83	2.816890207	59.3120	43.2934		
OTf	Toluene	136	100000	20.02	3.022614249	64.2496	47.2423		
OTf	Toluene	135	100000	19.73	2.901346602	60.7751	45.0186	45.1848	1.9797
Cl_3	Toluene	120	1000	20.66	1.529766999	0.3355	0.2796		
Cl_3	Toluene	119	1000	19.62	1.709928903	0.3562	0.2993		
Cl_3	Toluene	117	1000	20.23	1.64173555	0.3527	0.3015	0.2935	0.0120
Cl	Et_2O	79	1000	19.53	0.571663554	0.1185	0.1500		
Cl	Et_2O	78	1000	20.13	0.466631058	0.0997	0.1279		
Cl	Et_2O	76	1000	20.15	0.233139202	0.0499	0.0656	0.1145	0.0438
Br	Et_2O	104	1000	19.91	0.135596744	0.0287	0.0276		
Br	Et_2O	97	1000	21.01	0.103491804	0.0231	0.0238		
Br	Et_2O	95	1000	20.63	0.181414931	0.0397	0.0418	0.0311	0.0095
I	Et_2O	129	1000	19.97	0.093957803	0.0199	0.0154		
I	Et_2O	124	1000	19.72	0.040143258	0.0084	0.0068		
I	Et_2O	123	1000	20.04	0.060270092	0.0128	0.0104	0.0109	0.0044
OTf	Et_2O	139	100000	20.90	2.229353848	49.4670	35.5878		
OTf	Et_2O	135	100000	19.77	2.534146748	53.1912	39.4009		
OTf	Et_2O	134	100000	19.90	2.358939102	49.8358	37.1909	37.3932	1.9146
Cl_3	Et_2O	119	1000	19.22	6.127642742	1.2506	1.0509		
Cl_3	Et_2O	115	1000	19.54	6.698877024	1.3896	1.2083		
Cl_3	Et_2O	113	1000	19.27	6.785615863	1.3881	1.2284	1.1626	0.0972

Neat Glyme Solutions

X	Ligand	Initial Mass (mg)	Dilution Factor 1	Dilution Factor 2	ICP-MS Raw Data (ppb)	Final Mass	% Uptake	Avg (%)	Stdev
Br	DME	54	1000	7.82	0.424036174	0.0352	0.0652		
Br	DME	53	1000	6.82	1.676491511	0.1214	0.2290		
Br	DME	50	1000	6.42	1.909896767	0.1302	0.2604	0.1849	0.1048
*Br	Triglyme	56	1000	19.46	2.200688232	0.4548	0.8121	0.8121	
Br	Tetraglyme	61	1000	19.03	2.913855245	0.5888	0.9652		
Br	Tetraglyme	55	1000	18.44	2.391577748	0.4682	0.8512		
Br	Tetraglyme	52	1000	18.80	2.045431152	0.4084	0.7853	0.8672	0.0910
I	DME	68	1000	18.90	0.282402673	0.0567	0.0834		
I	DME	66	1000	19.20	0.93763073	0.1911	0.2896		
I	DME	65	1000	19.78	0.166346131	0.0349	0.0538	0.1422	0.1285
I	Triglyme	69	1000	18.94	0.688555484	0.1385	0.2007		
I	Triglyme	67	1000	19.19	0.644051191	0.1313	0.1959		
I	Triglyme	62	1000	19.52	0.768254567	0.1592	0.2568	0.2178	0.0339
I	Tetraglyme	77	1000	19.39	0.919557843	0.1893	0.2458		
I	Tetraglyme	75	1000	19.83	1.069881953	0.2253	0.3004		
I	Tetraglyme	72	1000	19.23	1.406965862	0.2873	0.3990	0.3151	0.0776
OTf	2DME	75	50000	19.67	2.913782973	30.4232	40.5643		
OTf	2DME	68	50000	19.52	2.705745998	28.0458	41.2438		
OTf	2DME	67	50000	19.14	2.711014876	27.5430	41.1089	40.9723	0.3598
OTf	Triglyme	72	50000	19.37	2.797282605	28.7658	39.9524		
OTf	Triglyme	70	50000	19.55	2.67940252	27.8141	39.7345		
OTf	Triglyme	68	50000	19.67	2.300521175	24.0186	35.3215	38.3361	2.6130
OTf	Tetraglyme	73	50000	19.76	3.12757101	32.8159	44.9533		
OTf	Tetraglyme	73	50000	19.25	3.062315944	31.2974	42.8731		
OTf	Tetraglyme	73	50000	19.73	2.867416554	30.0423	41.1538	42.9934	1.9026
Cl_3	DME	55	50000	19.87	1.844845406	19.4654	35.3917		
Cl_3	DME	54	50000	19.56	1.809977913	18.7918	34.7997		
Cl_3	DME	54	50000	19.32	2.504557692	25.6902	47.5744	39.2553	7.2107
Cl_3	Triglyme	64	1000	19.43	137.02581	28.2718	44.1747		
Cl_3	Triglyme	59	1000	19.44	101.0414445	20.8615	35.3584		
Cl_3	Triglyme	56	1000	19.63	101.4245386	21.1453	37.7594	39.0975	4.5579
Cl_3	Tetraglyme	59	50000	19.22	1.87254536	19.1051	32.3816		
Cl_3	Tetraglyme	57	50000	19.61	2.479227161	25.8046	45.2713		
Cl_3	Tetraglyme	54	50000	19.39	2.105795583	21.6783	40.1449	39.2659	6.4896

*Only one trial was run

2.7 References

[1] Pardoe, J. A. J.; Downs, A. J., *Chem. Rev.* **2007,** *107*, 2.
[2] Schneider, U.; Kobayashi, S., *Acc. Chem. Res.* **2012,** *45*, 1331.
[3] Andrews, C. G.; Macdonald, C. L. B., *Angew. Chem., Int. Ed.* **2005,** *44*, 7453.
[4] Tuck, D. G., *Chem. Soc. Rev.* **1993,** *22*, 269.
[5] Green, S. P.; Jones, C.; Stasch, A., *Chem. Commun.* **2008**, 6285.
[6] Green, S. P.; Jones, C.; Stasch, A., *Angew. Chem., Int. Ed.* **2007,** *46*, 8618.
[7] Cole, M. L.; Jones, C.; Kloth, M., *Inorg. Chem.* **2005,** *44*, 4909.
[8] Fischer, E. O.; Hofmann, H. P., *Angew. Chem., Int. Ed.* **1957,** *69*, 639.
[9] Beachley, O. T.; Pazik, J. C.; Glassman, T. E.; Churchill, M. R.; Fettinger, J. C.; Blom, R., *Organometallics* **1988,** *7*, 1051.
[10] Fitz, H.; Muller, B. G., *Z. Anorg. Allg. Chem.* **1997,** *623*, 579.
[11] Macdonald, C. L. B.; Corrente, A. M.; Andrews, C. G.; Taylor, A.; Ellis, B. D., *Chem Commun.* **2004**, 250.
[12] Cooper, B. F. T.; Hamaed, H.; Friedl, W. W.; Stinchcombe, M. R.; Schurko, R. W.; Macdonald, C. L. B., *Chem. Eur. J.* **2011,** *17*, 6148.
[13] Bandyopadhyay, R.; Cooper, B. F. T.; Rossini, A. J.; Schurko, R. W.; Macdonald, C. L. B., *J. Organomet. Chem.* **2010,** *695*, 1012.
[14] Macdonald, C. L. B.; Bandyopadhyay, R.; Cooper, B. F. T.; Friedl, W. W.; Rossini, A. J.; Schurko, R. W.; Eichorn, S. H.; Herber, R. H., *J. Am. Chem. Soc.* **2012,** *134*, 4332.
[15] Schmidbaur, H., *Angew. Chem.* **1985,** *97*, 893.
[16] Schmidbaur, H.; Schier, A., *Organometallics* **2008,** *27*, 2361.
[17] Mishra, S. K.; Yadav, R. K. S.; Singh, V. B.; Rai, S. B., *J. Phys. Chem. Ref. Data* **2004,** *33*, 453.
[18] Pearson, R. G., *J. Am. Chem. Soc.* **1963,** *85*, 3533.
[19] Pearson, R. G., *J. Chem. Educ.* **1968,** *45*, 581.
[20] Pearson, R. G., *J. Chem. Educ.* **1968,** *45*, 643.
[21] Pangborn, A. B.; Giardello, M. A.; Grubbs, R. H.; Rosen, R. K.; Timmers, F. J., *Organometallics* **1996,** *15* (5), 1518.
[22] *SAINTPlus*, Bruker AXS Inc.: Madison, WI, 2008.
[23] *SADABS*, Bruker AXS Inc.: Madison, WI, 2008.
[24] Sheldrick, G. M., *Acta Crystallogr., Sect. A: Found. Crystallogr.* **2008,** *64* (1), 112.
[25] Farrugia, L. J., *J. Appl. Crystallogr.* **1999,** *32*, 837.
[26] Becke, A. D., *J. Chem. Phys.* **1993,** *98* (7), 5648.
[27] Perdew, J. P.; Burke, K.; Wang, Y., *Phys. Rev. B* **1996,** *54*, 16533.
[28] Perdew, J. P.; Chevary, J. A.; Vosko, S. H.; Jackson, K. A.; Pederson, M. R.; Singh, D. J.; Fiolhais, C., *Phys. Rev. B* **1992,** *46*, 6671.
[29] Frisch, M. J.; Trucks, G. W.; Schlegel, H. B.; Scuseria, G. E.; Robb, M. A.; Cheeseman, J. R.; Scalmani, G.; Barone, V.; Mennucci, B.; Petersson, G. A.; Nakatsuji, H.; Caricato, M.; Li, X.; Hratchian, H. P.; Izmaylov, A. F.; Bloino, J.; Zheng, G.; Sonnenberg, J. L.; Hada, M.; Ehara, M.; Toyota, K.; Fukuda, R.; Hasegawa, J.; Ishida, M.; Nakajima, T.; Honda, Y.; Kitao, O.; Nakai, H.; Vreven, T.; Montgomery, J., J. A.; Peralta, J. E.; Ogliaro, F.; Bearpark, M.; Heyd, J. J.;

Brothers, E.; Kudin, K. N.; Staroverov, V. N.; Kobayashi, R.; Normand, J.; Raghavachari, K.; Rendell, A.; Burant, J. C.; Iyengar, S. S.; Tomasi, J.; Cossi, M.; Rega, N.; Millam, N. J.; Klene, M.; Knox, J. E.; Cross, J. B.; Bakken, V.; Adamo, C.; Jaramillo, J.; Gomperts, R.; Stratmann, R. E.; Yazyev, O.; Austin, A. J.; Cammi, R.; Pomelli, C.; Ochterski, J. W.; Martin, R. L.; Morokuma, K.; Zakrzewski, V. G.; Voth, G. A.; Salvador, P.; Dannenberg, J. J.; Dapprich, S.; Daniels, A. D.; Farkas, Ö.; Foresman, J. B.; Ortiz, J. V.; Cioslowski, J.; Fox, D. J. *Gaussian 09*, A.1; Gaussian Inc.: Wallingford, CT, 2009.

[30] Reed, A. E.; Curtiss, L. A.; Weinhold, F., *Chemical Reviews* **1988,** *88* (6), 899.

[31] Glendening, E. D.; Reed, A. E.; Carpenter, J. E.; Weinhold, F. *NBO Version 3.1*, Madison, Wisconsin.

Chapter 3: Insertion of InOTf into carbon-halogen bonds

3.1 - Introduction

The electron-rich nature of indium in the +1 oxidation state has given rise to a considerable amount of chemistry that can be done utilizing these centres. It should come as no surprise that the majority of the chemistry that these types of compounds undergo involves oxidative addition reactions which generates In(II) or In(III) species. Previously, it has been shown that indium(I) halides readily insert into dichalcogens, Grignard-type reagents, as well as several other species (Scheme 3.1).[1] One of the most important reactions of this class is the insertion of In(I)X species into carbon-halogen bonds which was first reported by Tuck and co-workers. They showed that In(I)X can be generated electrochemically *in situ* when in the presence of H_2CX_2 (X = Br, I). Production of In(I)X in the presence of excess dihalomethanes yielded organoindium(III) compounds of the type $X_2In\text{-}CH_2X$.[2-3] This work was later extended to haloforms (CHX_3; X = Cl, Br, I) and produced analogous products, $X_2In\text{-}CH_2X$.[4-5]

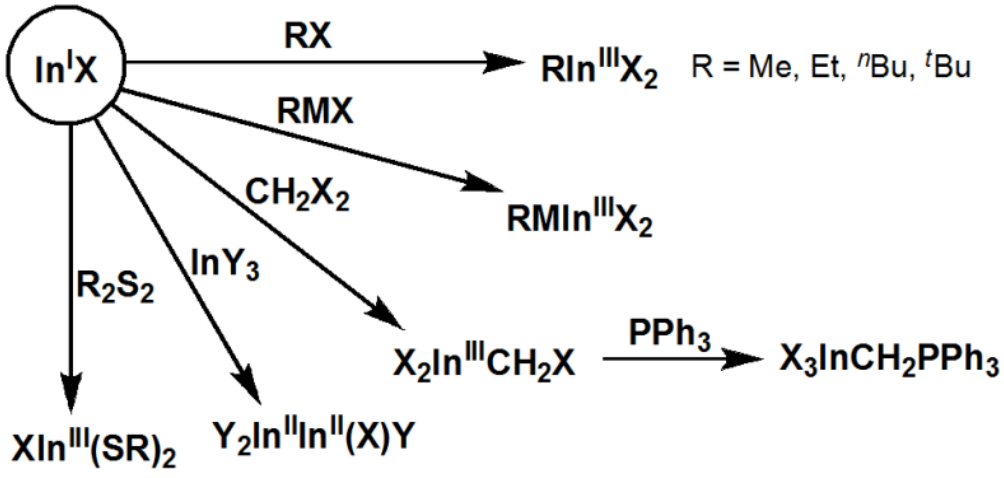

Scheme 3.1: Reaction wheel illustrating several of the oxidative addition reactions of In(I)X explored by Tuck.

While the pioneering work done by Tuck focused on the insertion chemistry of In(I)X, there are now many examples in the literature where various chelated In(I) compounds undergo oxidative addition reactions with R-X. Hill's [In][NacNac] complex was shown to add oxidatively to ^{i}Pr-Br/I, ^{t}Bu-Br/I and MeI.[6] However, as with Tuck's earlier work, the insertion into carbon-chlorine bonds was not observed.

Macdonald *et al*. attempted to achieve these same types of inserted products using the more stable and soluble InOTf salt instead of indium(I) halides. Perhaps surprisingly, the addition of pure InOTf to H_2CCl_2 or $HCCl_3$ yielded no reaction, in contrast to the reactivity of InCl or InBr observed by Tuck. However, ligation of [18]crown-6 to InOTf was found to alter the reactivity of the salt. While no reaction was observed for "free" InOTf, "crowned" InOTf in the form of [In([18]crown-6)][OTf] was shown to rapidly and quantitatively insert into the carbon-chlorine bond of H_2CCl_2 or $HCCl_3$.[7] This difference in reactivity between the free and encapsulated InOTf was initially postulated to be attributable to reduced agglomeration of the salt, but then later rationalized in terms of the destabilization of the 5s orbital, as briefly mentioned in Chapter 2. In summary, the structural changes caused by the presence of the [18]crown-6 ligand (and the counter anion) raises the energy of the 5s electrons sufficiently to undergo the oxidative addition reaction (Figure 3.1).

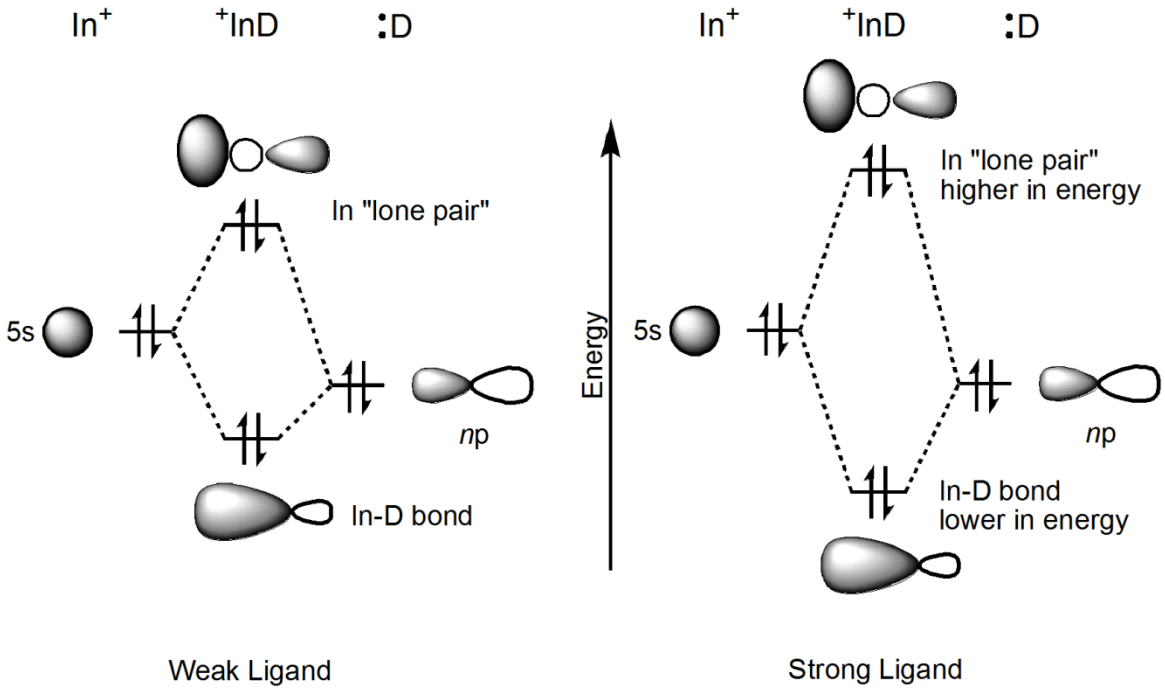

Figure 3.1: Simplified molecular orbital diagram of the interaction with donor molecules and In^{+}. A stronger In-D bond will result in a lower σ orbital, increasing the energy of the σ* orbital, resulting in a more reactive "lone pair".[8]

It was also shown that the addition of KX to [In([18]crown-6)][OTf] resulted in "crowned" potassium, [K([18]crown-6)][OTf] as well as In(I)X, which then rapidly underwent disproportionation yielding In^{0}.[9] This chapter explores the *in situ* generation of In(I)X by salt metathesis from $[R_4N][X]$, followed by subsequent insertion into carbon-halogen bonds before disproportionation can occur. Additionally, expanding upon the insertion chemistry achieved with "crowned" InOTf, other ligands are explored that will potentially destabilize the "lone pair" of electrons so as to promote oxidative addition.

3.2 - Experimental Results and Discussion

3.2.1 In situ generation of In(I)Cl

The addition of dichloromethane or chloroform to a flask charged with InOTf appeared to give no reaction on the basis of the physical and spectroscopic features of the mixture. However, the slow addition of a stoichiometric amount of Bu_4NCl immediately produced a bright yellow precipitate, consistent with the formation of In(I)Cl. Upon continued stirring for 18 hours, the reaction decolourized. Removal of all volatile components *in vacuo* produced a white precipitate (Scheme 3.2).

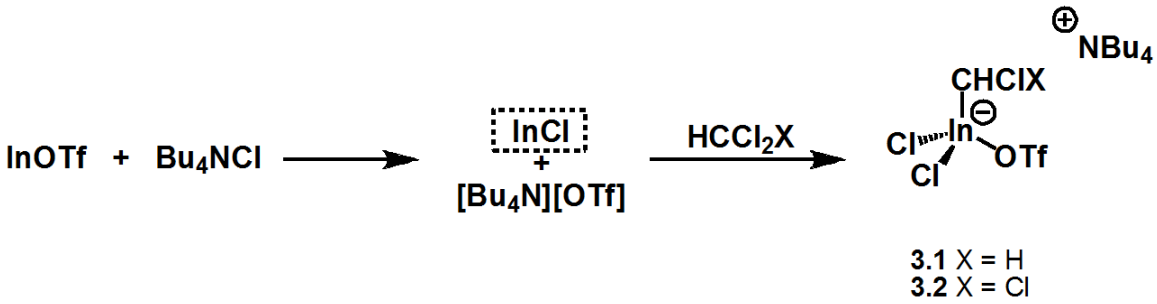

Scheme 3.2: Insertion reactions of InCl generated *in situ* from Bu_4NCl and InOTf.

The nature of the product, which is a very tacky substance, made characterization very difficult as it could not be packed into melting point tubes or accurately weighed into tin boats for elemental analysis. Additionally, the material was not receptive to positive ion mass spectrometry and exhibited no peaks that corresponded to product. However, the product is extremely soluble in acetonitrile which made analysis by NMR spectroscopy facile. Distinct upfield shifts in the ^1H NMR spectra reveal a drastic environmental change (Table 3.1). This upfield shift is consistent with a more electron-rich environment around the carbon centre and is consistent with a carbon that is adjacent

to a metal centre. Importantly, the shifts observed for the inserted products are comparable to those reported by Tuck *et al*.[1]

Table 3.1: ^{1}H NMR spectral shifts of chloroform and dichloromethane and the corresponding inserted product.

Compound	Substrate	Starting Material (ppm)	Inserted Product (ppm)	Change (ppm)
3.1	H_2CCl_2	5.45	3.86	-1.59
3.2	$HCCl_3$	7.58	5.54	-2.04

Attempts to grow crystals of **3.1** or **3.2** were unsuccessful. Many group 13 compounds have a propensity to symmetrize and as a result the only crystals obtained from these reactions were $[Bu_4N][InCl_4]$ or the metathesis byproduct $[Bu_4N][OTf]$. This behavior is not surprising given that previous attempts to grow crystals of the inserted products encapsulated by "crowns" were also often unsuccessful and the quality of the crystallographic data obtained was usually relatively poor.[7]

Analogous indium(I) insertion reactions into several other chlorinated organic compounds (^{n}BuCl, ^{i}PrCl, PhCl and $PhCH_2Cl$) were attempted using the same approach but none produced conclusive evidence for formation of the targeted products. In particular, the addition of Bu_4NCl to a solution of ^{n}BuCl, ^{i}PrCl, or PhCl (neat) and InOTf resulted in a dark, forest green precipitate. Concentration of the reaction mixture resulted in disproportionation and only signals from the starting materials were observed in the ^{1}H NMR spectra. Prolonged stirring of the solutions resulted in decolourization; however, once again, only signals from the cation, Bu_4N^{+}, were observed by ^{1}H NMR spectroscopy.

When Bu_4NCl was added to benzyl chloride and InOTf, the solution turned a dark, forest green colour. Continued stirring overnight resulted in a peach coloured, glassy substance. Characterization by ^1H NMR spectroscopy revealed very large, broad peaks in the aromatic and benzylic regions, consistent with polymerization of the solvent ($PhCH_2Cl$). Although the formation of this polymer was unexpected, it is not unreasonable given that benzyl radicals are readily produced and that the oxidative addition reactions of indium(I) compounds are proposed to occur through radical processes.[10-11] Specifically, the oxidation of indium(I) compounds are proposed to go through a 1 electron oxidation, generating an indium(II) centre, followed by a rapid 1 electron oxidation once again to generate the final indium(III) product.

Given the foregoing, the attempted insertion reactions into ^{n}BuCl, ^{i}PrCl and PhCl may not have proceeded due to the relative instability of the corresponding organic radical intermediates. In contrast, both dichloromethane and chloroform are more capable of stabilizing radical species due to the presence of geminal chlorine atoms on the carbon (the stability of organic radicals can be likened to the stability of carbocations, as radicals are also electron deficient).[12] The intense green colour generated from the reactions involving ^{n}BuCl, ^{i}PrCl and PhCl may originate from an organic radical that is then quenched upon concentration. Consequently, it is possible that no products were observed in the ^1H NMR spectra due to their paramagnetic nature.

All attempts to isolate the proposed In(I)Cl intermediate were unsuccessful. The addition of Bu_4NCl to InOTf in toluene resulted in the characteristic bright yellow precipitate, which then slowly decomposed to indium metal over the course of a couple of hours and may be from formation of $[In(toluene)_2][InCl_4]$. The melting point obtained

for this yellow precipitate was well below the literature value for InCl (*cf.* 225˚C) and is likely a consequence of melting point suppression caused by the presence of impurities and by-products (e.g. $[Bu_4N][OTf]$, and any In(II) or In(III) products generated during disproportionation).

3.2.2 In situ generation of In(I)Br

Analogous to the insertion reactions involving the generation of InCl, the salt Et_4NBr was used to generate InBr *in situ*. The addition of this salt to solutions of InOTf and bromoform or BuBr resulted in the formation of a bright orange precipitate, consistent with the production of an InBr intermediate. The solutions completely decolourized upon stirring for 48 hours, and the final products were analyzed by ^{1}H NMR spectroscopy. As with the chlorinated insertion products mentioned above, characteristic upfield shifts were observed in the ^{1}H NMR spectra of the products (Table 3.2).

Table 3.2: ^{1}H NMR spectral shifts of bromoform and n-bromobutane and the corresponding inserted product.

Compound	Substrate	Starting Material (ppm)	Inserted Product (ppm)	Change (ppm)
3.3	H_2CBr_2	5.08	2.76	-2.32
3.4	^{n}BuBr	3.48 (α)	$^{\#}$1.21	-2.27
		1.82 (β)	1.65	-0.17
		1.44 (γ)	1.38	-0.06
		0.92 (δ)	0.90	-0.02

$^{\#}$This signal overlaps with the cation Et_4N^+, however the integration of this signal is consistent with a peak buried underneath.

The kinetics for the reaction of *in situ* generation of InBr are noticeably slower than those observed for the analogous reactions involving chlorine and the reactions take up to twice as long to go to completion. One thing worthy to note is that InBr appeared to insert into ^{n}BuBr, which was not the case for ^{n}BuCl and InCl and is most likely a consequence of the stability of intermediate products. A discussion on the mechanism and proposed intermediates is found below in section 3.3: Theoretical Calculations.

3.2.3 Ligand-Destabilized Insertions

In most cases, ligands are employed successfully to either stabilize or solubilize metal centres (with ns^0 electron configurations) by filling vacant orbitals. However, for indium(I) compounds (with $5s^2$ electron configurations), strong interactions from ligands often results in disproportionation, as discussed in Chapter 2. Although such behavior is usually considered to be problematic, we reasoned that it should be possible to exploit the destabilization of the 5s orbital in a controlled manner in order to induce controlled reactivity. As mentioned above, such induced reactivity was observed unexpectedly for "crowned" InOTf. The cyclic crown ether is weakly donating enough to avoid disproportionation, but is destabilizing enough to promote oxidative addition of certain substrates. In order to explore this potential methodology, a series of ligands were added to solutions of InOTf and dichloromethane to see if they would cause destabilization of the $5s^2$ electrons and promote insertion of InOTf into carbon-chlorine bonds (Scheme 3.3)

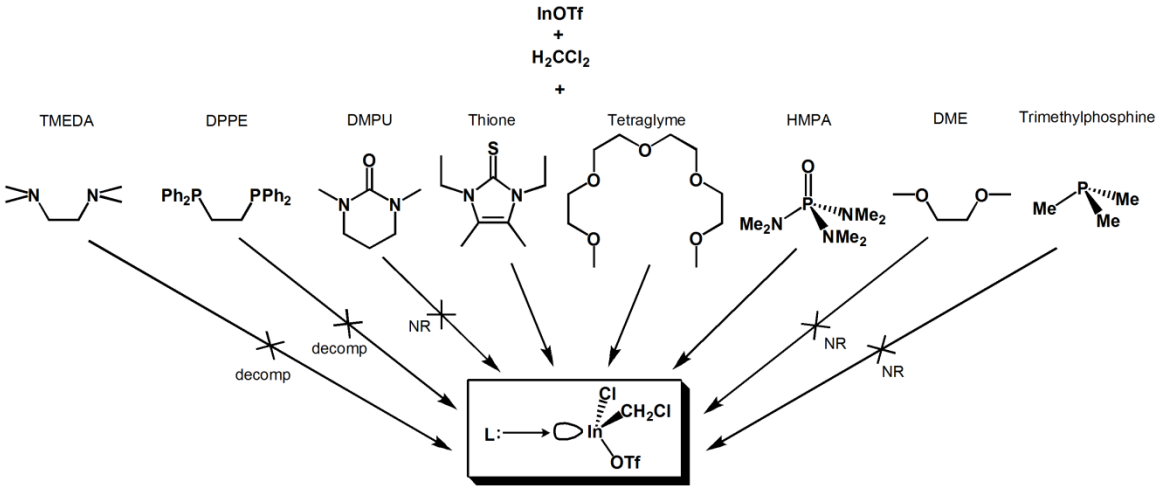

Scheme 3.3: Ligands tested to promote oxidative addition of InOTF into dichloromethane. [decomp= decomposed; NR=no reaction]

The addition of the bidentate ligands TMEDA (tetramethylethylenediamine) and DPPE (diphenylphosphinoethane) both resulted in disproportionation with no evidence for the production of any inserted product. The addition of TMEDA to the solution of InOTf in H_2CCl_2 resulted in disproportionation almost immediately, producing a black precipitate. At low temperatures (-78˚C), TMEDA did not cause disproportionation. However, slowly warming to room temperature resulted in decomposition and suggests that TMEDA is too strong a donor and that the kinetics for disproportionation are faster than those of insertion. In contrast, the addition of trimethylphosphine or DMPU (dimethylpropyleneurea) to solutions of InOTf and H_2CCl_2 produced no observable reaction and only starting materials were observed in the ^{1}H NMR spectra.

Gratifyingly, three of the eight ligands examined were found to promote insertion of the In(I) centre into dichloromethane: the thione (which is one of Kuhn's precursors to *N*-heterocyclic carbenes[13]), tetraglyme ($MeO(CH_2CH_2O)_4Me$) and HMPA

(hexamethylphosphoramide). In each case, the characteristic upfield shift to around 3.8 ppm was observed in the ^{1}H NMR spectra of the reaction mixtures.

Fortunately, crystals suitable for single crystal X-ray diffraction were obtained for the thione-mediated insertion of InOTf into chloroform (Figure 3.2). There is a minor disorder problem involving one of the triflate groups but the structure clearly establishes the connectivity of the molecule and the presence of the dichloromethyl fragment derived from the insertion. The In-C distance of 2.208(6)Å is significantly longer than those found for the corresponding adducts of [18]crown-6 (2.174(7) and 2.182(15)Å); this difference is likely a consequence of the dramatically different coordination environments about the In(III) centres in these classes of insertion products. It should be noted that an analogous structure was also obtained for the insertion product with dichloromethane, however the data from the crystal were very poor and thus have not been included.

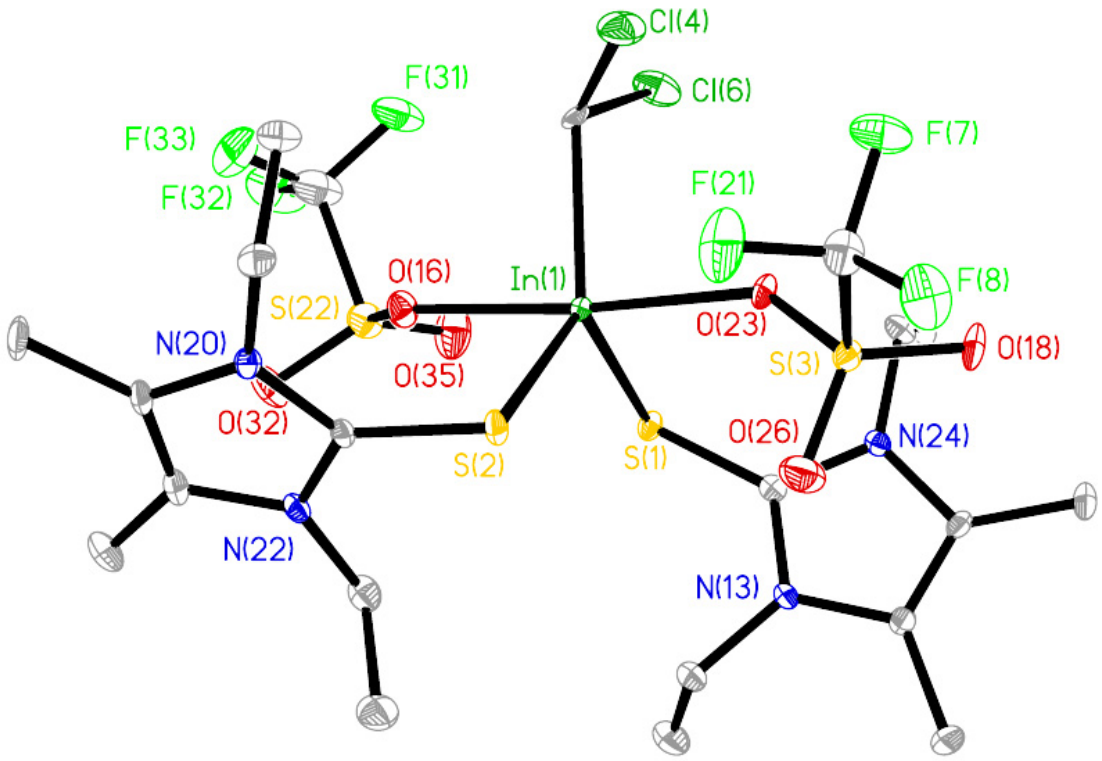

Figure 3.2: Solid state structure from the reaction of "thione" with InOTf and chloroform with 30% thermal ellipsoids. Selected bond distances (Å) and angles (˚): In-C: 2.208(6); In-O(11): 2.258(4); In-O(21): 2.330(4); In-S(3): 2.4667(16); In-S(4): 2.4772(16); S(3)-C: 1.728(6); S(4)-C: 1.734(6). S(3)-In-S(4): 114.07(6); O(11)-In-O(21): 175.30(16). Hydrogen atoms have been omitted for the sake of clarity.

3.3 - Theoretical Calculations

3.3.1 Chelation of In^+

To gain insight into the electronics of these insertion reactions, a computational study was undertaken to examine the effects that a series of ligands have on an indium cation. A "free" In^+ cation was chosen, rather than the full InOTf salt, in order to reduce computational time and cost. Additionally, as mentioned in Chapter 2, InOTf dissociates

completely in many solutions so gas phase calculations using a full InOTf model may not give results that are applicable to the systems we have studied experimentally. The results from these calculations are summarized below in Tables 3.3-3.5 and are divided into three categories: monodentate, bidentate and polydentate ligands, so that relevant comparisons between systems can be made. In addition to the ligands that were used experimentally, several other ligands were calculated to compare and contrast donor molecules from the same group.

It is worthy to note that the NBO analyses of all optimized structures that feature sulfur as the binding site suggest the presence of covalent In-S bonds. This behavior is perhaps most easily rationalized in terms of hard-soft acid-base theory.[14-16] Sulfur, which is "softer" than oxygen, forms a stronger bond with indium, which is also "soft".

Table 3.3: Selected energies obtained from computational analysis of model $[Donor \rightarrow In]^+$ complexes of *monodentate* ligands. Although not drawn explicitly, an indium cation is present in each calculation; pictures of the optimized structures are presented in Figure 3.6.1 of the supporting information. InCl has been included in the table for reference.

Ligand	Ligand Structure	NBO "Lone Pair" Energy (eV)	SCF HOMO Energy (eV)	NBO Wiberg Bond Index
NMe_3	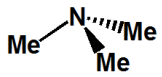	-13.37	-11.49	0.1156
PMe_3	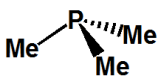	-13.31	-10.76	0.2250

DMPU	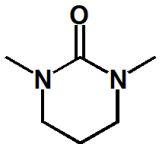	-12.23	-10.23	0.1221
DMPTU*	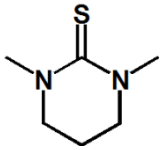	-12.48	-10.25	0.2928
TMIO	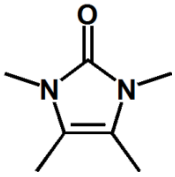	-12.20	-9.43	0.1224
TMIT	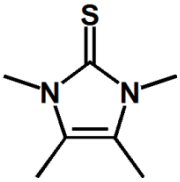	-11.34	-9.47	0.3010
HMPA	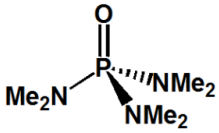	-12.00	-10.07	0.1178
HMPAT	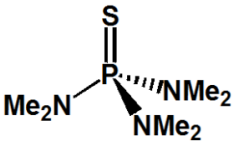	-12.09	-10.34	0.2246
Cl	Cl^-	-9.15	-7.21	0.5635

*The optimized structure exhibits an imaginary frequency (i.e. is a transition structure). Although the magnitude is small (*ca.* 4 cm^{-1}), comparisons to its oxygen analogue must be done with caution.

Of the monodentate ligands, only two were found to insert into carbon-chlorine bonds experimentally: the imidazole-thione and HMPA. For the computational investigation, the ethyl groups on the imidazole-thione were replaced with methyl groups and will be referred to as TMIT (tetramethylimidazolethione). The results from the

computational investigation reveal that coordination of In^+ to TMIT and HMPA results in the highest lone pair energies (-11.34 and -12.00, respectively) and HOMO energies.

It is also worth noting that for the majority of these compounds the "lone pair" on indium is not the HOMO, but rather ascribable to a lower energy orbital. This is likely a consequence of the π-systems and/or other non-bonding electrons that many of these models possess; this is, of course, not the case for NMe_3 and PMe_3 (note that the differences in the energies of the HOMO and LP energies in all of the models described above is a result of differing orbital definitions in the NBO and SCF treatments).

Examination of the model complexes featuring the NMe_3 and PMe_3 ligands shows that the "softer" phosphorus ligand results in a higher HOMO energy and produces a more reactive indium centre. Similarly, the energy of the "lone pair" in TMIT is higher in energy than its oxygen analogue, TMIO. The sulfur ligand has a stronger interaction with the indium centre (again, this is readily rationalized using HSAB considerations) and therefore destabilizes the "lone pair" of electrons more effectively. However, this observation fails to hold true for the comparison of HMPA and HMPAT and may be a consequence of the increased conjugation from flanking NMe_2 groups.

The Wiberg Bond Index of the In-E bond shows that complexes derived from the heavier congeners of the ligands always contain a more covalent bond due to the increased interaction between the donating atom and the indium centre.

Table 3.4: Selected energies obtained from computational analysis of model [Donor·In]$^+$ complexes of *bidentate* ligands. Although not drawn explicitly, an indium cation is present in each calculation; pictures of the optimized structures are presented in Figure 3.6.1 of the supporting information.

Ligand	Ligand Structure	NBO "Lone Pair" Energy (eV)	SCF HOMO Energy (eV)	NBO Wiberg Bond Index (average)
TMEDA		-11.82	-10.21	0.1073
DMPE	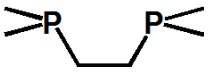	-12.85	-9.79	0.2305
DME		-12.37	-11.47	0.0864
DMEDT		-12.67	-10.58	0.1787

In contrast to the calculations including the monodentate ligands above, the model complexes derived from bidentate ligands all show "lone pair" character on the indium in the HOMO, and therefore comparisons between the different ligands can be made. The results from the calculation on [TMEDA·In]$^+$ show the least stable "lone pair" energy (-11.82 eV) as well as the second least stable HOMO energy (-10.21 eV). The complex with the highest HOMO energy was found to be [DMPE·In]$^+$, and is significantly higher in energy than that of the TMEDA complex (-9.79 eV). Although the "lone pair" energy for this complex is actually the lowest in the series (-12.85 eV), this ligand was found to cause disproportionation without insertion. These results suggest that predictions in reactivity cannot be done simply by examining "lone pair" energy or the HOMO energy independently. These observations are especially true for the case of [DME·In]$^+$.

Although the DME complex has a higher "lone pair" energy than the DMPE complex, its HOMO energy is the lowest in the series (-11.47 eV) and provides insight into why no insertion was observed experimentally when using DME. Much like the monodentate ligands described above, heavier atom chelates have higher WBIs and thus bonds with more covalent character with the indium centre.

Table 3.5: Selected energies obtained from computational analysis of model $[Donor{\cdot}In]^{+}$ complexes of *polydentate* ligands. Although not drawn explicitly, an indium cation is present in each calculation; pictures of the optimized structures are presented in Figure 3.6.3 of the supporting information.

Ligand	Ligand Structure	NBO "Lone Pair" Energy (eV)	SCF HOMO Energy (eV)	NBO Wiberg Bond Index (average)
Diglyme	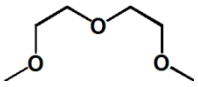	-11.52	-10.51	0.0756
Triglyme	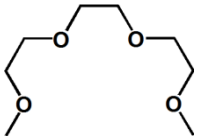	-11.12	-9.94	0.0569
Tetraglyme	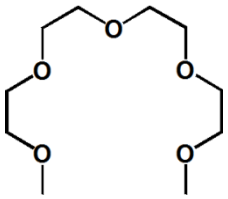	-10.90	-9.70	0.0495

Of the three polydentate ligands calculated, only tetraglyme was used experimentally and was found to promote insertion of dichloromethane into InOTf. However, the results from all of the acyclic polyether ligands model complex calculations are fairly similar and suggest that triglyme may also be used to promote insertion. All

complexes exhibit very low bond WBI values and suggest these are all weak donor-acceptor type complexes, as one would anticipate.

Optimized structures and molecular orbital diagrams of all the $[Donor{\cdot}In]^+$ complexes are located in the supporting information at the end of this chapter.

3.3.2 Mechanism of InX into R-X

One can envision three possible types of intermediates for the step-wise insertion of InX into RX: an anionic intermediate, where the indium bears a negative charge; a cationic intermediate, with a positive charge on the indium; and a radical intermediate. Each pathway is depicted in Scheme 3.4. Although a concerted mechanism is possible, one could not be located on the potential energy surface for the insertion reaction.

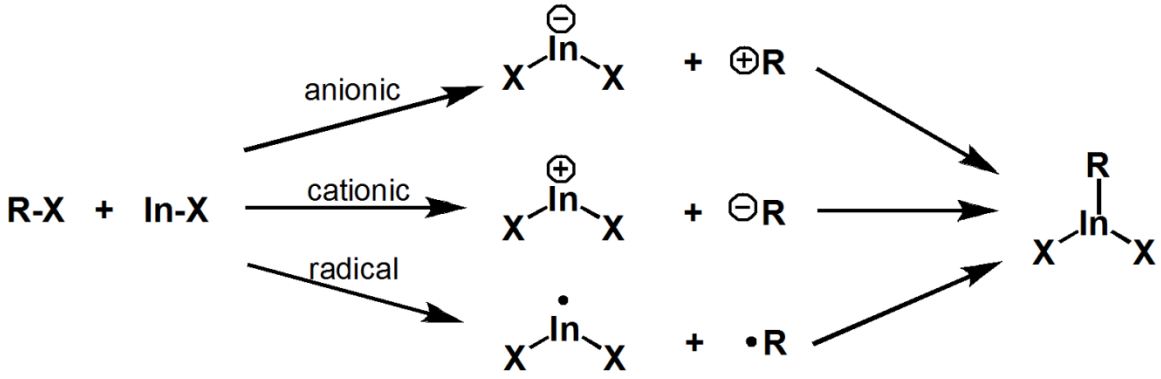

Scheme 3.4: Possible step-wise mechanisms for insertion of InX into R-X.

The relative stabilities of the intermediates are therefore related to the nature of the R-X species and, in particular, the ability of the R group to support and stabilize either a radical, or positive or negative charge. A wide range of substrates were

calculated: HCX_3, H_2CX_2, ^{i}PrX, ^{n}BuX, PhX and $PhCH_2X$ (X=Cl, Br, I) and a summary of the energy data obtained is presented in Table 3.6.

Table 3.6: Relative energies for the intermediates and products for the reaction of InX and RX.

Substrate	Intermediates: Relative E (kJ/mol)			Products (ΔE, kJ/mol)
	Anion	Radical	Cation	
CH_2Cl_2	686.04	125.37	934.03	-97.11
CH_2Br_2	629.83	107.10	838.71	-111.83
CH_2I_2	597.05	98.20	770.99	-119.29
$CHCl_3$	630.17	109.26	825.02	-95.52
$CHBr_3$	553.61	83.91	718.46	-121.71
CHI_3	505.75	68.94	647.83	-134.66
^{i}PrCl	533.04	135.43	1043.48	-76.23
^{i}PrBr	496.53	116.17	978.66	-81.85
^{i}PrI	482.56	102.45	921.40	-86.05
BuCl	547.36	138.65	1023.60	-94.40
BuBr	513.73	122.27	961.66	-98.40
BuI	503.83	112.62	908.47	-98.02
PhCl	718.67	236.49	1007.52	-52.46
PhBr	623.60	158.67	884.14	-114.69
PhI	610.88	146.21	828.14	-118.23
$PhCH_2Cl$	461.91	81.61	868.24	-113.28
$PhCH_2Br$	429.81	66.76	807.83	-112.91
$PhCH_2I$	421.93	59.14	756.66	-111.59

For every substrate examined, it is clear that the radical intermediate is significantly lower in energy. It is therefore most likely that the reaction of InX with RX proceeds through a radical intermediate. These computational results thus concur with experimental evidence presented in the literature.[10-11] The intermediates for $PhCH_2X$ are the lowest in energy for the series and support the production of the benzyl-derived polymer that was discussed earlier in this chapter. Expectedly, the intermediates for the anionic pathway are lower in energy than for the cationic pathway, as the organic

fragments in the model complexes we examined are more suitable at stabilizing a positive charge rather than a negative one.

3.4 - Conclusions

Indium(I) halides can be generated *in situ* from the addition of a halide source. By generating indium(I) halides in this way, it is possible to circumvent the lattice energy/solubility problems that plague the indium(I) halides and may help to improve reactivity. Although InOTf is more stable than the indium halides and does not insert into carbon-halogen bonds, the reactivity can be fine tuned through the use of ligands which sufficiently destabilize the "lone pair" of electrons on indium and allow for such reactions to proceed. Ligands with heavier atoms (e.g. sulfur) form stronger bonds with indium and are therefore more suitable for the destabilization of the metal centre. However, ligands which interact too strongly result in decomposition, rather than insertion and therefore a delicate balance between destabilization and reactivity needs to be met.

3.5 - Experimental

3.5.1 General Methods

All manipulations were carried out using standard Schlenk and glove box techniques under an atmosphere of either argon or nitrogen, respectively. Solution phase NMR spectra were recorded at room temperature on a Bruker Avance 300 MHz spectrometer. Chemical shifts are reported in ppm, relative to external standards ($SiMe_4$ for ^{1}H and ^{13}C NMR) and were run in MeCN-d3. InOTf and the thione ligand were prepared according to reported procedures.[13, 17] The remaining ligands were purchased

from Sigma-Aldrich. Polyether ligands were dried over sodium followed by distillation at reduced pressure. HMPA, DMPU and halogenated solvents (excluding DCM) were dried over CaH_2 followed by distillation. Dichloromethane was dried using a series of Grubbs'-type columns.[18]

3.5.2 General Synthetic Procedures for in situ generation of InX

In a typical experiment, InOTf (100 mg, 0.38 mmol) and the desired halogenated solvent (15 mL) were added to a Schlenk flask. Whilst stirring, a solution of Bu_4NCl (95 mg, 0.38 mmol), Et_4NBr (74 mg, 0.38 mmol) or the desired ligand (0.38 mmol) in MeCN was slowly added. The mixture was allowed to stir overnight and volatile components were removed under reduced pressure and the product was obtained as a powder. Crystals from the reaction of InOTf, $HCCl_3$ and "thione" were obtained from slow concentration of the reaction mixture.

3.5.3 ^1H NMR Shifts

RCl + InOTF + Bu_4NCl →

Substrate	Inserted Product shifts	Bu_4NCl shifts
H_2CCl_2	3.86, br s, 2H	3.09, m, J_{HH} = 8.4 Hz, 8H 1.60, m, J_{HH} = 7.8 Hz, 8H 1.34, ddt, J_{HH} = 7.5 Hz, 8H 0.96, t, J_{HH} = 7.5 Hz, 12H
$HCCl_3$	5.54, s, 1H	3.04, m, 8H, J_{HH} = 8.4 Hz, 8H 1.54, m, 8H, J_{HH} = 7.8 Hz, 8H 1.29, ddt, 8H, J_{HH} = 7.5 Hz, 8H 0.90, t, 12H, J_{HH} = 7.5 Hz

RBr + InOTf + Et_4NBr →

Substrate	Inserted Product	Et_4NBr shifts
H_2CBr_2	2.76, s, 2H	3.17, q, J_{HH} = 7.2 Hz, 8H 1.20, tt, J_{HH} = 7.2 Hz, J_{HH} = 1.8, 12H
BuBr	1.65, ddd, J_{HH} = 7.5 Hz, β 1.38, ddt, J_{HH} = 7.5 Hz, γ 0.90, t, J_{HH} = 7.2 Hz, δ *α signal buried beneath cation shifts	3.17, q, J_{HH} = 7.2 Hz, 8H 1.21, tt, J_{HH} = 7.2 Hz, J_{HH} = 2.1 Hz, 12H

R-X + InOTf + Ligand →

Substrate	Ligand	Inserted Product shifts	Ligand Shifts
H_2CCl_2	Thione	3.22, s, 2H	Et: 1.30, t, J_{HH} = 7.5 Hz, 6H Et: 4.21, q, J_{HH} = 7.5 Hz, 4H CH_3: 2.22, s, 6H
$HCCl_3$	Thione	5.64, s, 1H	Et: 1.32, t, J_{HH}=7.5 Hz, 6H Et: 4.22, q, J_{HH} = 7.5 Hz, 4H CH_3: 2.22, s, 6H
H_2Br_2	Thione	2.80, s, 2H	Et: 1.32, t, J_{HH}=7.5 Hz, 6H Et: 4.22, q, J_{HH} = 7.5 Hz, 4H CH_3: 2.22, s, 6H
BuBr	Thione	1.64, ddd, J_{HH} = 7.5 Hz, 2H, β 0.90, t, J_{HH} = 7.2 Hz, 3H, γ *α and γ buried beneath ligand shifts	Et: 1.31, t, J_{HH} = 7.2 Hz, 6H Et: 4.21, q, J_{HH} = 7.2 Hz, 4H CH_3: 2.22, s, 6H
H_2CCl_2	HMPA	3.21, s 2H	2.62, s, 9H 2.66, s 9H
H_2CCl_2	Tetraglyme	3.07, s 2H	3.47, s, 6H 3.79, m, 18H

3.5.4 Crystallographic Methods

Crystals for investigation were covered in Nujol®, mounted into a goniometer head, then rapidly cooled under a stream of cold N_2 from the low-temperature apparatus (Kryoflex) attached to the diffractometer. The data were collected using the SMART

software suite on a Bruker APEX CCD diffractometer using a graphite monochromator with MoKα radiation (λ=0.71073 Å). A hemisphere of data was collected using either 10 or 30 seconds/frame at 173 K. APEX-II[19] software was used for data reductions and absorption corrections (semi-empirical from equivalents). Structures were solved and refined using the SHELX[20] suite of programs as implemented in WinGX.[21]

3.5.5 Crystallographic Parameters

Identification code	p21n	
Empirical formula	$C_{21}H_{33}Cl_2F_6InN_4O_6S_4$	
Formula weight	865.47	
Temperature	150(2) K	
Wavelength	0.71073 Å	
Crystal system	Monoclinic	
Space group	P2(1)/n	
Unit cell dimensions	a = 13.683(2) Å	α= 90°.
	b = 17.792(3) Å	β= 113.497(2)°
	c = 15.043(2) Å	γ = 90°.
Volume	3358.5(9) $Å^3$	
Z	4	
Density (calculated)	1.712 Mg/m^3	
Absorption coefficient	1.186 mm^{-1}	
F(000)	1744	
Crystal size	0.40 x 0.30 x 0.20 mm^3	
Theta range for data collection	1.70 to 27.50°.	
Index ranges	$-17 \leq h \leq 17$	
	$-22 \leq k \leq 22$	
	$-19 \leq l \leq 19$	
Reflections collected	38288	
Independent reflections	7660 [R(int) = 0.0826]	
Completeness to theta = 27.50°	99.3 %	
Absorption correction	Semi-empirical from equivalents	
Max. and min. transmission	0.789 and 0.656	

Refinement method	Full-matrix least-squares on F^2
Data / restraints / parameters	7660 / 0 / 397
Goodness-of-fit on F^2	1.037
Final R indices [I>2sigma(I)]	R1 = 0.0649, wR2 = 0.1443
R indices (all data)	R1 = 0.0993, wR2 = 0.1666
Largest diff. peak and hole	6.270 and -1.417 e.$Å^{-3}$

3.5.6 Computational Methods

All density functional theory (DFT) calculations were performed using the B3PW91 method[22-24] using the Gaussian 09[25] suites using the SHARCNET high-performance computing network (www.sharcnet.ca). Where applicable, the Stuttgart group (SDD) effective core potentials (ECP) and corresponding basis sets were used for indium atoms and the 6-31+G(d) basis set was used for all lighter atoms. Natural bond order (NBO) analyses[26] to determine orbital contributions, Wiberg Bond Indices and HOMO/LUMO energies were obtained using the routine included in the Gaussian distributions.[27] All stationary points were confirmed to be minima exhibiting no imaginary frequencies unless otherwise stated. Output files generated from calculations can be found on the electronic media accompanying this work.

3.6 - Supporting Information

3.6.1 Optimized Structures and Molecular Orbital Diagrams

$[NMe_3 \cdot In]^+$

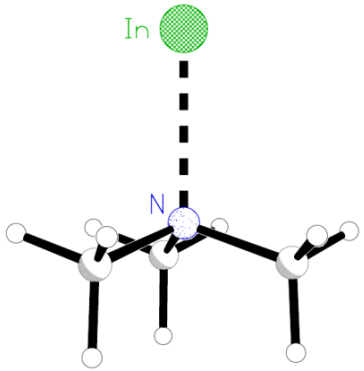

HOMO

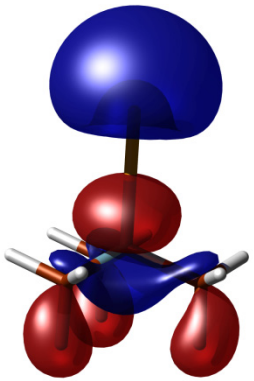

LUMO

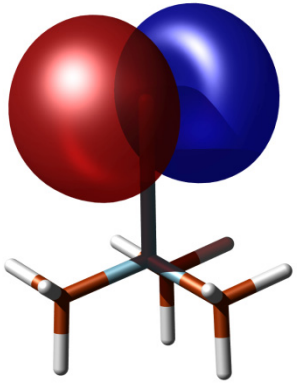

$[PMe_3 \cdot In]^+$

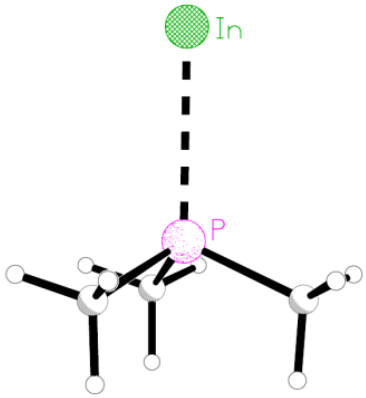

HOMO

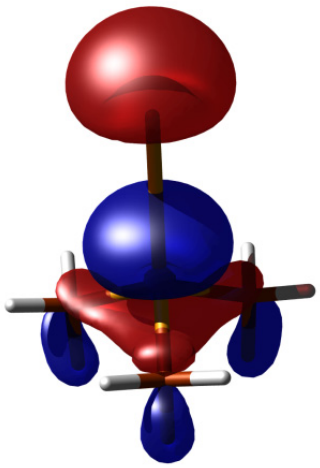

LUMO

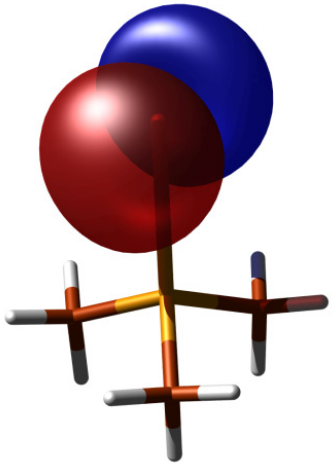

[DMPU·In]$^+$

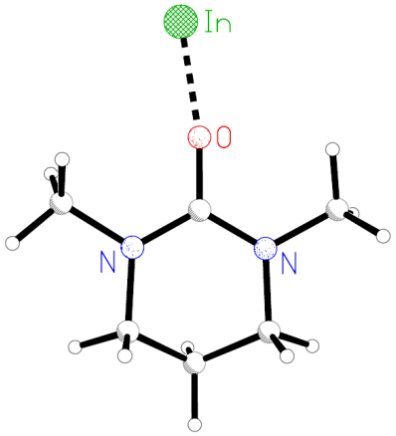

HOMO-2

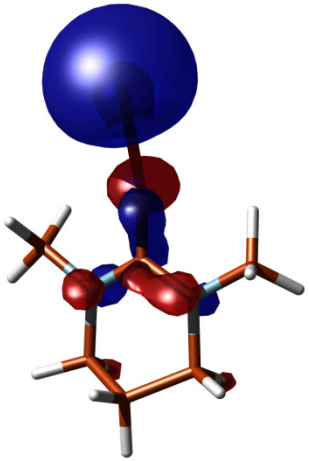

HOMO

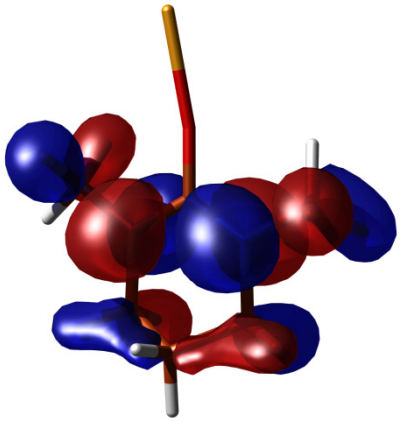

LUMO

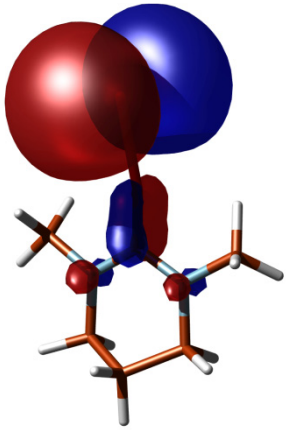

[DMPTU·In]$^+$

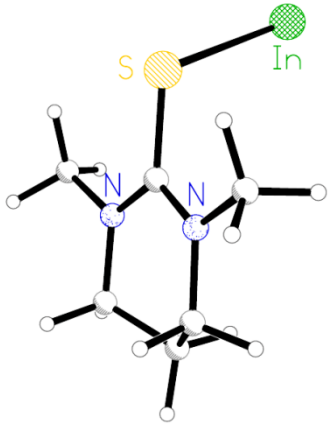

HOMO

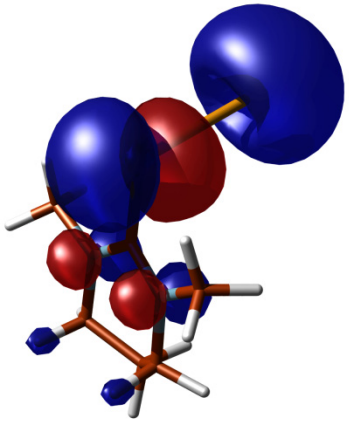

LUMO

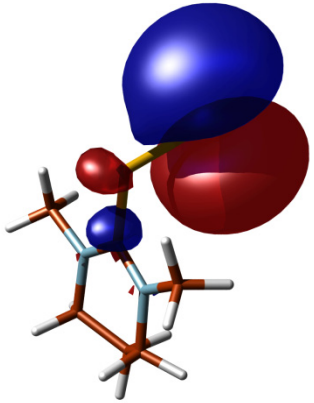

[TMIO·In]$^+$

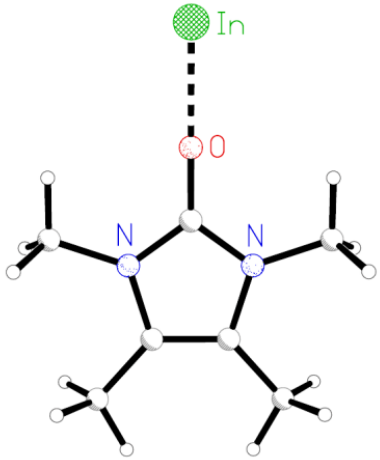

HOMO-2

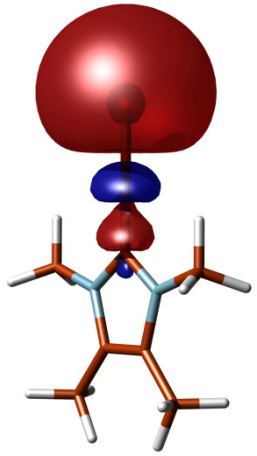

HOMO

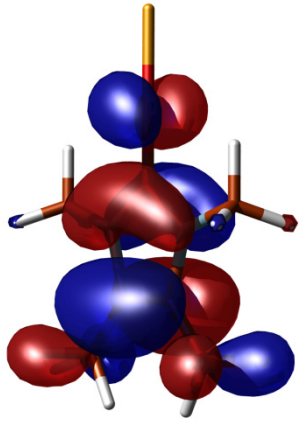

LUMO

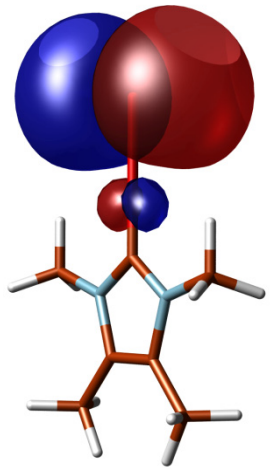

[TMIT·In]$^+$

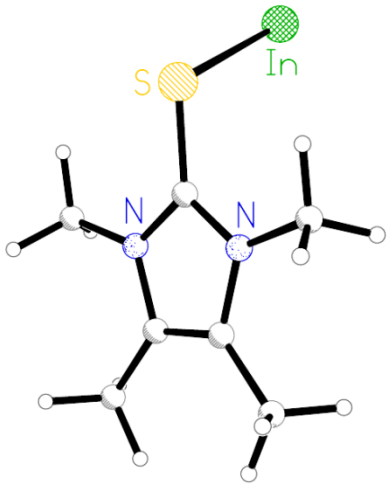

HOMO-2

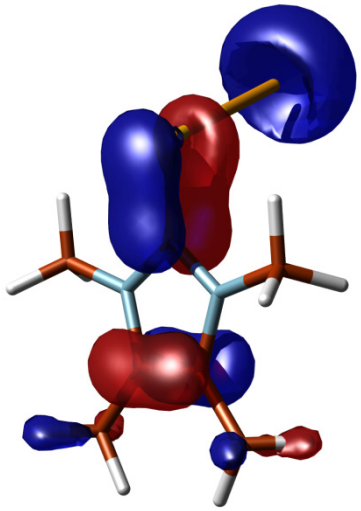

HOMO

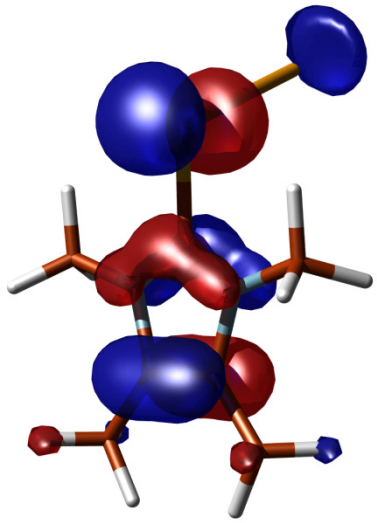

LUMO

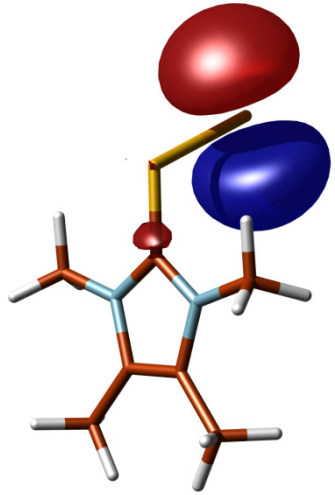

[HMPA·In]$^{+}$

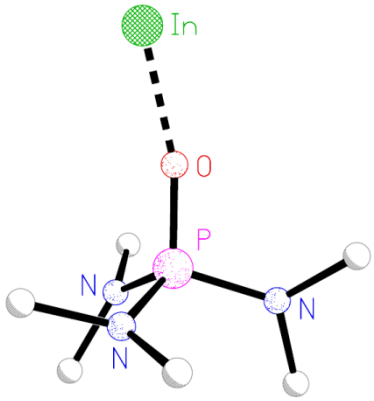

HOMO-2

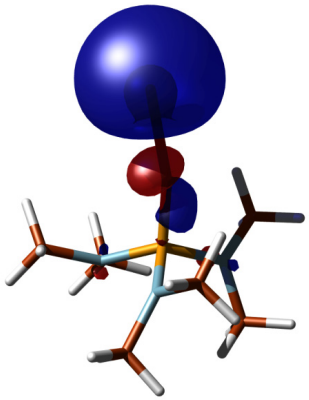

HOMO

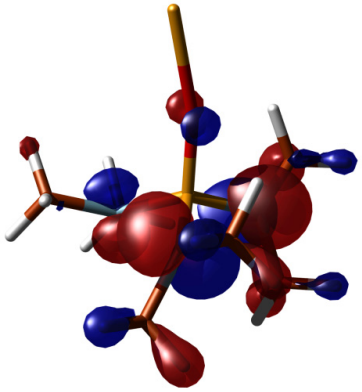

LUMO

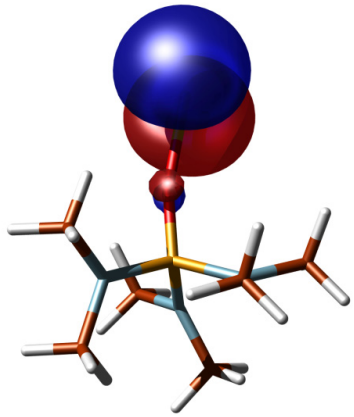

[HMPAT·In]$^{+}$

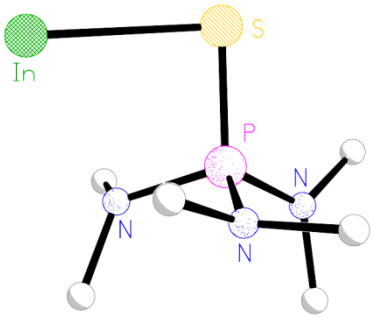

HOMO

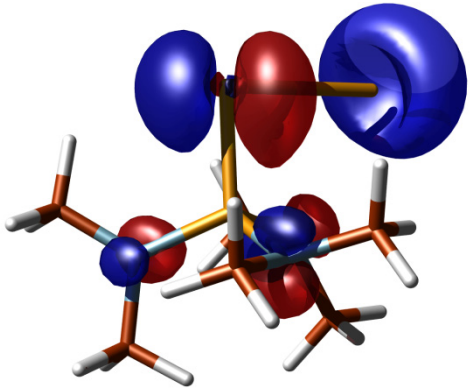

LUMO

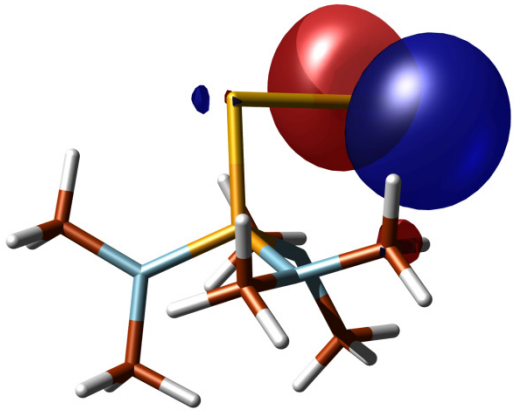

[TMEDA·In]$^+$

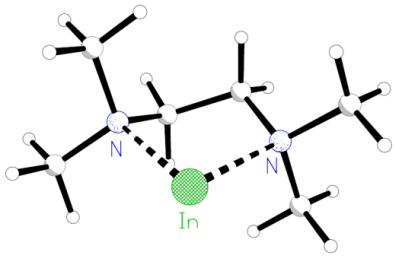

HOMO

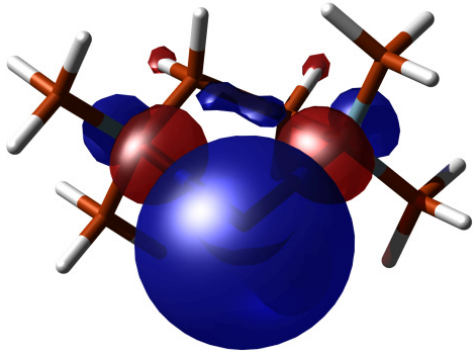

LUMO

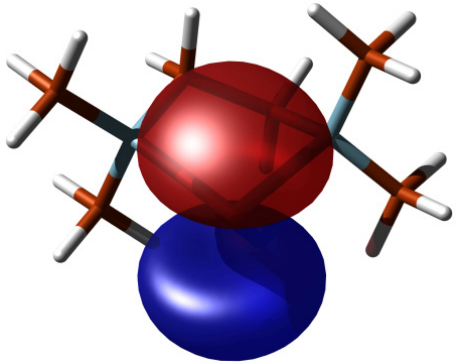

[DME·In]$^+$

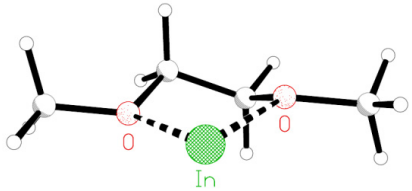

HOMO

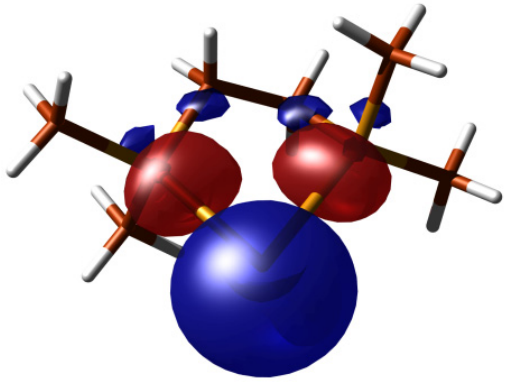

LUMO

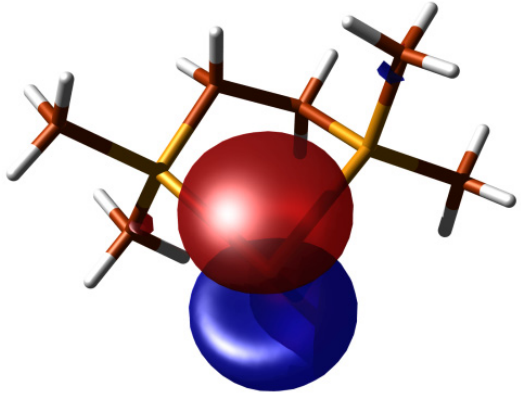

[DMSE·In]$^+$

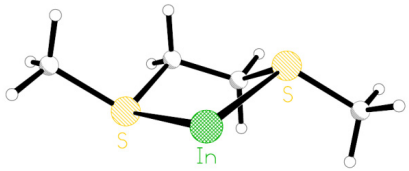

HOMO

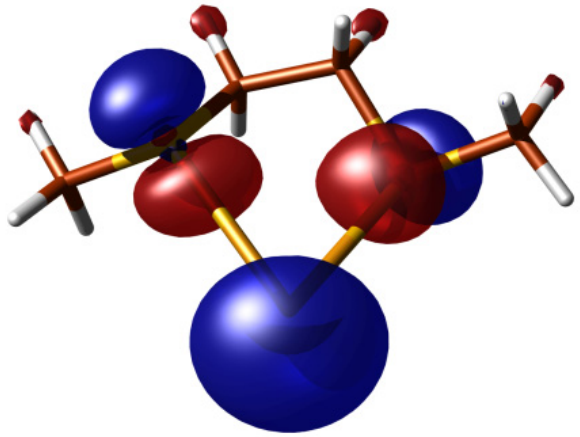

LUMO

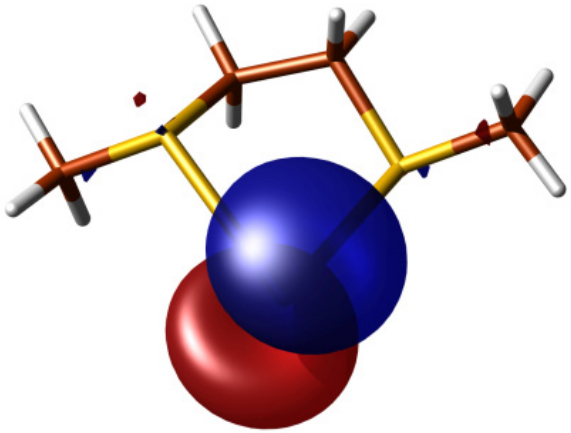

[Diglyme·In]$^+$

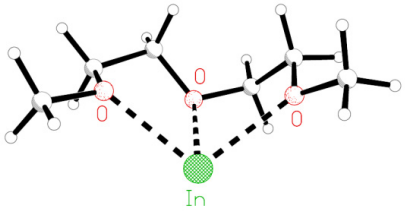

HOMO

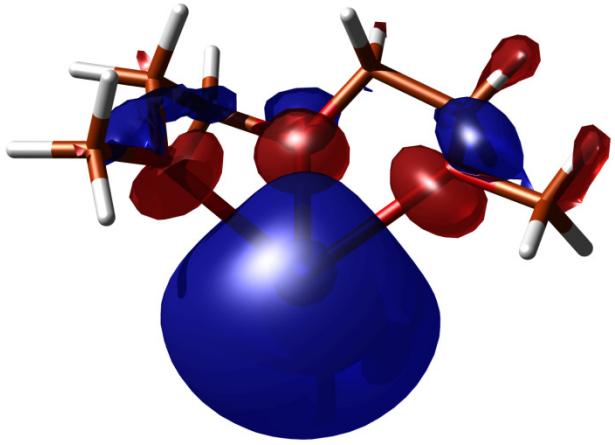

LUMO

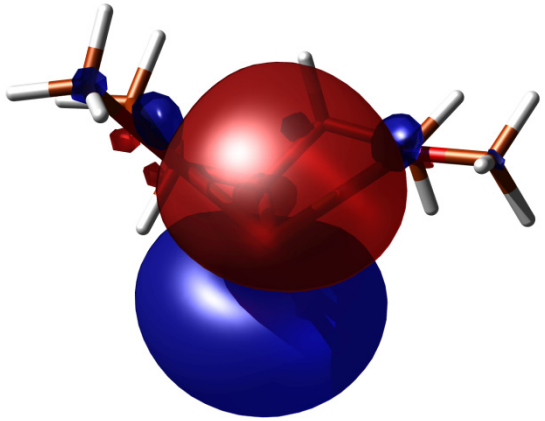

[Triglyme·In]$^{+}$

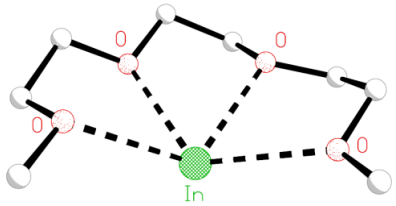

HOMO

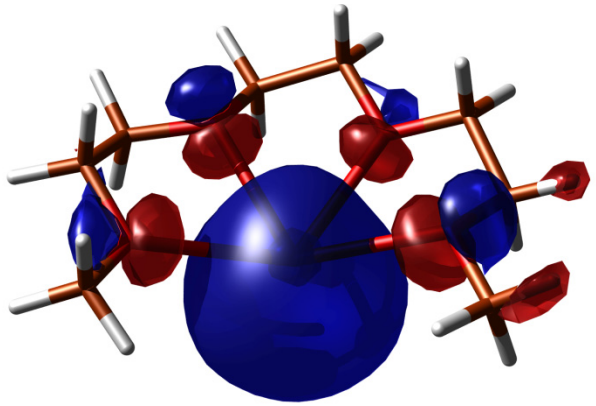

LUMO

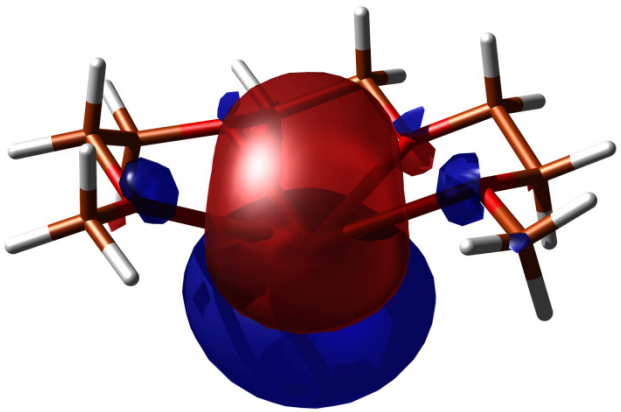

[Tetraglyme·In]$^{+}$

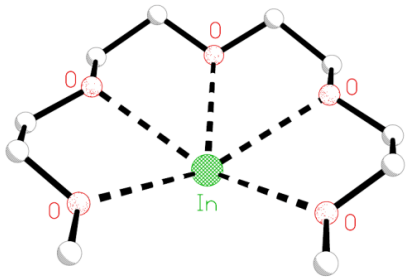

HOMO

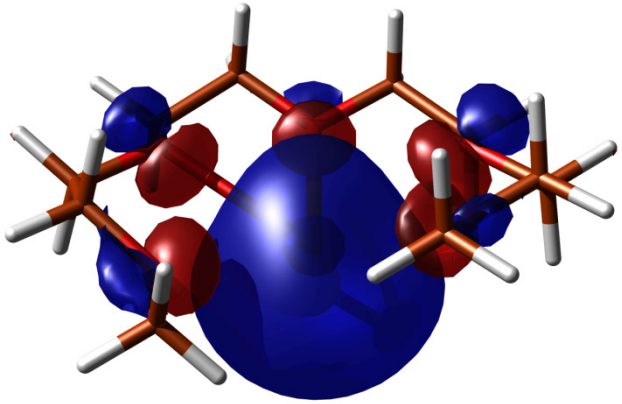

LUMO

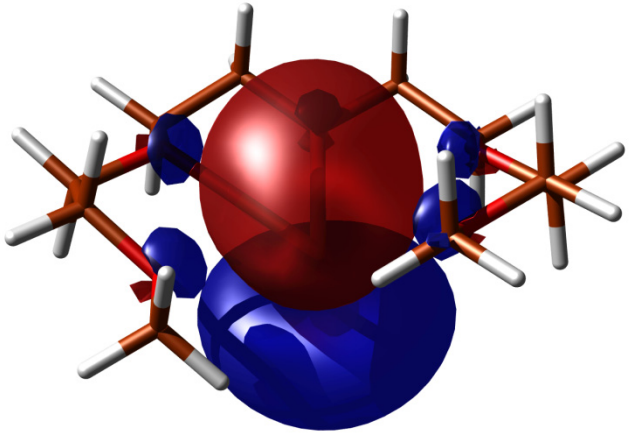

3.7 - References

[1] Tuck, D. G., *Chem. Soc. Rev.* **1993,** *22*, 269.

[2] Khan, M. A.; Peppe, C.; Tuck, D. G., *Organometallics* **1986,** *5*, 525.

[3] Annan, T. A.; Tuck, D. G.; Khan, M. A.; Peppe, C., *Organometallics* **1991,** *10*, 2159.

[4] dosSantos, J. E.; Peppe, C.; Brown, M. A.; Tuck, D. G., *Organometallics* **1996,** *15*.

[5] Peppe, C.; Tuck, D. G.; de Andrale, F. M.; Nobrega, J. A.; Brown, M. A.; Burrow, R. A., *J. Organomet. Chem.* **2005,** *690*, 925.

[6] Hill, M. S.; Hitchcock, P. B.; Pongtavornpinyo, R., *Inorg. Chem.* **2007,** *46*, 3783.

[7] Cooper, B. F. T.; Andrews, C. G.; Macdonald, C. L. B., *J. Organomet. Chem.* **2007,** *692*, 2843.

[8] Bandyopadhyay, R.; Cooper, B. F. T.; Rossini, A. J.; Schurko, R. W.; Macdonald, C. L. B., *J. Organomet. Chem.* **2010,** *695*, 1012.

[9] Cooper, B. F. T.; Macdonald, C. L. B., *Main Group Chem.* **2010,** *9*, 141.

[10] Annan, T. A.; Chadha, R. K.; Doan, P.; McConville, D. H.; McGarvey, B. R.; Ozarowski, A.; Tuck, D. G., *Inorg. Chem.* **1990,** *29*, 3936.

[11] Yang, Z. Y.; Gould, E. S., *Dalton Trans.* **2004**, 1858.

[12] Hioe, J.; Zipse, H., *Org. Biomol. Chem.* **2010,** *8*, 3609.

[13] Kuhn, N.; Kratz, T., *Synthesis* **1993**, 561.

[14] Pearson, R. G., *J. Am. Chem. Soc.* **1963,** *85*, 3533.

[15] Pearson, R. G., *J. Chem. Educ.* **1968,** *45*, 581.

[16] Pearson, R. G., *J. Chem. Educ.* **1968,** *45*, 643.

[17] Cooper, B. F. T.; Macdonald, C. L. B., *New J. Chem.* **2010,** *34*, 1551.

[18] Pangborn, A. B.; Giardello, M. A.; Grubbs, R. H.; Rosen, R. K.; Timmers, F. J., *Organometallics* **1996,** *15*, 1518.

[19] *APEX-II*, Bruker ASX, Inc: Madison, WI, 2013.

[20] Sheldrick, G. M., *Acta Crystallogr., Sect. A: Found. Crystallogr.* **2008,** *64* (1), 112.

[21] Farrugia, L. J., *J. Appl. Crystallogr.* **1999,** *32*, 837.

[22] Perdew, J. P.; Chevary, J. A.; Vosko, S. H.; Jackson, K. A.; Pederson, M. R.; Singh, D. J.; Fiolhais, C., *Phys. Rev. B* **1992,** *46*, 6671.

[23] Perdew, J. P.; Burke, K.; Wang, Y., *Phys. Rev. B* **1996,** *54*, 16533.

[24] Becke, A. D., *J. Chem. Phys.* **1993,** *98*, 5648.

[25] Frisch, M. J.; Trucks, G. W.; Schlegel, H. B.; Scuseria, G. E.; Robb, M. A.; Cheeseman, J. R.; Scalmani, G.; Barone, V.; Mennucci, B.; Petersson, G. A.; Nakatsuji, H.; Caricato, M.; Li, X.; Hratchian, H. P.; Izmaylov, A. F.; Bloino, J.; Zheng, G.; Sonnenberg, J. L.; Hada, M.; Ehara, M.; Toyota, K.; Fukuda, R.; Hasegawa, J.; Ishida, M.; Nakajima, T.; Honda, Y.; Kitao, O.; Nakai, H.; Vreven, T.; Montgomery, J., J. A.; Peralta, J. E.; Ogliaro, F.; Bearpark, M.; Heyd, J. J.; Brothers, E.; Kudin, K. N.; Staroverov, V. N.; Kobayashi, R.; Normand, J.; Raghavachari, K.; Rendell, A.; Burant, J. C.; Iyengar, S. S.; Tomasi, J.; Cossi, M.; Rega, N.; Millam, N. J.; Klene, M.; Knox, J. E.; Cross, J. B.; Bakken, V.; Adamo, C.; Jaramillo, J.; Gomperts, R.; Stratmann, R. E.; Yazyev, O.; Austin, A. J.; Cammi, R.; Pomelli, C.; Ochterski, J. W.; Martin, R. L.; Morokuma, K.; Zakrzewski, V. G.; Voth, G. A.; Salvador, P.; Dannenberg, J. J.; Dapprich, S.;

Daniels, A. D.; Farkas, Ö.; Foresman, J. B.; Ortiz, J. V.; Cioslowski, J.; Fox, D. J. *Gaussian 09*, A.1; Gaussian Inc.: Wallingford, CT, 2009.
[26] Reed, A. E.; Curtiss, L. A.; Weinhold, F., *Chem. Rev.* **1988,** *88*, 899.
[27] Glendening, E. D.; Reed, A. E.; Carpenter, J. E.; Weinhold, F. *NBO Version 3.1*, Madison, Wisconsin.

Chapter 4: Non-Innocent Ligand Effects on Low Oxidation State Indium Complexes

4.1 - Introduction

The term "non-innocent" is used to describe ligands which have the potential to undergo redox behaviour that may result in some ambiguity in the assignment of an oxidation state of the metal to which they are bound.[1-3] Thus, ligands that have a propensity to undergo redox chemistry may render simple electron counting of the metal difficult and require the use of more sophisticated techniques in order to determine the most appropriate oxidation states of the species involved. From a practical point of view, the redox flexibility of such systems can engender a large variety of interesting and useful chemistry.

Ligands that can be described as "non-innocent" range from small molecules such as O_2 or RN=NR to larger, more conjugated ligands like *o*-quinone and unsaturated C_n chains. These types of ligands occur frequently in naturally occurring biological systems,[4] have many potential applications in devices such as NIR harvesting compounds[5] and can also play an important role as ligands for transition metal catalysts.[6] Given the foregoing, the chemistry exhibited by "non-innocent" ligands has been reviewed extensively.[2-3]

One of the most important classes of non-innocent ligands used regularly in inorganic chemistry are the 1,4-diazabutadienes (DAB).[7-9] These α-diimine ligands are able to undergo two sequential one e^- reductions to form radical anionic or dianionic ligands, respectively, and can thus potentially oxidize an element or complex in the process (Scheme 4.1).

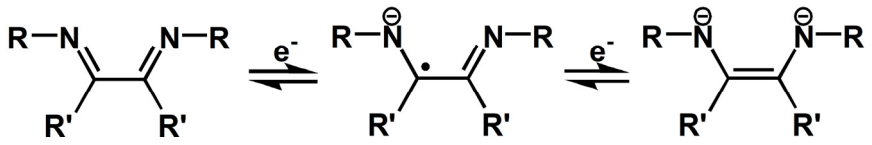

Scheme 4.1: Reduction process of $^{R}DAB^{R'}$.[8]

When coordinated to low oxidation state main group atoms or ions, these complexes can generate the main group analogues of *N*-heterocyclic carbenes. The preparation, structure and reactivity of these carbenoids have been under investigation for many years.[10-12] For example, the groups of Cowley and Macdonald showed that when they are treated with univalent phosphorus precursors, DAB ligands undergo a formal $2e^-$ reduction, oxidizing the group 15 element from +1 to +3.[13-14] The relative instability of the P^I oxidation state invariably leads to oxidation of the phosphorus, regardless of the R or R′ group. A similar two-electron ligand reduction was also observed in the coordination of Al(I)Cp* and Ga(I)Cp* to neutral DAB ligands.[15-16] In both cases, the resultant heterocycles are best-described as being composed of dianionic DAB fragments bonded to Al(III) or Ga(III) centres, which are substituted by the Cp* ligands in an η^1- or η^5-fashion, respectively. Cowley also showed that reduction of the DAB ligand prior to reaction with $GaCl_3$ generates related Ga(III) complexes.[17] In contrast, the groups of Jutzi and Jones found that the addition of DAB ligands to "GaI" and InCl resulted in a series of paramagnetic Ga(II), Ga(III)[18-19] and In(II)[20] products which were formed through various disproportionation pathways (Scheme 4.2). Jones *et al.* also showed that the addition of InCl to pre-reduced lithiated DAB ligands results in disproportionation reactions, yielding the radical complex ($^{Dipp}DAB^{H}$)$InCl_2$(THF).[21]

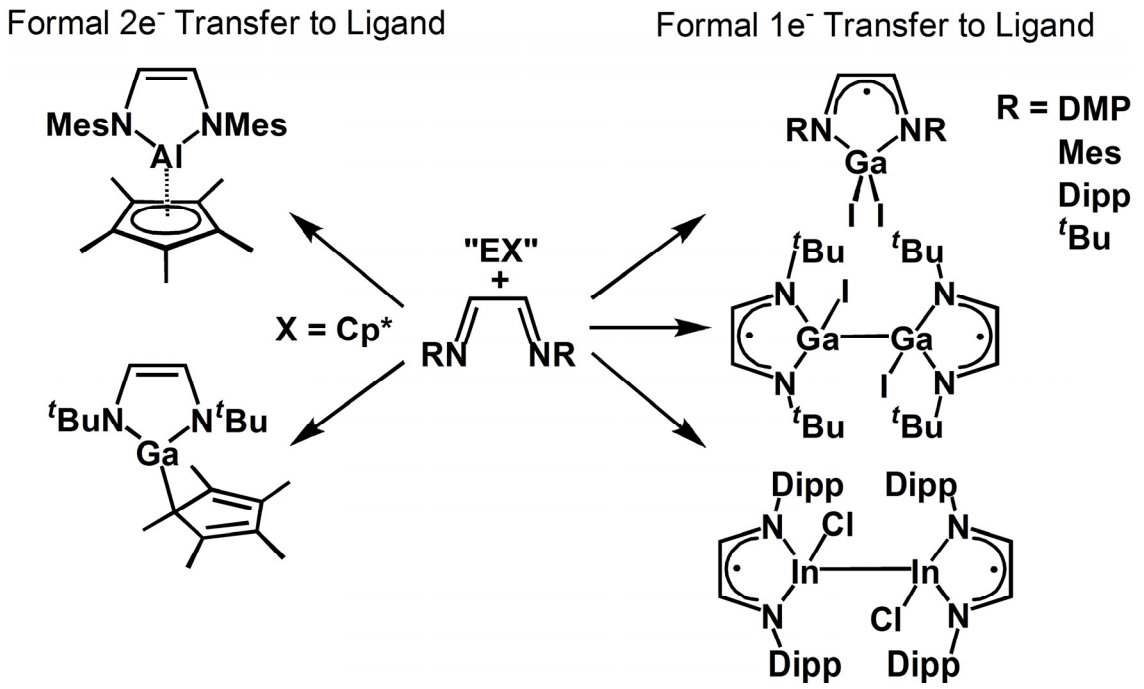

Scheme 4.2: Reaction of DAB ligands with Ga(I), Al(I) and In(I) halides and Cp* compounds.

The ability of univalent indium to act a Lewis acid (and base) has been under investigation for many years.[22-24] Although the more core-like nature of the valence *s*-orbital is anticipated to lead to a greater degree of stability for the indium(I) oxidation state in relation to the lighter group 13 elements, attempts to ligate bases, including DAB ligands as described above, to In(I) halides typically leads to disproportionation resulting in the production of indium metal and the generation of higher-oxidation-state species.[25-27] Oligomeric clusters are typically observed in the solid state for related E(I) halide complexes.[25, 28] Notably, Jones *et al*. showed in 2007 that it is indeed possible to isolate the donor-stabilized complex InBr·TMEDA (TMEDA = tetramethylethylenediamine) at temperatures between -30°C and -20°C, however, disproportionation to In_2Br_4·2TMEDA is observed above this temperature. Similar attempts to coordinate TMEDA to InI

resulted in the formation of the mixed valent indium cluster, $In_6I_8 \cdot 4TMEDA$.[25] Likewise, attempts to incorporate indium(I) halides into cyclic ether ligands at room temperature result in the formation of mixed-valent In(I)-In(III) donor-acceptor complexes.[29]

In contrast to the univalent halides, we have previously shown that the more stable indium(I) triflate, InOTf,[30-31] can form a monomeric donor-stabilized species in the presence of appropriate ligands.[32-33] Although the treatment of InOTf with TMEDA results in immediate disproportionation, the reaction with crown ethers produces remarkably robust species. In fact, the complex [In([18]crown-6)][OTf] was the first stable monomeric complex in which an inorganic In(I) centre acts as an acceptor. Likewise, Richeson and co-workers were also able to obtain stable complexes of tridentate 2,6-diiminopyridyl (dimpy) ligands with InOTf but not with the monovalent indium halides.[34-35] The important role of the cation-anion interactions in determining the stability of such complexes was further emphasized by Krossing and others, who demonstrated that univalent group 13 salts of non-coordinating anions can also function as acceptors without decomposing.[36-38]

One electronic feature common to both the stable cyclic polyether complexes and the dimpy complexes is the apparent absence of strong covalent bonding interactions between the ligand and the indium centre.[35] It is noteworthy that these N-donor dimpy ligands appear to behave as "innocent" ligands to indium in spite of their more complex behavior when binding to the heavier chalcogens.[39-41]

In this chapter, the role of the substitution pattern on a series of DAB ligands in the formation of Lewis adducts with a low oxidation state indium centre is elucidated and

the experimental results reveal that the outcome of each reaction is remarkably dependent on the electron releasing/withdrawing properties of the substituents on the DAB framework.

4.2 - Results

4.2.1 Synthesis and Crystallography

As indicated above, all previous attempts to coordinate indium(I) halides to DAB ligands have resulted in disproportionation leading to chelated In(II)[21] or In(III) species.[20] In light of the poor solubility and relative instability of the indium(I) halides, we selected the more stable and soluble InOTf reagent for the attempts to synthesize indium(I) diimine complexes.

The treatment of equimolar amounts of InOTf and either functionalised $^{R}DAB^{R'}$ or bis(aryl)acenaphthenequinonediimine (^{R}BIAN) ligands in toluene results in marked colour changes and the generation of intensely coloured solutions from which a range of solids **4.1** – **4.6** (Figure 4.3) were isolated. In stark contrast to the reaction of the In(I) halides, there is no evidence for any deposition of indium metal and microanalytical data confirmed the formation of 1:1 adducts in each case. The orange to red colors observed for **4.5** and **4.6** are indicative of the formation of radical anion fragments of the type $[^{R}BIAN]^{\bullet-}$,[42] but, given the non-innocent nature of the diimine ligands, the nature of these complexes required structural and/or spectroscopic authentication.

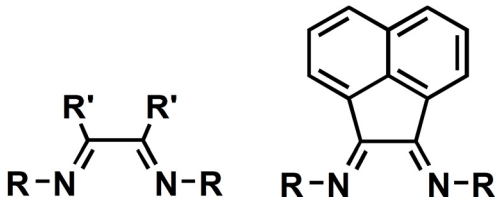

4.1 [^{Mes}DAB^{Me}In][OTf] R = Mes, R′ = Me

4.2 [^{Mes}DAB^{H}In][OTf] R = Mes, R′ = H

4.3 [^{Dipp}DAB^{Me}In][OTf] R = Dipp, R′ = Me

4.4 [^{Dipp}DAB^{H}In][OTf] R = Dipp, R′ = H

4.5 [^{Mes}BIANIn][OTf] R= Mes

4.6 [^{Dipp}BIANIn][OTf] R = Dipp

(Mes = 2,4,6-$Me_3C_6H_2$; Dipp = 2,6-($^{i}Pr)_2C_6H_3$)

Figure 4.1: ^{R}DAB$^{R'}$ and ^{R}BIAN Ligands

The attempted recrystallization of these 1:1 adducts from a range of solvents persistently afforded amorphous or poorly crystalline materials but in two cases, crystals of sufficient quality were isolated and allowed for the constitution, connectivity and gross structural features of each complex to be determined unambiguously. Each structure features a remarkably different bonding pattern and the results suggest a marked dependence on the seemingly minor changes to the ligand framework. The complex ^{Mes}DAB^{Me}InOTf (**4.1**) crystallizes in the space group *P*bca and comprises a three coordinate pyramidal In centre with a sum of 233.5° for the angles around indium (Figure 4.2). The In-N bond distances (2.4925(4) – 2.5091(4) Å) are comparable to those reported by Richeson for the In-$N_{(pyridine)}$ dative bonds in the In(I) dimpy complexes of 2.495(5) – 2.502(5) Å; in contrast, In(III) to N distances are typically shorter than 2.4 Å.[34-35] Furthermore, examination of the metrical parameters within the ligand framework confirms that the molecular geometry is consistent with the formulation of **4.1** as a bis-

imine complex of In(I). The C(1)-C(2) distance of 1.520(19) Å and the C-N bond lengths of 1.242(16) and 1.292(16) Å are consistent with those of neutral imine compounds, i.e. those with predominantly C=N and C−C character.

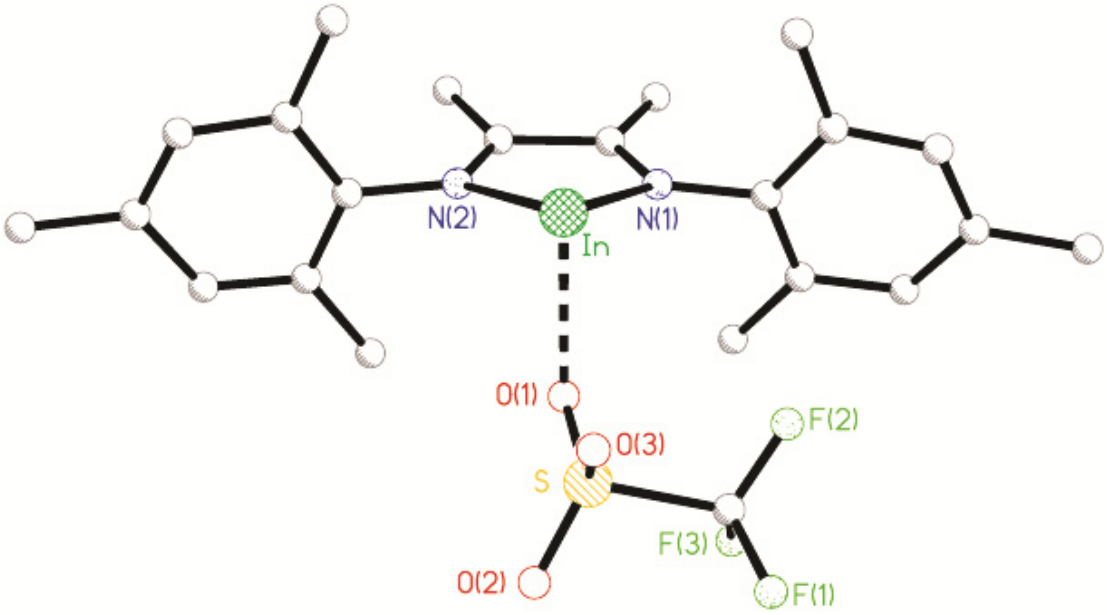

Figure 4.2: Solid state structure of **4.1**. Selected bond distances (Å) and angles (˚): In(1)-N(1): 2.448(11); In(1)-N(2): 2.459(11); In(1)-O(1): 2.450(10); N(1)-C(1): 1.292(16); N(2)-C(2): 1.242(16); C(1)-C(2): 1.520(19); S-$O_{(range)}$: 1.433(10)-1.467(10); N(1)-In(1)-N(2): 65.1(4); N(X)-In(1)-O(1): 83.7(4)-84.7(3); $\Sigma_{<@In}$: 233.5(11). Hydrogen atoms and a toluene of crystallization are omitted for clarity.

In a similar manner, the reaction of InOTf with $^{Mes}DAB^{H}$ provided crystals of the complex (**4.2**) suitable for analysis by single-crystal X-ray diffraction. Although hampered by persistently poor crystal quality, structure solution clearly revealed the atomic connectivity. The material crystallizes in the triclinic space group *P*-1 with four formula units of "$^{Mes}DAB^{H}InOTf$" in the asymmetric unit. In spite of the similarity of the

empirical formulae, the structure of **4.2** (Figure 4.3) is dramatically different from that of **4.1**.

The most immediately apparent difference between **4.1** and **4.2** is the presence of an In−In bond (In(1)-In(2) and In(3)-In(4) of 2.656(1) and 2.665(1) Å, respectively). These distances are considerably shorter than the 2.7280(9) Å reported by Jones for a related In(II) DAB complex[20] and are also shorter than the majority of other In-In bonds previously reported.[43] The shortness is likely a consequence of the bonds in **4.2** each being supported by two bridging μ–κ^2-O,O′-triflate groups. Moreover, the observed In-N bond lengths at each of the crystallographically independent In centres are distinctly different and include one short In-N bond (2.050(7) – 2.075(7) Å) and one long In-N bond (2.216(7) – 2.256(7) Å). The former distances are comparable with other covalent In-N bonds. The latter are more similar to those observed in **4.1**, consistent with a dative covalent In(II)-N bond (*cf*. 2.168 - 2.237 Å).[44-45] In addition, there are substantial differences within the ligand framework of **4.2** as compared to **4.1**, as demonstrated by the data in Table 4.1. For example, there are two clearly different C-N bond distances within each DAB ligand: one longer (1.446(10) – 1.476(9) Å) and one shorter (1.291(10) – 1.309(10) Å). Even more importantly, one of the C atoms from the DAB heterocycle is *tetracoordinate* and features a new C-C bond formed (1.483(11) – 1.509(11) Å) to an adjacent unit of **4.2**. These distances are typical of C-C single bonds and do not merit further discussion.

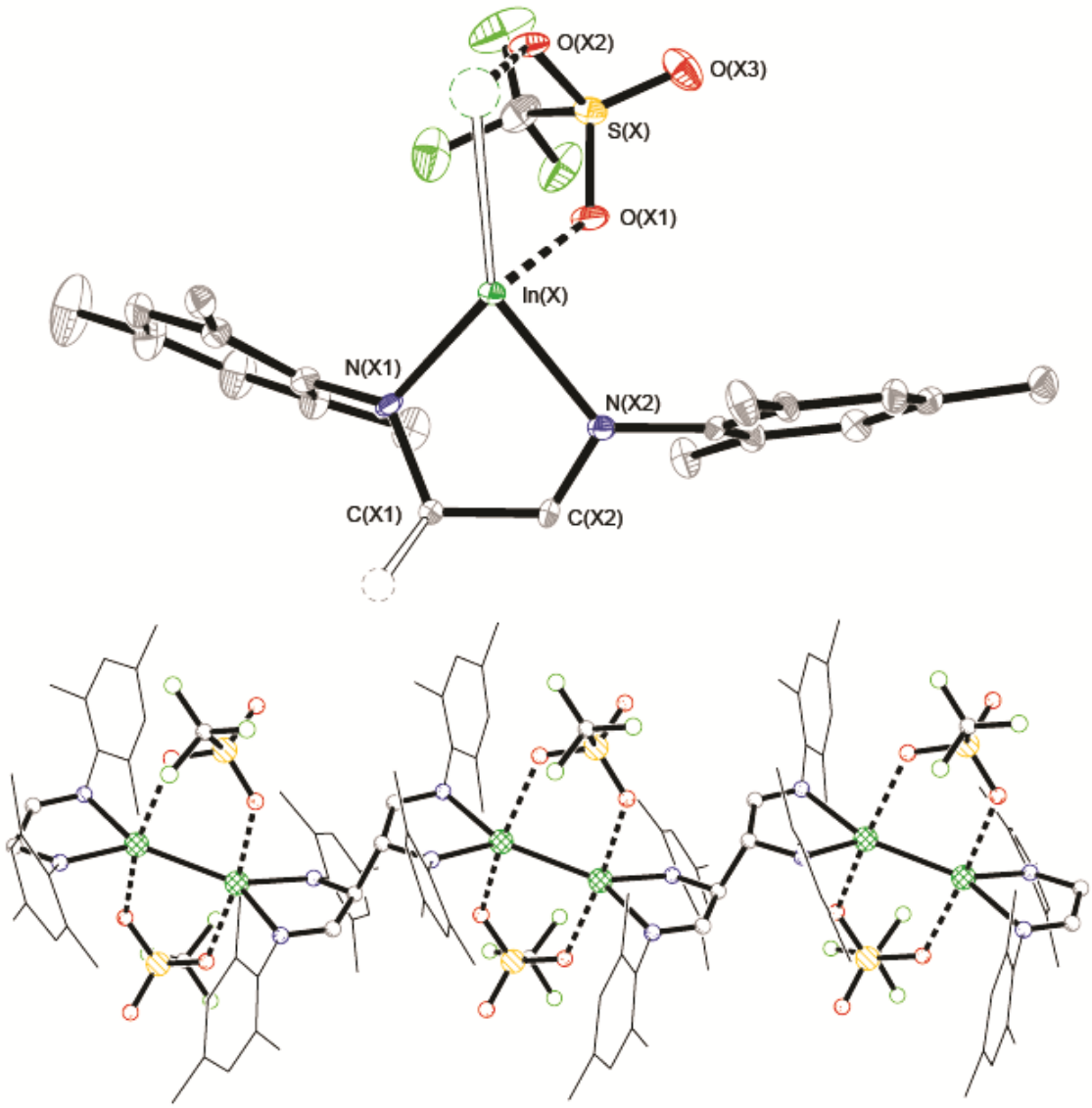

Figure 4.3: Top: thermal ellipsoid plot of one of the four crystallographically independent formula units of **4.2** in the asymmetric unit (20% probability surface). Open circles indicate the connections to adjacent molecules. Bottom: the polymeric structure of **4.2**. Hydrogen atoms are omitted for clarity.

Table 4.1: Selected bond lengths (Å) in **4.2**.

	X=1	X=2	X=3	X=4
InX-NX1	2.235(6)	2.241(6)	2.216(7)	2.256(7)
InX-NX2	2.063(7)	2.057(7)	2.075(7)	2.050(7)
NX1-CX1	1.292(10)	1.301(10)	1.291(10)	1.309(10)
NX2-CX2	1.446(10)	1.476(9)	1.454(10)	1.475(10)
CX1-CX2	1.500(11)	1.496(11)	1.483(11)	1.509(11)
InX-In(X+1)	2.656(1)		2.665(1)	
In1-O11	2.362(6)		In3-O31	2.418(6)
In1-O22	2.578(6)		In3-O42	2.489(6)
In2-O21	2.360(6)		In4-O41	2.373(6)
In2-O12	2.581(5)		In4-O32	2.509(6)
C11-C21	1.586(11)		C31-C41	1.587(12)

4.2.2 Cyclic Voltammetry

In order to quantify the different redox properties of the ^{R}DAB$^{R'}$ ligands, cyclic voltammetry was employed. Analogous CV investigations on a series of ^{R}BIAN ligands have been reported recently and confirm that such ligands always much easier to reduce than the corresponding DAB ligands: e.g. the first reduction wave for ^{Mes}BIAN is found at ca. –0.97 V vs. SHE.[46-48]

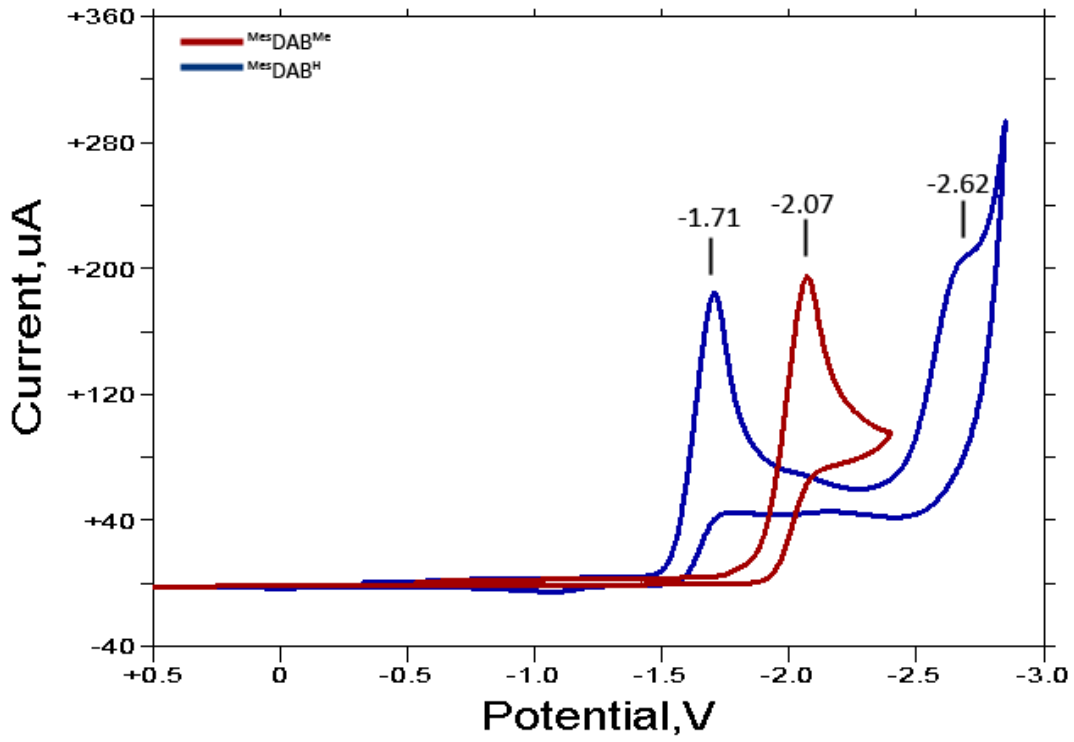

Figure 4.4: Cyclic voltammograms of $^{Mes}DAB^{H}$ (blue) and $^{Mes}DAB^{Me}$ (red) at the same concentration. Reduction of the solvent (MeCN) prevented observation of the second reduction wave for $^{Mes}DAB^{Me}$.

Both ligands appear to undergo two $1e^-$ reductions, with the $^{Mes}DAB^{H}$ ligand being more readily reduced (by 0.36 V) than $^{Mes}DAB^{Me}$ (Figure 4.4, Table 4.2). Cyclic voltammetry was also conducted on InOTf and it was found to have a relative oxidation potential (E_{pa1}) of *ca.* +0.79 V (*ca.* +1.02 V vs. SHE) in the absence of donor ligands. This potential is considerably smaller in magnitude than E_{pc1} of $^{Mes}DAB^{H}$ and the result suggests that destabilization of the non-bonding electrons on In(I) by the donor is important in this system.[49] Such destabilization is apparently sufficient to drive the first reduction of the $^{Mes}DAB^{H}$ ligand but not that of the methyl derivative. It is noteworthy that after addition of a stoichiometric amount of InOTf to the electrochemical cell, the

first reduction wave for $^{Mes}DAB^{H}$ rapidly diminishes in intensity but that of the second reduction wave remains unchanged, suggesting that **4.2** has a very similar reduction potential to $[^{Mes}DAB^{H}]^{\bullet-}$. In stark contrast, the addition of InOTf to a cell containing $^{Mes}DAB^{Me}$ does not alter the appearance of the voltammogram, indicating that coordination to In(I) does not affect the electrochemistry of the $^{Mes}DAB^{Me}$ ligand.

Table 4.2: Cathodic reduction potentials for $^{R}DAB^{R'}$ ligands (E_{pc} vs. Ag/AgCl; o/w = outside window).

	E_{pc1} (V)	E_{pc2} (V)
$^{Mes}DAB^{H}$	–1.71	–2.62
$^{Dipp}DAB^{H}$	–1.72	–2.73
$^{Mes}DAB^{Me}$	–2.10	o/w
$^{Dipp}DAB^{Me}$	–2.11	o/w

4.2.3 Electron Paramagnetic Resonance Studies

The solid state structure of **4.2** suggested the presence of radical intermediates so we pursued EPR investigations to confirm this hypothesis. In fact, although the solid state structure of **4.2** at 173K is consistent with a diamagnetic system, EPR investigations reveal the presence of paramagnetic species at elevated temperatures in the solid state and in solution at ambient temperature.

A solution of **4.2** in toluene exhibited a rich EPR spectrum, revealing hyperfine coupling to two equivalent N atoms (I = 1), two H atoms (I = ½) and ^{115}In (I = 9/2). The similarity in the ^{14}N and ^{1}H hyperfine constants give rise to an apparent decet of non-

binomial septets with g=2.0034. The g-value is consistent with a ligand-based reduction affording a g-value close to the free electron value (g_e=2.0036); an indium-based radical would give rise to a large deviation from g_e due to significant spin-orbit coupling (which scales as Z^4).[50] The large hyperfine coupling to In is not a reflection of large quantities of electron density on In but of a particularly high sensitivity factor.[51]

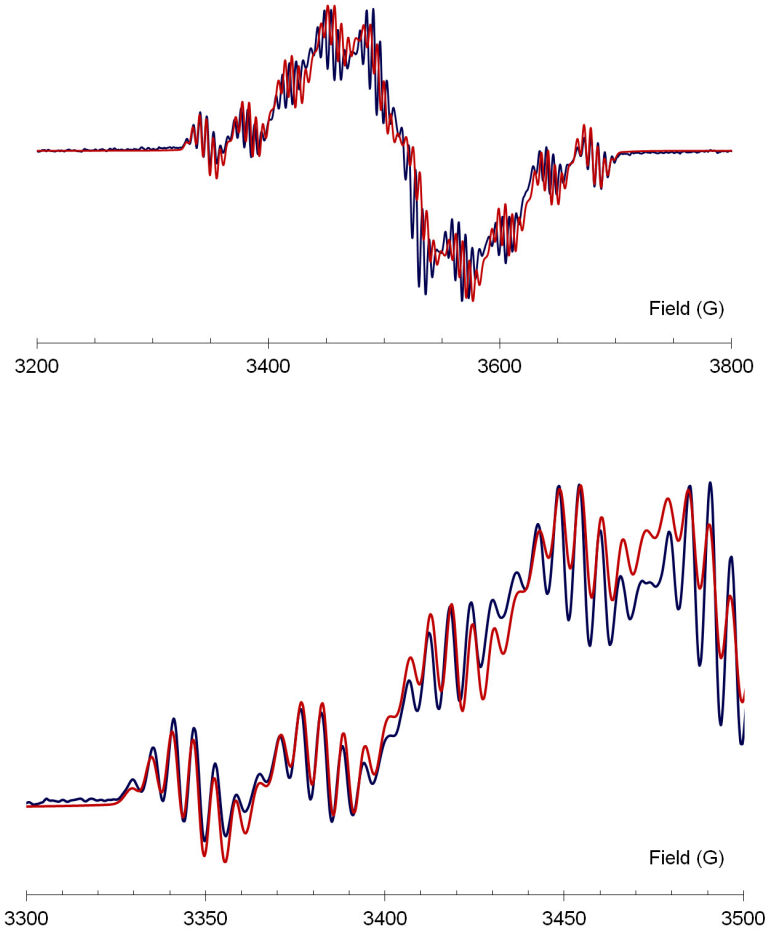

Figure 4.5: Top: Full solution EPR spectrum of **4.2** displaying broad underlying feature; bottom: expansion of the low field region detailing hyper-fine coupling. Blue = experimental, red = simulated.

This complex hyperfine pattern is overlaid on a broader unresolved (and persistent) feature which is attributed to some degree of aggregation in solution or formation solid **4.2** based on the same g-value or another poorly resolved species (see the EPR of **4.4**, *vide infra*). The low field portion of the EPR spectrum is shown in Figure 4.5 along with a simulation (a_{In} = 36.00 G, a_N = 5.80 G and a_H = 5.05 G, ΔH_{pp} =2.2 G). Notably, simulation of the entire spectrum using a first order approximation proved impossible due to the large indium hyperfine which reveals second order effects in the spectrum, i.e. a slightly unequal spacing of the spectral lines with an incremental increase of *ca.* 0.5 G in the measured indium hyperfine coupling constant with increasing field. Such behaviour is particularly prevalent for large couplings to high spin nuclei.[52] An analysis of the second order behaviour gives a_{In} = 36.9 G. These parameters are comparable to those previously reported by Jones *et al*.[20] (g = 2.0012, a_{In} = 26.2 G, a_N = a_H = 5 G) though their ^{14}N and ^{1}H couplings did not appear well resolved.

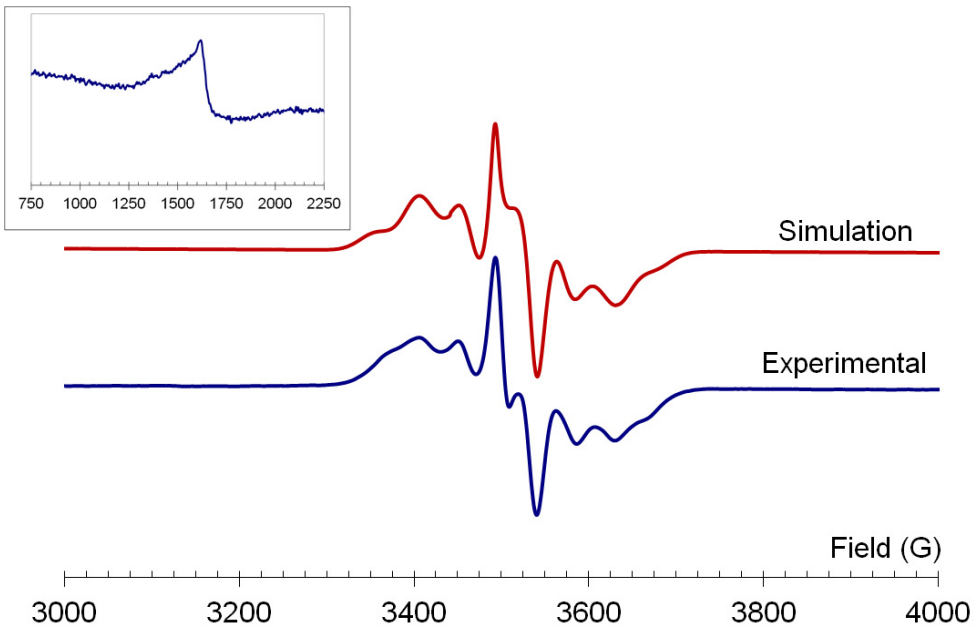

Figure 4.6: Solid state EPR spectrum of **4.2** at room temperature (g = 2.0 |D| = 0.0152, |E| = 0.002 cm^{-1}) with (inset) the $\Delta M_S = \pm 2$ half-field transition.

The solid state EPR spectrum of **4.2** at room temperature revealed a complex multiplet centred at g = 2.0 but which proved to be strongly temperature dependent. This was modelled as a superposition of an approximately axial S = ½ radical and an S = 1 species with a small zero field splitting (|**D**| = 0.0152 cm^{-1}, |**E**| = 0.002 cm^{-1}) expected for an organic radical with minimal anisotropy. The observation of the formally spin-forbidden half field resonance around 1650 G provided confirmation of the assignment as a spin-triplet (Figure 4.6 inset). On cooling to 273 K, the EPR signal was entirely quenched, indicating that the presence of the spin triplet is a thermally activated process. This process seemed entirely reversible and suggests a possible phase transition between a spin-paired low temperature phase (consistent with the crystal structure at 173 K) and a

paramagnetic phase associated with rupture of the C-C bond in the polymeric structure (Scheme 4.3).

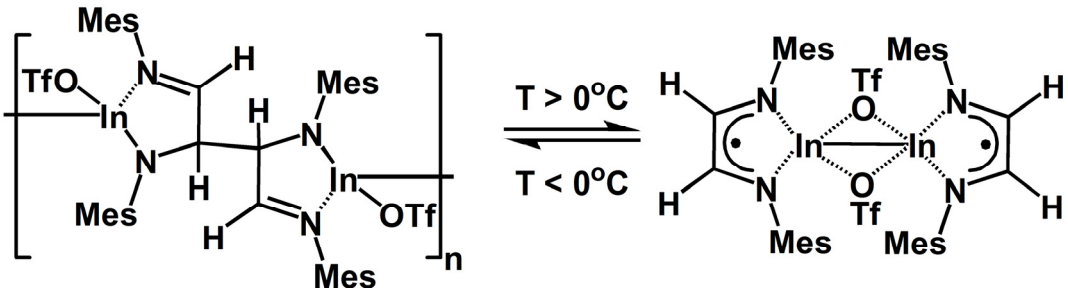

Scheme 4.3: Model for the temperature-dependent behavior of **4.2**.

Indeed the reversible nature of the phase transition would indicate that the structures of the high and low temperature phases are similar and therefore that radicals generated by C-C bond cleavage are in close proximity (Scheme 4.3). This would lead to strong magnetic exchange between the two S = ½ radicals generated by C-C bond cleavage leading to the presence of a thermally accessible spin triplet. The presence of such thermally accessible spin-triplets associated with weak dimerization has been observed in both main group radical dimers[53-55] and organic radicals[56-58].

The EPR-active nature of **4.2** prompted us to reinvestigate **4.1** in solution and this too was found to be EPR active, indicative of a reversible electron-transfer from In(I) to the ligand in solution, in spite of its apparent conventional solid state structure. The g-factor and hyperfine coupling constants (g = 2.002, a_{In} = 24.0 G, a_N = 6.6 G and a_H = 5.0G) are comparable to those observed in **4.2**, though the coupling to 6 methyl-H leads to a distinctly different hyperfine structure (Figure 4.7).

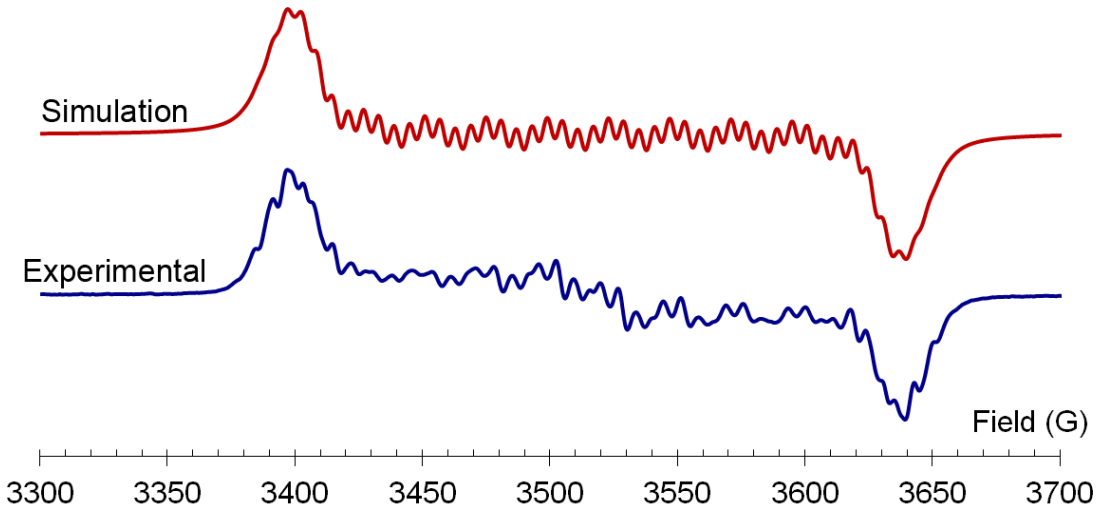

Figure 4.7: Room temperature solution EPR spectrum of **4.1** prepared *in situ* (blue = experimental, red = simulation).

An initial room temperature solution EPR spectrum of **4.4** comprises a single EPR-active species consistent with an N-based radical with the unpaired electron coupling to ***four*** N atoms associated with two $^{Dipp}DAB^{H}$ units (g = 2.0022, 4 x a_N = 6.5 G). On standing, a second EPR-active species becomes apparent, which exhibits hyperfine coupling to In (g = 2.0008, a_{In} = 29.9 G, 2 x a_N = 6.0 G, 2 x a_H = 4.8 G, ΔH_{pp} = 2.2 G), comparable with that observed for **4.2** and which similarly exhibits second order effects due to the large In hyperfine coupling (Figure 4.8).

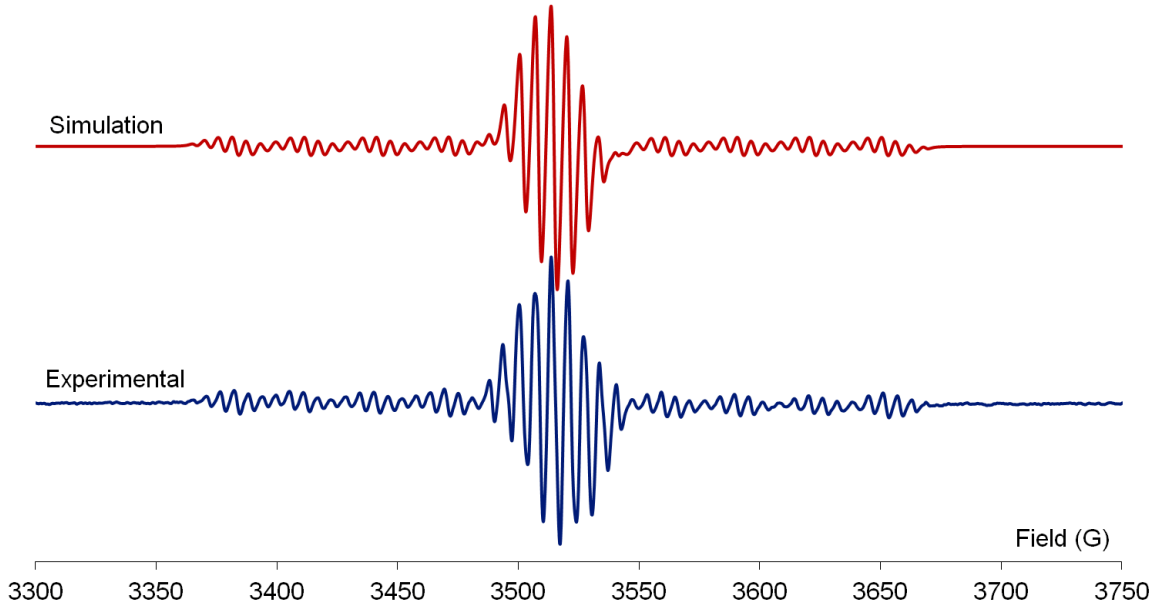

Figure 4.8: EPR spectrum of **4.4** at room temperature.

Further investigations probed the more extensively conjugated BIAN derivatives based on ^{Mes}BIAN and ^{Dipp}BIAN. In these cases the electron-transfer appears more complete, affording entirely ligand-based radicals with no evidence for indium hyperfine coupling. The EPR spectra of ^{Mes}BIANInOTf (**4.5**) and ^{Dipp}BIANInOTf (**4.6**) both reveal coupling to just two equivalent ^{14}N nuclei and two ^{1}H nuclei from the ligand framework (Figure 4.9). These couplings are similar to those of other BIAN-complexed main group species reviewed by Cowley and co-workers.[42]

Notably, **4.3** did not appear EPR active, consistent with the near identical electrochemical behaviour of the ^{Mes}DAB^{Me} and ^{Dipp}DAB^{Me} ligands and the structural features of **4.1** that suggest a formal In(I) species.

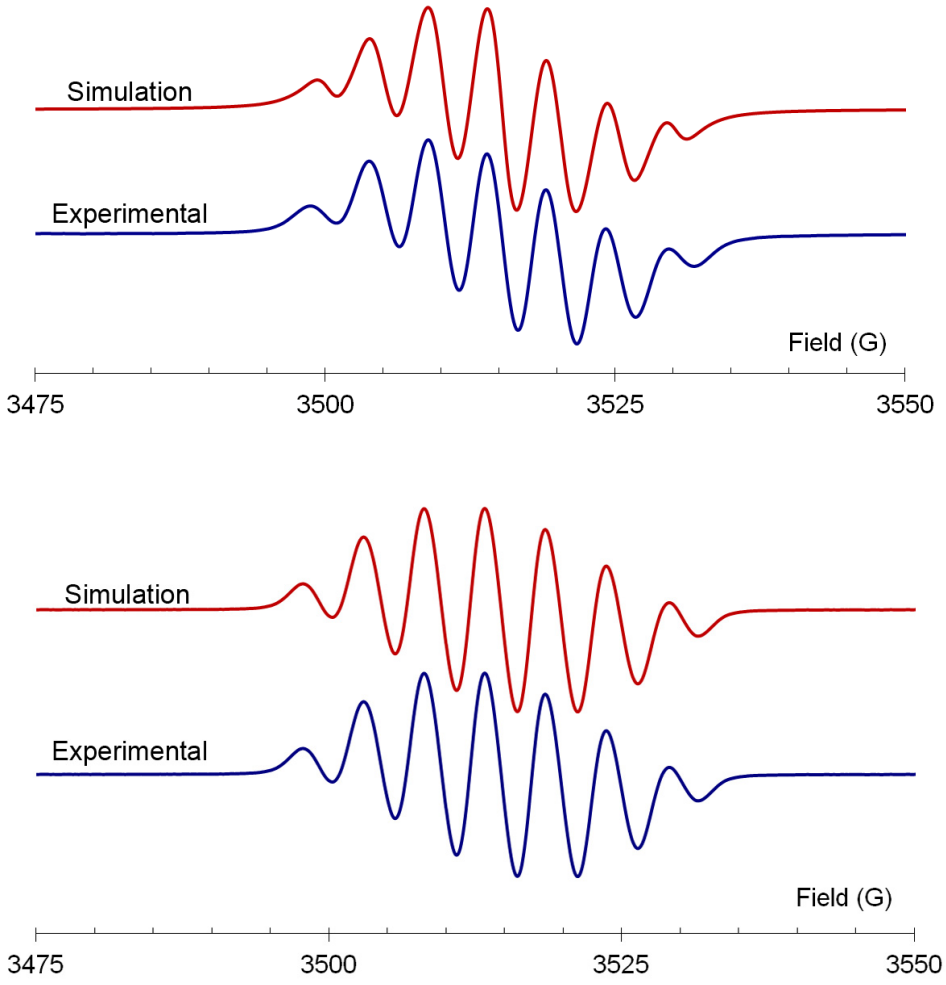

Figure 4.9: EPR spectrum of (top) **4.5** and (bottom) **4.6** at room temperature. For **4.5**: g = 2.0025, a_N = 5.4 G, a_H = 4.5 G; for 6: g = 2.0027, a_N = 4.8 G, a_H = 6.0 G.

4.3. Discussion of Experimental Work

The structural features of **4.1** are consistent with simple *N,N′*-chelation of the In(I) centre by the $^{Mes}DAB^{Me}$ ligand and are not suggestive of any metal-to-ligand electron transfer. The sum of the angles around indium in **4.1** (233.5°) is consistent with the presence of a stereochemically-active "lone pair" of electrons on the indium centre and the metrical parameters suggest a neutral DAB ligand. The "innocent" behavior of the

DAB ligand in **4.1** is unprecedented for indium(I) and lighter monovalent group 13 species. In contrast, the indium centre in **4.2** displays a strikingly more trigonal planar geometry as indicated by the sum of angles around indium (357.67-359.04°), indicative of a higher oxidative species.

The In−In distance in **4.2** (2.656-2.665 Å) is substantially less than twice the van der Waals radius of In (3.86 Å) and is at the short end of the range observed for other In-In bonds reported in the literature (*cf.* 2.646-2.938 Å[43, 59-62]), most likely as a consequence of the bridging triflate groups. Analysis of all of the metrical parameters in **4.2** suggests the monomer structure depicted in Scheme 4.4.

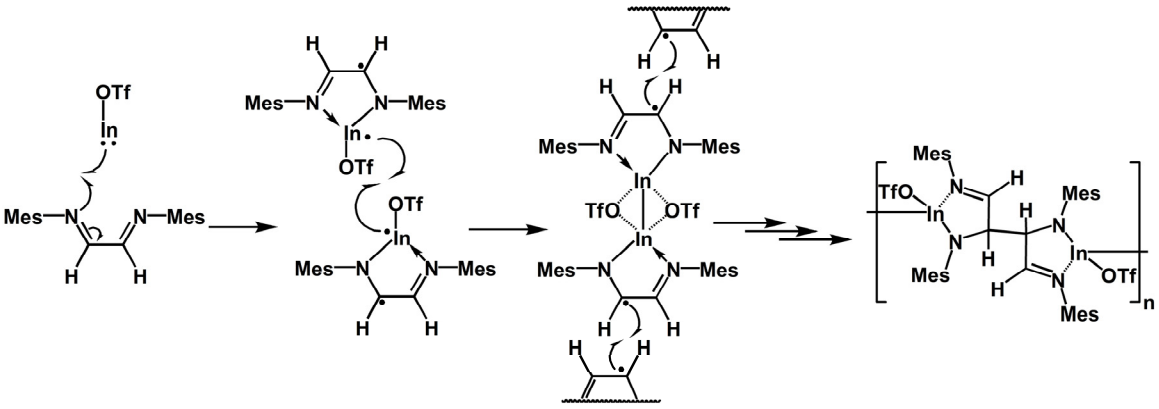

Scheme 4.4: Proposed mechanism for polymerization of **4.2**.

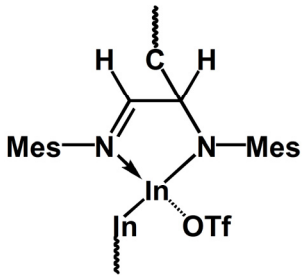

Figure 4.10: Monomer structure of **4.2**, illustrating the localized C=N double bond and different nitrogen-indium(II) bonding modes.

Overall, the presence of both an In−In bond and a C−C bond between adjacent units of **4.2** leads to a one-dimensional polymeric structure. The metrical parameters and coordination geometries in this polymer are consistent with the presence of In(II) centres generated by single electron transfer to the ligand framework with concomitant C−C coupling *via* radical dimerization of the ligand backbone (Figure 4.10).

The dramatically different structures of **4.1** and **4.2** suggest that the outcome of the reaction is highly sensitive to the redox properties of the ligand. In particular, it appears as if the replacement of the electron-releasing methyl substituents in $^{Mes}DAB^{Me}$ by H renders the $^{Mes}DAB^{H}$ ligand a superior electron acceptor. The polymeric structure of **4.2** is consistent with our electrochemical studies that indicate that the presence of hydrogen substituents on the backbone results in a more electron-poor ligand that is considerably easier to reduce than the methyl-substituted analogue. The CV studies also suggest that destabilization of the non-bonding electrons on indium(I) is necessary to render the redox process favorable.

The fact that the EPR spectrum of **4.2** appears as a ligand-based S = ½ species suggests that σ-dimerization at the indium centres is substantially stronger than dimerization *via* C−C bond formation. Indeed, cleavage of the weak C−C bond is partially offset by π-delocalisation of the resultant radical (Figure 4.7).

The electrochemical and EPR investigations of the corresponding complexes of $^{Dipp}DAB^{R'}$ ligands, **4.3** and **4.4**, suggest that these ligands result in chemistry that features similar backbone-dependence as that of the mesityl-substituted ligands. In spite of the similar electronic behavior, the discrete structure of the diradical [$^{Dipp}DAB^{H}In(Cl)In(Cl)^{Dipp}DAB^{H}$] reported by Jones and co-workers[20] suggests that the

larger steric bulk of the Dipp substituents may tend to inhibit the coupling of the DAB fragments observed for the mesityl analogs. However, it should be noted that this inhibition does not completely preclude coupling: the solid state structure of the radical [^{Dipp}DAB^{H}AlCl$_2$], prepared by the *in situ* reduction of an adduct of the ligand and aluminum trichloride, is dimeric and similar to **4.2** but features a very long 1.585(9) Å C-C bond that cleaves upon dissolution.[63] In contrast, the analogous iodide radical [^{Dipp}DAB^{H}AlI$_2$] remains monomeric in the solid state,[18] so it appears as if *N*-Dipp substituents provide DAB radicals that are at the energetic boundary of radical coupling.

Given the foregoing, it follows that the much-more-readily-reduced ^{R}BIAN ligands produce paramagnetic complexes **4.5** and **4.6** under all conditions. The analytical data, physical properties and spectroscopic data suggests that these are probably dimeric In(II)-In(II) compounds bearing two independent, and comparatively stable, [^{R}BIAN]$^{\bullet-}$ radical anion fragments that are inherently much less prone to coupling than the DAB analogues (*cf.* the high-temperature form of **4.2** illustrated in Figure 4.6).

4.4 - Computational Investigations

Several previous computational investigations into group 13 *N*-heterocyclic carbene (NHC) analogues have focused on analyses of anionic group 13 diazabutadiene (DAB) compounds (Figure 4.11) and suggest that the bonding between indium and the nitrogen atoms of the DAB ligand is primarily electrostatic in nature.[10, 64-66] It is perhaps worth noting that the anions of this type are typically synthesized by reduction of existing E(II) dimers related to **4.2** (or their isomers in the case of Ga) and cleavage of an E-E bond.[67]

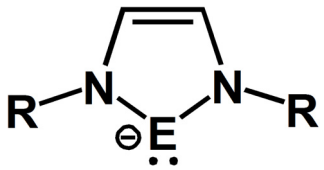

Figure 4.11: Group 13 NHC analogues.

The previous computational work on neutral group 13 DAB complexes has concentrated on the modeling of EPR parameters for the reported radical metal dihalides.[19, 63, 68] There has been virtually no work on cations or neutral molecules of the kind described above in particular regard to whether electron transfer has occurred (or should occur) so computational investigations of model DAB complexes of E-X species were pursued in order to provide insight into the nature of bonding and substituent effects in these systems. As previously noted, Richeson *et al.* find very little covalent interaction between diiminopyridine ligands and the indium centres in their dimpy complexes and proposed that a lower 5s orbital contribution to the HOMO of the diiminopyridine complex is consistent with a more stable molecule.[29, 35, 46]

Herein, we employ Natural Bond Order (NBO) analyses, Wiberg Bond Indices (WBI), and geometrical analyses in an effort to rationalize the similarities and differences observed experimentally between the closely related diimine complexes described above.

The nature of the bonding between the metal centre and the DAB fragment in a formal complex derived from the formal combination of a neutral DAB ligand and a neutral univalent group 13 species (EX) can be described by three different canonical structures as illustrated in Scheme 4.5. The bonding motifs in these possible structures include: a more covalent ligand-metal interaction wherein both electrons of the "lone

pair" of electrons on the metal are formally transferred to the DAB ligand (E^{III}/DAB^{2-}); a diradical species derived from single electron transfer from the metal to the ligand (E^{II}/DAB^{-}); and, a donor-acceptor complex in which the "lone pair" remains associated with the metal centre (E^{I}/DAB). Analysis of the geometrical features and electron distributions in such neutral complexes can provide insight into the nature of the bonding within the complex.

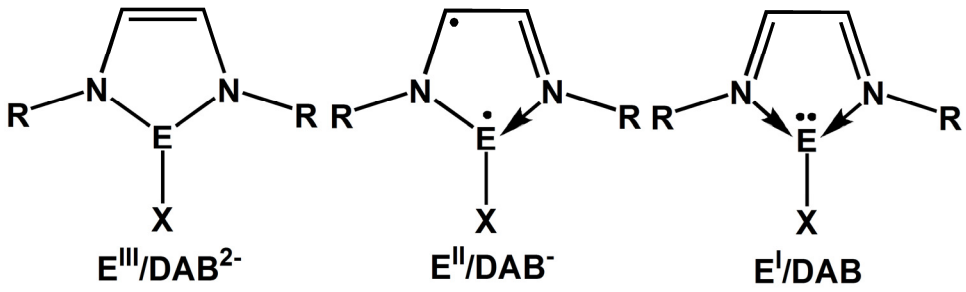

Scheme 4.5: Potential canonical forms for DAB complexes of E-X species; (i) ligand reduction and covalent bonding; (ii) partial ligand reduction with dative and covalent bonding; (iii) donor-acceptor complex formation.

Initial geometry optimizations were performed on model complexes of the form $EX{\cdot}^{H}DAB^{H}$ (E = Ga, In; X = Cl, OTf) in order to establish the ideal structures adopted by these four species. The gallium analogues were calculated in order to asses the reliability of our computational approach for the examination the formal "ligand reduction" that may occur. The isovalent gallium models are insightful because the oxidation of Ga(I) to Ga(III) is always considerably more favourable than it is for the indium analogue and, more importantly, because 2-electron transfer products have been characterized experimentally for gallium.[16, 69-70]

The B3PW91 optimized structures (Figure 4.12, Table 4.3) demonstrate that a pyramidal geometry is favored for the metal in both indium models regardless of the identity of the substituent X and is in agreement with the structural data for **4.1**. For the triflate salt the sum of the bond angles at In is 269°. In contrast, for gallium, two different structures are observed depending on the identity of the substituent. For the weakly interacting triflate, a pyramidal geometry at gallium is observed as evidenced by a sum of the bond angles equal to 307°. The trend toward trigonal planarity is complete for the chloro analogue and suggests two electron transfer and formation of a gallium(III) complex occurs in the latter. The metrical parameters, NBO analyses and Wiberg Bond indices of the DAB fragments in the models are all consistent with this interpretation: the C-C and C-N distances in the GaCl model suggest a reduced DAB^{2-} anion, those in the InOTf model are consistent with a neutral DAB ligand, and those in the other models are intermediate between the two extremes.

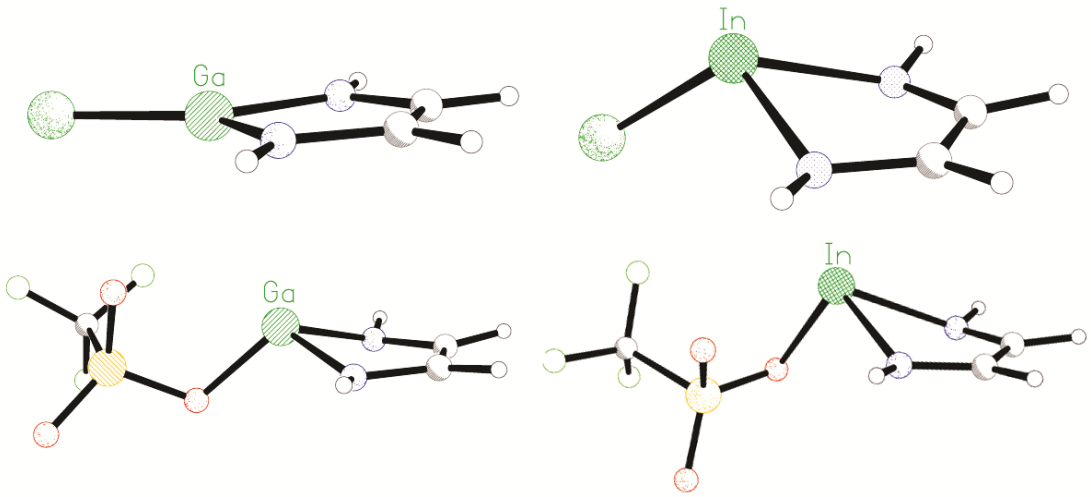

Figure 4.12: Optimized structures of $ECl{\cdot}^{H}DAB^{H}$ (top) and $EOTf{\cdot}^{H}DAB^{H}$ (bottom).

Table 4.3: Selected metrical parameters for optimized ECl·^{H}DAB^{H} and EOTf·^{H}DAB^{H} structures; distances are reported in Å and angles in degrees. Average NBO Wiberg Bond Indices are in parentheses.

	GaCl	InCl	GaOTf	InOTf
C-C	1.358	1.404	1.384	1.431
	(1.697)	(1.353)	(1.484)	(1.216)
C-N	1.395	1.339	1.360-1.361	1.313-1.314
	(1.354)	(1.420)	(1.295)	(1.582)
N-E	1.837	2.364	1.905-1.910	2.230-2.270
	(0.725)	(0.562)	(0.664)	(0.432)
E-X	2.119	2.364	1.913	2.230
	(0.842)	(0.595)	(0.362)	(0.197)
$\Sigma_{<@E}$	360.00	308.06	307.28	269.25

The NBO charges associated with the EOTf fragment and the DAB ligand in the model complex provides a simple estimate of the degree of formal charge transfer from the metal centre to the ligand. As expected, the gallium analogue has a larger formal net charge transfer to the DAB ligand: an overall ligand charge of –0.71 is found for E = Ga versus –0.35 for E = In. The differing degree of charge transfer is also evident from the NBO analyses: a "lone pair" of electrons is still identified on the indium centre, while no "lone pair" is identified in the analysis of the gallium analogue. Furthermore, the NBO analyses confirm the diene-like bonding in the DAB fragment of the InOTf model but suggest a more delocalized ene-like model for GaOTf.

Having established that our computational approach reproduces the experimental observations at a coarse level using simple models, we sought to elucidate the effects of changing substituents. For computational efficiency, models using only hydrogen or methyl substituents on the nitrogen and carbon atoms of the DAB fragments were examined initially in order to probe the effects of electron-rich vs. electron-poor ligands. However, test calculations using a full model InOTf·^{Mes}DAB^{Me} revealed that the substituents on nitrogen have a significant influence on the electronic properties of the system; for that model, the formal charge transfer from the InOTf to the ligand drops to a negligible 0.04. The optimized In-N distances in that model average 2.446 Å and all of the other geometrical parameters match the experimental values of **4.1** closely. Model complexes featuring phenyl groups on the nitrogen atoms (i.e. InOTf·^{Ph}DAB$^{R'}$) also reproduced the experimental geometries more accurately (e.g. the avg. In-N distance calculated for InOTf·^{Ph}DAB^{Me} is 2.527 Å) and provided electronic properties similar to the complete model (e.g. formal charge transfer of 0.08) so the results from these models are the most relevant.

As confirmed by the EPR investigations described above, radical species are often formed in the reaction of InOTf with ^{R}DAB$^{R'}$. Thus, a series of triplet-singlet energy gap calculations were performed to assess the relative stabilities and properties of these paramagnetic models (Table 4.4). In each of the triplet systems, the Mulliken spin density analysis indicates that one unpaired electron is localized on the indium atom and that the other unpaired electron is delocalized in the π-system of the DAB ligand, as suggested by the (E^{II}/DAB^{-}) canonical structure in Scheme 4.5. It should also be

emphasized that no evidence was found for any unusually stable singlet diradical species (broken symmetry singlets) in these isolated gas-phase model systems.

Table 4.4: Singlet-Triplet and HOMO-LUMO energy differences for InOTf·^{R}DAB$^{R'}$ complexes; a positive value indicates that the triplet state is higher in energy than the singlet state (s = singlet; t = triplet).

	Singlet-Triplet ($kJmol^{-1}$)	HOMO-LUMO (eV)[a]
R=H	18.3	s: 2.317
R′=H		t: 2.201
R=H	30.0	s: 2.444
R′=Me		t: 2.050
R=Me	38.8	s: 2.711
R′=H		t: 1.948
R=Me	47.3	s: 2.615
R′=Me		t: 1.849
R=Ph	21.0	s: 2.269
R′=H		t: 1.765
R=Ph	40.6	s: 2.764
R′=Me		t: 1.979

[a]For triplet species, the value reported is the smallest SOMO-LUMO energy difference.

In all cases, the singlet model is predicted to be more stable than the triplet and the complexes with the H-backbone substituents exhibit lower triplet-singlet energy barriers than do the corresponding Me-subtituted models. Most importantly for the

systems we examined experimentally, the model complex InOTf·^{Ph}DAB^{H} has a singlet-triplet energy gap of only *ca.* 21 kJ/mol, suggesting that both diamagnetic and paramagnetic species may exist in solution simultaneously. In contrast, the singlet-triplet gap for the corresponding methyl-substituted model InOTf·^{Ph}DAB^{Me} is nearly twice as large.

Regardless of the nature of the substituents, the appearance of the frontier orbitals for the singlet models of all of the InOTf·^{R}DAB$^{R'}$ complexes suggest these are all best understood as coordination complexes in which there has been minimal formal metal to ligand charge transfer. For example, the frontier orbitals of InOTf·^{Ph}DAB^{H} (Figure 4.13) and InOTf·^{Ph}DAB^{Me} are nearly identical and are consistent with the presence of a "lone pair" on indium in the HOMO and a ligand-based LUMO. Most importantly, the LUMO of each system is the ligand-based π-type orbital that would produce C=C double bond character if it were populated; in fact, the ligand-based fragment of this orbital is almost identical to the LUMO of the *cisoid* form of the uncomplexed DAB ligand. Finally, it is worth noting that the two SOMO orbitals of the triplet model of InOTf·^{Ph}DAB^{H} are almost identical in appearance to those depicted in Figure 4.13 and are consistent with Mulliken spin density analysis that indicates that one unpaired electron is localized on In and the other is delocalized on the ligand.

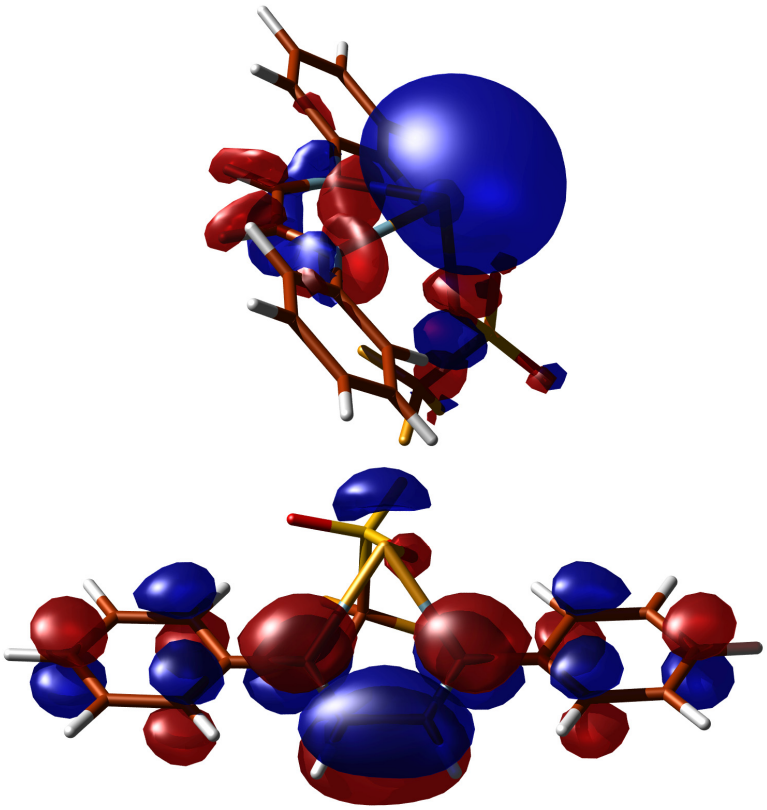

Figure 4.13: Frontier orbitals for singlet InOTf·^{Ph}DAB^{H}; top: HOMO, bottom: LUMO.

As a note of caution, we wish to emphasize that simple calculations of the energy differences between the complexes and their component donor and acceptor fragments do not adequately illustrate the differences attributable to substitution effects. For example, bond snapping[71] and fragment relaxation[72-73] energies calculated for the singlet InOTf·^{Ph}DAB$^{Me/H}$ model complexes (Scheme 4.6) reveal that it takes considerably more energy to break the bonds between the ligand and the In atom for the methyl-substituted model than for the hydrogen model. One would anticipate that the more electron-rich methyl-substituted ligand should form a stronger dative bond with the indium, and these calculations are consistent with that expectation. However, more energy is released by

the relaxation of the $^{Me}DAB^{Me}$ ligand and the overall energies associated with decomplexation are virtually identical for $^{Me}DAB^{Me}$ and $^{Me}DAB^{H}$.

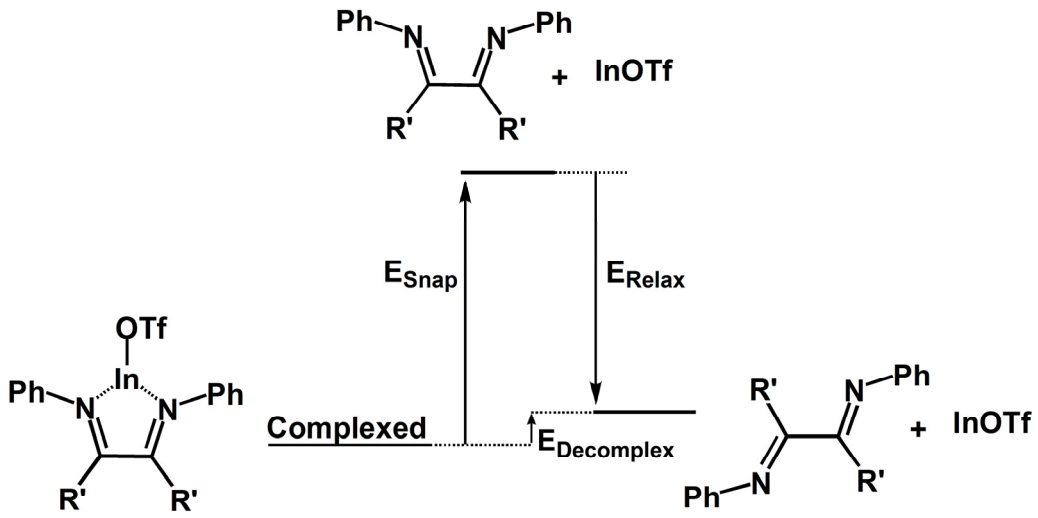

	R' = H	R' = Me
E_{Snap}	75.0	91.2
E_{Relax}	-59.5	-75.7
$E_{Decomplex}$	15.5	15.5

Scheme 4.6: Snapping, relaxation and decomplexation energies (kJ mol^{-1}) calculated for $InOTf{\cdot}^{Ph}DAB^{(Me/H)}$.

Finally, it should be noted that simple H-substituted models of the dimeric diradicals were optimized (Figure 4.14) both with and without the bridging triflate groups. The dicationic model $[^{Me}DAB^{H}In\text{-}In\ ^{Me}DAB^{H}]^{2+}$ features a very flat potential energy surface with respect to rotation about the In-In bond and the minimum is a singlet diradical with a nearly co-planar arrangement of DAB heterocycles. The analogous triplet has almost nearly indistinguishable structure and is less than 3 kJ mol^{-1} higher in

energy. Both of these models have virtually identical spin distributions with *ca*. 0.21 e^- on each indium atom and the rest of the spin density delocalized on the DAB ligand; overall, there is one one unpaired electron for each InDAB fragment and the spins are anti-parallel for the singlet and parallel for the triplet. The inclusion of the bridging OTf groups enforces the planar arrangement and results in a shortening of the In-In bond from ca. 2.774 (s)-2.784 (t) Å to 2.747 (both s and t models) Å. The presence of bridging triflates also diminishes the spin density on the indium atoms to produce exclusively ligand based radicals and, consequently, the singlet diradical and triplet models have identical energies. These predictions are consistent with the conclusions we reached on the basis of the experimental data and are consistent with previous computational work.[68]

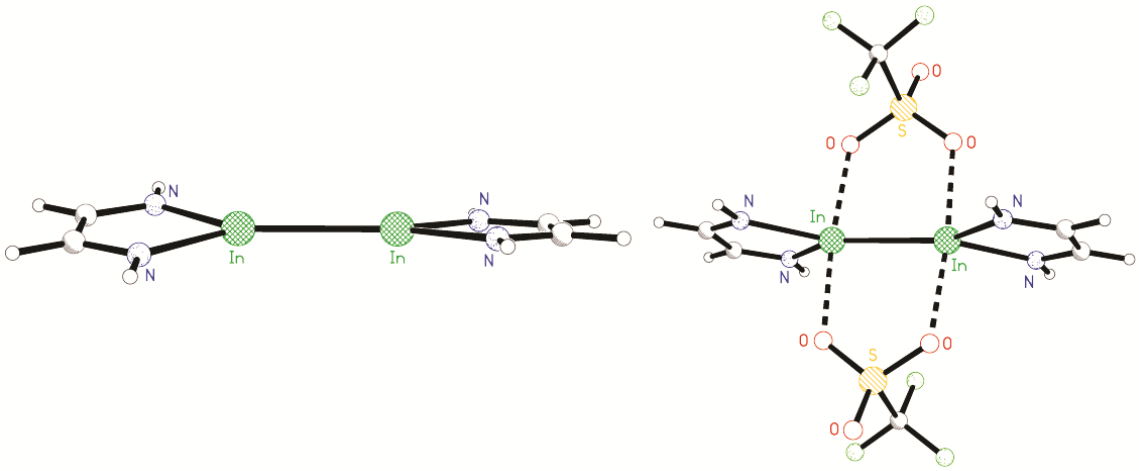

Figure 4.14: Optimized structures for [^{H}DAB^{H}In-In^{H}DAB^{H}]$^{2+}$ (left) and [^{H}DAB^{H}In(OTf)-In(OTf)^{H}DAB^{H}] (right).

4.5. Conclusions

The reaction of InOTf with a variety of α-diimines generates dramatically different products depending on the nature of the ligand substitution. The redox active (non-innocent) nature of the α-diimine allows for electron-transfer from the In(I) to the ligand framework and the degree of electron-transfer, evidenced by EPR spectroscopy and cyclic voltammetry, is sensitive to the substituents on the α-diimine. In particular, electron-releasing *C*-Me backbones on the DAB ligand appear to diminish or inhibit electron-transfer from indium to the ligand, as reflected by non-reactivity or by larger hyperfine coupling constants to In when paramagnetic species are observed, in comparison to the H-functionalized variants. Conversely use of the conjugated BIAN ligand facilitates one electron-transfer.

The variations in redox behavior are also manifested in the solid state structures of the complexes that were amenable to crystallographic investigation. Thus the coordination geometry of **4.1** is consistent with a formal indium(I) centre and a neutral DAB ligand, the more electron-accepting nature of the $^{Mes}DAB^{H}$ variant in **4.2** affords a formal indium(II) structure with a ligand-based radical which undergoes reversible oligomerization. These assignments as indium(I) and indium(II) are supported by computational studies and rationalized in terms of both electrochemical studies on the parent ligand and the analysis of computational results. Notably, these studies also confirm that the nature of the counterion on the metal is an important factor in determining complex stability with indium(I) triflate being substantially more stable to redox chemistry than the univalent indium halides.[74] More strongly interacting anions and donors have been demonstrated to destabilize the "lone pair" of electrons on low

valent main group metals and to render them more reactive.[49] In this vein, it is perhaps not surprising that the pentamethylcyclopentadienyl substituents in Cp*E actually promote *two* electron transfer from the metal to DAB ligands.[15-16] Conversely, univalent triel salts with extremely non-interacting anions appear to be even more amenable to the formation of stable donor-acceptor adducts without decomposition.[75-76]

Finally the degree of charge transfer from In to the ligand appears amenable to tuning on the backbone of the DAB ligand. Thus whilst electron-releasing *C*-methyl suppresses metal-ligand electron transfer, electron withdrawing and π-conjugated backbones should facilitate the generation of stable radicals. Indeed in the case of BIAN electron transfer appears essentially 100% complete with no evidence for In hyperfine coupling in the EPR spectrum.

4.6. Experimental

4.6.1 General Procedures

All manipulations were carried out using standard Schlenk techniques and solvents were dried using a series of Grubbs'-type columns and degassed prior to use.[77] Melting points were obtained using an Electrothermal® melting point apparatus on samples sealed in glass capillaries under dry nitrogen. Solution phase NMR spectra were recorded at room temperature on a Bruker Avance 300-MHz spectrometer. Chemical shifts are reported in ppm, relative to external standards ($SiMe_4$ for ^1H and ^{13}C NMR). InOTf and $^{Mes}DAB^{R'}$ (and all other ligands) were prepared according to reported procedures. Elemental analysis was run on a Perkin Elmer 2400, Series II CHNS/O analyzer, calibrated with acetanilide.

4.6.2 General Synthetic Procedures of InOTf with diimines

In a typical experiment toluene (20 mL) was added to InOTf (0.200 g, 0.758 mmol) and a toluene (15 mL) diimine (0.758 mmol) solution was added. The mixture was stirred overnight and volatile components were removed under reduced pressure and the product was obtained as a powder. In the case of $^{Mes}DAB^{(H/Me)}$, crystals were obtained from slow concentration of toluene solutions. In spite of the relatively low quality of the crystals, the data are more than sufficient to establish connectivity unambigously.

*Synthesis of **4.1**, InOTf:$^{Mes}DAB^{Me}$*

InOTf (0.200 g) and $^{Mes}DAB^{Me}$ (0.242 g) yielded 0.372 g (84.2 %) of an orange powder. Anal. (Calcd.): C% 48.11 (47.27), H% 4.69 (4.83), N% 4.80 (4.79). ^{1}H NMR (C_6D_6): δ = 1.20 (s, 12H, *o*-C*H*$_3$); 2.052 (s, 6H, *p*-C*H*$_3$); 2.22 (s, 6H, N=CC*H*$_3$); 6.843 (s, 4H, Aryl-C*H*). ^{13}C NMR (C_6D_6) δ = 16.16 (*p*-*C*H$_3$); 17.96 (*o*-*C*H$_3$); 20.84 (N*C*CH$_3$); 124.90 (*p*-Aryl*C*); 129.19 (*m*-Aryl*C*); 132.78 (*o*-Aryl*C*); 146.05 (*i*-Aryl*C*); 168.64 (N=*C*).

*Synthesis of **4.2**, InOTf:$^{Mes}DAB^{H}$*

InOTf (0.200 g) and $^{Mes}DAB^{H}$ (0.222 g) produced 0.422 g (100 %) of a brown-orange powder. Anal. (Calcd.): C% 43.27 (45.30), H% 4.97 (4.30), N% 4.41 (5.00).

^{1}H and ^{13}C NMR spectra contain a multitude of peaks in the methyl and aromatic region, consistent with several oligomers being present.

*Synthesis of **4.3**, InOTf:^{Dipp}DAB^{Me}*

InOTf (0.212 g) and ^{Dipp}DAB^{Me} (0.326 g) yielded 0.470 g (87.4 %) of an orange powder. Anal. (Calcd.): C% 52.85 (52.10), H% 6.42 (6.03), N% 4.14 (4.19). ^{1}H NMR (C_6D_6): δ = 1.16 (d, 12H, CH(CH_3)$_2$, J_{HH} = 6.9 Hz); 1.18 (d, 12H, CH(CH_3)$_2$, J_{HH} = 6.9 Hz); 2.87 (qq, 4H, CH(CH$_3$)$_2$, J_{HH} = 6.9 Hz); 2.14 (s, 6H, N=CCH_3); 7.18-7.10 (m, 6H, ArylH). ^{13}C NMR (C_6D_6): δ = 16.54 (N=CCH$_3$); 22.73 (CH(CH$_3$)$_2$); 23.25 (CH(CH$_3$)$_2$); 29.02 (CH(CH$_3$)$_2$); 123.53 (*p*-ArylC); 124.46 (*m*-ArylC); 135.22 (*o*-ArylC); 146.80 (*i*-ArylC); 168.50 (C=N).

*Synthesis of **4.4**, InOTf:^{Dipp}DAB^{H}*

InOTf (0.200 g) and ^{Dipp}DAB^{Me} (0.285 g) produced 0.485 g of a yellow powder. Anal. (Calcd.): C% 50.59 (50.60) H% 5.99 (5.70), N% 4.13 (4.40). ^{1}H NMR (C_6D_6): δ = 1.17 (d, 24H, CH(CH_3)$_2$, J_{HH} = 9.5 Hz); 3.12 (dq, 4H, CH(CH$_3$)$_2$) J_{HH} = 7.0 Hz); 7.14 - 7.23 (m, 6H, ArylCH); 8.18 (s, 2H, NCCH). ^{13}C (C_6D_6): δ = 23.47 (CH(CH$_3$)$_2$; 28.53 (CH(CH$_3$)$_2$); 123.56 (*m*-Aryl$C$); 124.45 (*p*-Aryl$C$); 136.93 (*o*-Aryl$C$); 128.95 (*i*-Aryl$C$); 163.49 (C=N).

*Synthesis of **4.5**, InOTf:^{Mes}BIAN*

InOTf (0.200 g) and ^{Mes}BIAN (0.315 g) produced 0.436 g (84.7 %) of a deep red/purple powder. Anal. (Calcd.): C% 52.17 (54.72), H% 4.25 (4.15), N% 3.79 (4.12). The paramagnetic nature of the compound and low solubility in C_6D_6 and other deuterated solvents precluded collection of meaningful NMR spectra.

*Synthesis of **4.6**, InOTf:^{Dipp}BIAN*

InOTf (0.200 g) and ^{Dipp}BIAN (0.378 g) produced 0.502 g (86.8 %) of an orange powder. Anal. (Calcd.): C% 57.59 (58.12), H% 5.21 (5.27), N% 3.31 (3.66). The paramagnetic nature of the compound and low solubility in C_6D_6 and other deuterated solvents precludes collection of meaningful NMR spectra.

4.6.3 Crystallographic Methods

Crystals for investigation were covered in Nujol®, mounted into a goniometer head, then rapidly cooled under a stream of cold N_2 from the low-temperature apparatus (Kryoflex) attached to the diffractometer. The data were collected using the SMART software suite on a Bruker APEX CCD diffractometer using a graphite monochromator with MoK_α radiation (λ=0.71073 Å). A hemisphere of data was collected using either 10 or 30 seconds/frame at 173 K. SAINT-Plus[78] software was used for data reductions and SADABS[79] was used for absorption corrections (semi-empirical from equivalents). Structures were solved and refined using the SHELX[80] suite of programs as implemented in WinGX.[81] For compound **4.1**, the crystals and data were of very low quality. A partial occupancy and highly-disordered toluene solvent of crystallization was best modeled as a C_6 hexagon of isotropic carbon atoms with fixed temperature factors. All attempts to improve the structure using the SQUEEZE routine in PLATON[82] to remove the solvent resulted in higher R-factors and non-positive definite ellipsoids.

4.6.4 Crystallographic Data

	4.1	**4.2**
Empirical formula	$C_{23}H_{28}F_3InN_2O_3S$ ·0.35(C_6)	$C_{21}H_{24}F_3InN_2O_3S$
Formula weight	609.58	556.30
Temp. (K)	173(2)	173(2)
Wavelength	0.71073 Å	0.71073 Å
Crystal system	Orthorhombic	Triclinic
Space group	Pbca	P-1
a (Å)	16.591(3)	9.083(3)
b (Å)	12.908(3)	23.902(9)
c (Å)	27.277(5)	25.234(9)
α (°)	90	62.720(4)
β (°)	90	81.535(5)
γ (°)	90	88.771(5)
V ($Å^3$)	5841.7(19)	4810(3)
Z	8	8
Density (calculated) ($g \cdot cm^{-3}$)	1.386	1.536
Absorption coefficient (mm^{-1})	0.926	1.116
F(000)	2469	2240
Crystal size (mm^3)	0.40 x 0.30 x 0.20	0.30 x 0.05 x 0.05
Theta range for data collection (°)	1.49 to 27.50	1.70 to 27.49
Index ranges	$-21 \leq h \leq 21$	$-11 \leq h \leq 11$
	$-16 \leq k \leq 16$	$-29 \leq k \leq 30$
	$-35 \leq l \leq 35$	$-32 \leq l \leq 32$
Reflections collected	59557	49648
Independent reflections	6644 [R(int) = 0.4293]	20257 [R(int) = 0.1061]

Completeness to theta = 27.50°	99.0 %	91.8 %
Absorption correction	SADABS: multi-scan semi-empirical from equivalents	
Max. and min. transmission	0.832 and 0.705	0.946 and 0.695
Refinement method	Full-matrix least-squares on F^2	
Data / restraints / parameters	6644 / 0 / 308	20257 / 0 / 1117
Goodness-of-fit on F^2	1.023	1.011
Final R indices [I>2sigma(I)]	R1 = 0.1105, wR2 = 0.2176	R1 = 0.0856, wR2 = 0.1902
R indices (all data)	R1 = 0.2902, wR2 = 0.3175	R1 = 0.1485, wR2 = 0.2189
Largest diff. peak and hole ($e \cdot Å^{-3}$)	1.166 and -1.026	1.396 and -2.392
CCDC submission codes	901801	901802

4.6.5 Computational Methods

All density functional theory (DFT) calculations were performed using the B3PW91 method[83-85] using the Gaussian 03[86] or Gaussian 09[87] suites using the SHARCNET high-performance computing network (www.sharcnet.ca). Where applicable, the Stuttgart group (SDD) effective core potentials (ECP) and corresponding basis sets were used for indium atoms and the 6-31+G(d) basis set was used for all lighter atoms. Natural bond order (NBO) analyses[88] to determine orbital contributions, Wiberg Bond Indicies and HOMO/LUMO energies were obtained using the routine included in the Gaussian distributions.[89] All stationary points were confirmed to be minima exhibiting no imaginary frequencies. Depictions of optimized geometries, summaries of results and atomic coordinates are included in the supporting information.

4.6.6 Cyclic Votlammetry

All voltammograms were done in a dry MeCN solution using a $[NBu_4][PF_6]$ (0.1 M) electrolyte. A glassy carbon electrode and a platinum wire were used as the working and auxiliary electrodes, respectively. All voltammographs are referenced to Ag/AgCl and were run with a scan rate of 100mV/s and a sensitivity of 100 μA/V. The analyte was run at a concentration of about 0.01 M. *Cisoidal* ligand conformations were promoted by adding stoichiometric amounts of KOTf. Electron integration was achieved by addition of a stoichiometric amount of ferrocene. Pictures of the all voltammograms are included in the supporting information.

4.6.7 EPR Spectroscopy

EPR spectra were recorded on a Bruker EMXplus X-band EPR spectrometer operating at X-band (ca. 9.8 GHz) using a cylindrical cavity. Simulations of the solution spectra were made using Winsim[90] to extract the ^{14}N and ^{1}H coupling constants and provide an initial estimate of the ^{115}In hyperfine which exhibited second order effects. Exact determination of the ^{115}In hyperfine was undertaken from the measurement of the position of the central peak of each multiplet from which the second order effects were determined manually. No attempt was made to model the 4% ^{113}In.

Variable temperature solid state EPR spectra on **4.2** were recorded in the region 500 – 8500 G in the temperature range from room temperature down to 150 K. No significant features were observed on cooling below 250 K. Simulations of the solid state spectra were undertaken using PIP run through the GUI "PIP for Windows" (J.M. Rawson, University of Windsor, 2011).[91] The orientation of the **D** and **E** tensors were

required to be slightly off-axis (< 5^{o}) in order to satisfactorily model all six peak positions associated with the spin triplet.

4.7 Supporting Information

4.7.1 Optimized Calculated Structures

InOTf•^{H}DAB^{H}

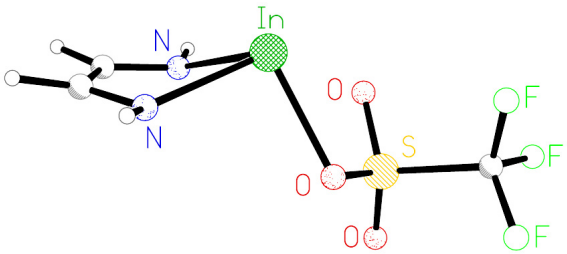

Singlet

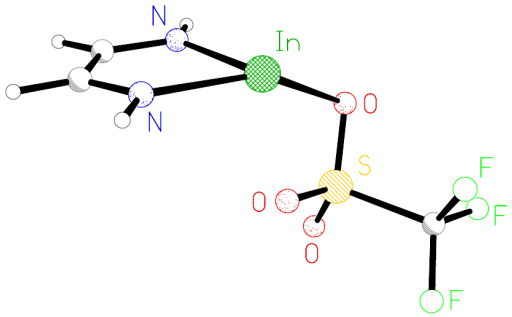

Triplet

InOTf•^{H}DAB^{Me}

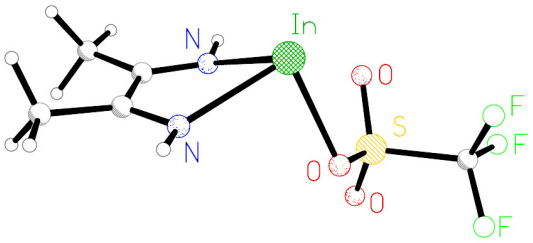

Singlet

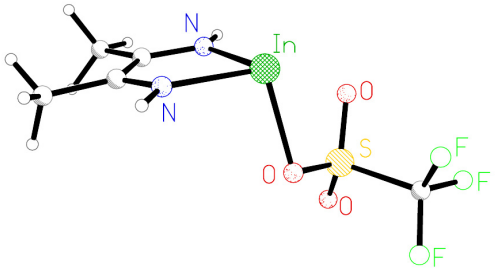

Triplet

InOTf•^{Me}DAB^{H}

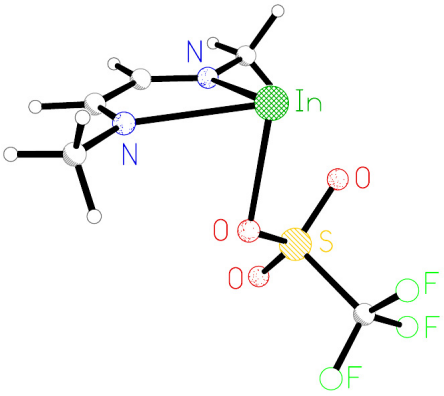

Singlet

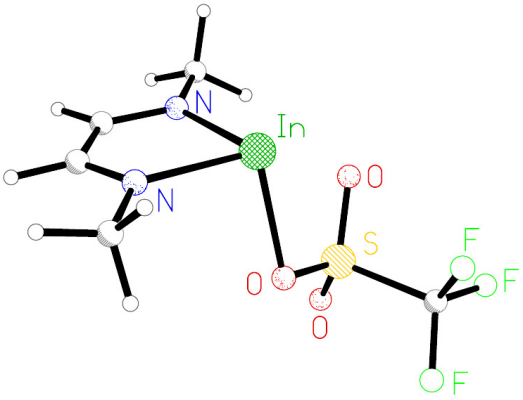

Triplet

InOTf•^{Me}DAB^{Me}

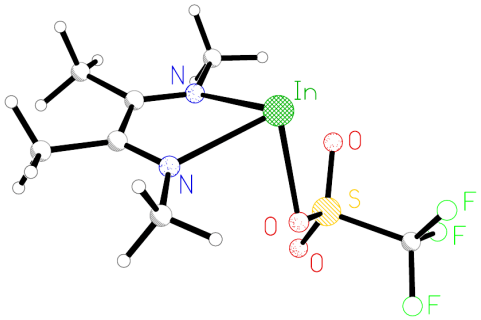

Singlet

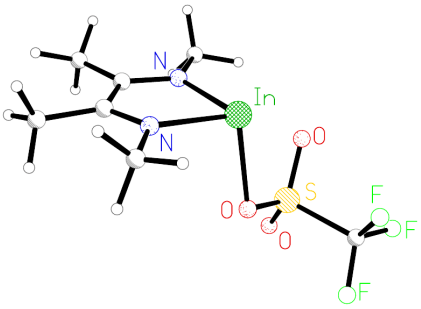

Triplet

InOTf•^{Ph}DAB^{H}

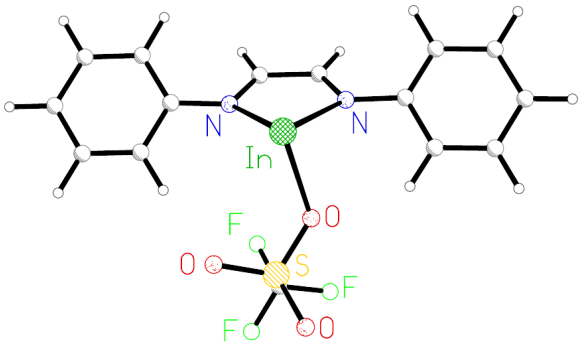

Singlet

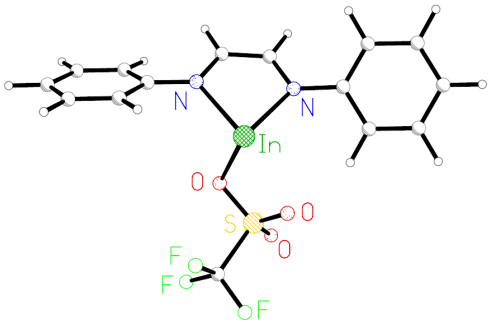

Triplet

InOTf•^{Ph}DAB^{Me}

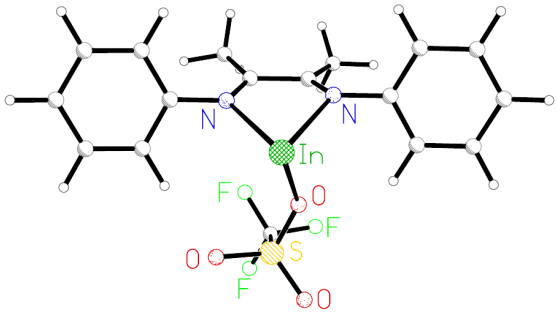

Singlet

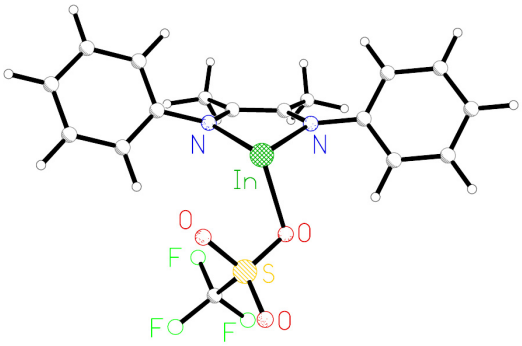

Triplet

InOTf•^{Mes}DAB^{Me}

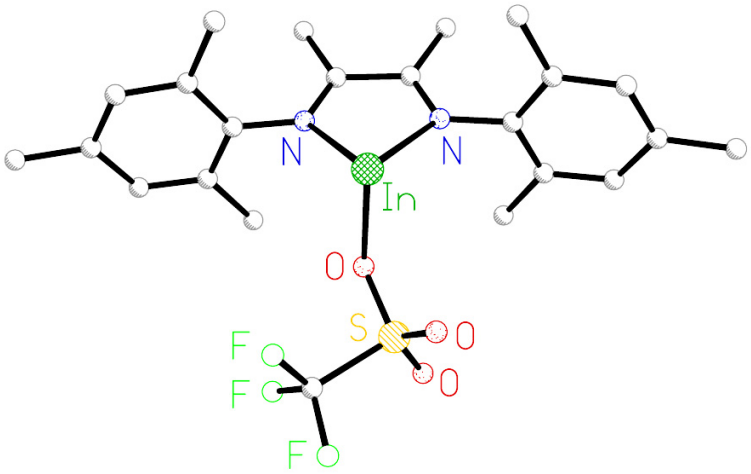

In•^{H}DAB^{H} dication dimer (planar starting geometry)

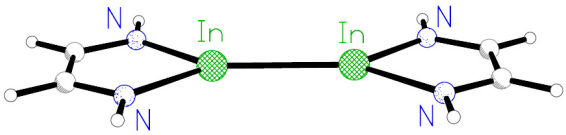

Singlet

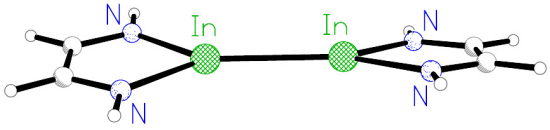

Triplet

In•^{H}DAB^{H} dication dimer (perpendicular starting geometry)

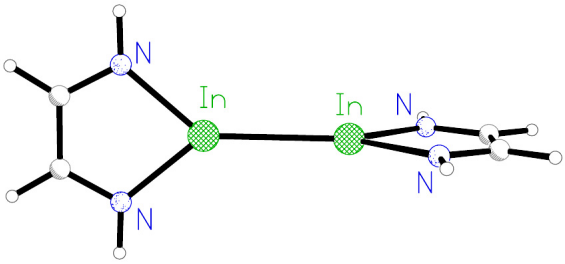

Singlet

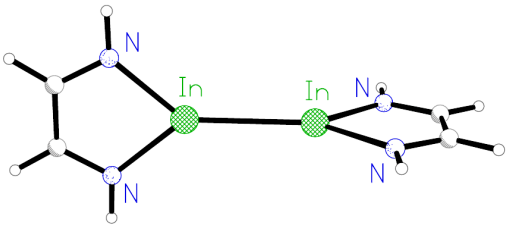

Triplet

InOTf•^{H}DAB^{H} dimer

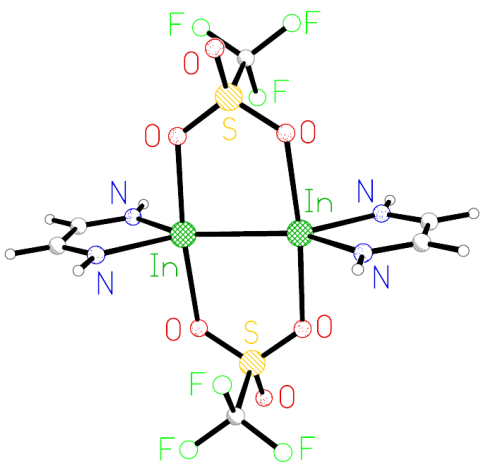

Singlet

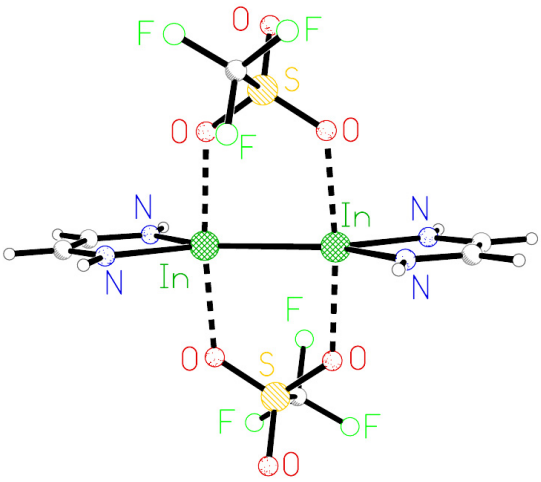

Triplet

4.7.2 Molecular Orbital Diagrams

InOTf•^{Ph}DAB^{H} (singlet)

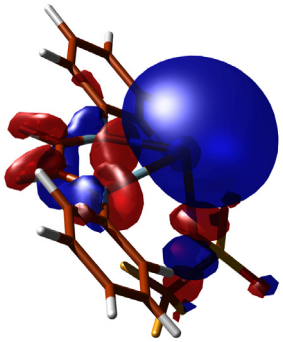

HOMO

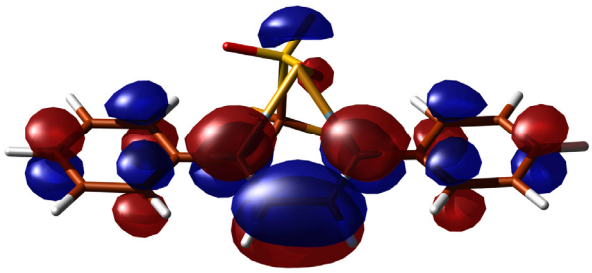

LUMO

InOTf•^{Ph}DAB^{Me} (singlet)

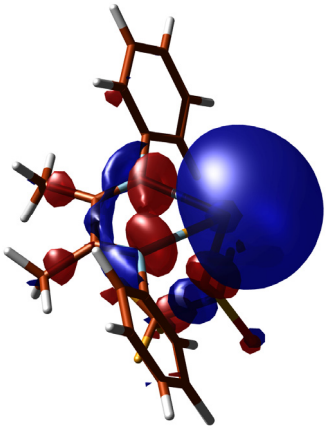

HOMO

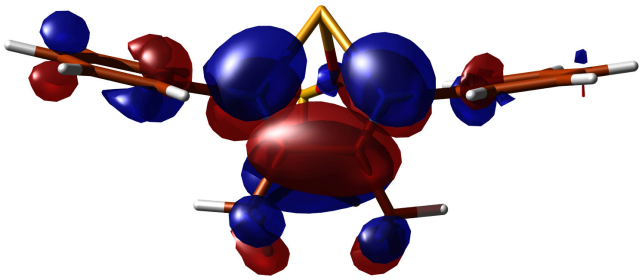

LUMO

InOTf•^{Ph}DAB^{H} (triplet)

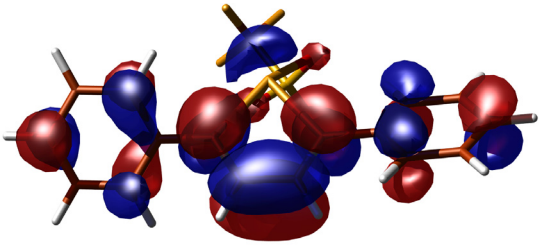

HOMO α-spin

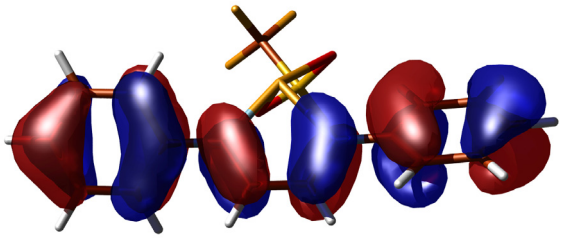

HOMO β-spin

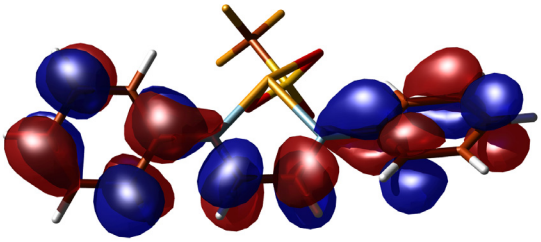

LUMO α-spin

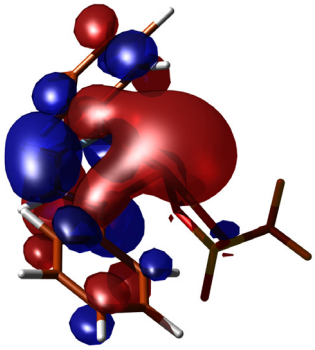

LUMO β-spin

InOTf•^{Ph}DAB^{Me} (triplet)

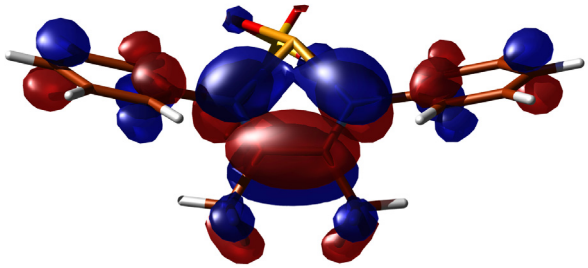

HOMO α-spin

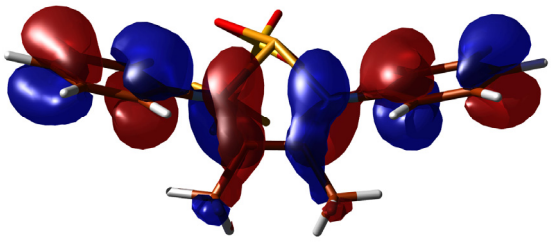

HOMO β-spin

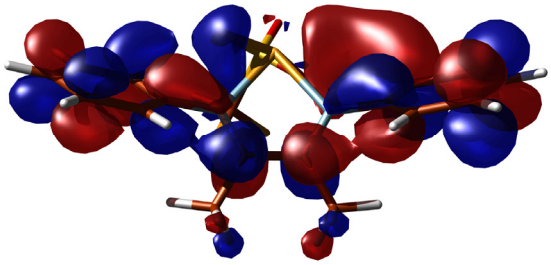

LUMO α-spin

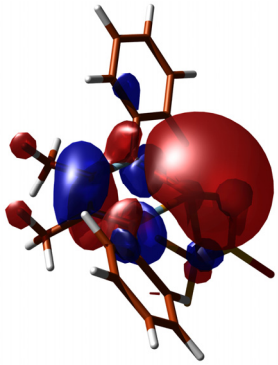

LUMO β-spin

4.7.3 Cyclic Voltammograms

^{Dipp}DAB^{Me}

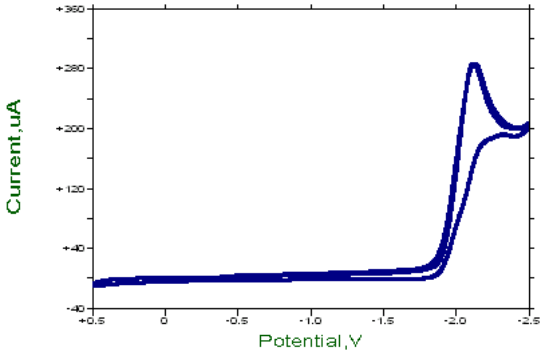

Cisoidal
E_{pc1} = -2.12 V

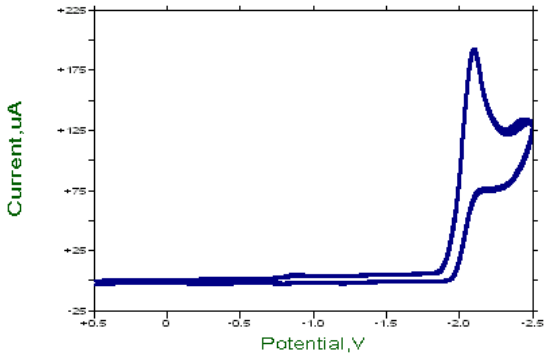

Transoidal
E_{pc1} = -2.11 V

$^{Dipp}DAB^{H}$

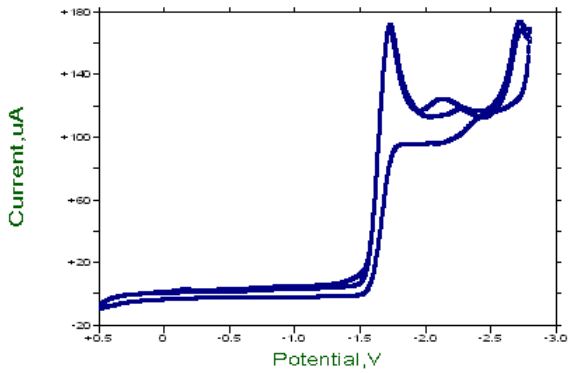

Cisoidal

E_{pc1} = -1.73; E_{pc2} = -2.73 V

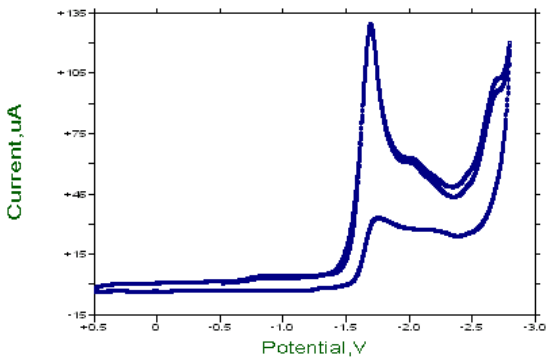

Transoidal

E_{re} = -1.72 & -2.73 V

$^{Mes}DAB^{H}$

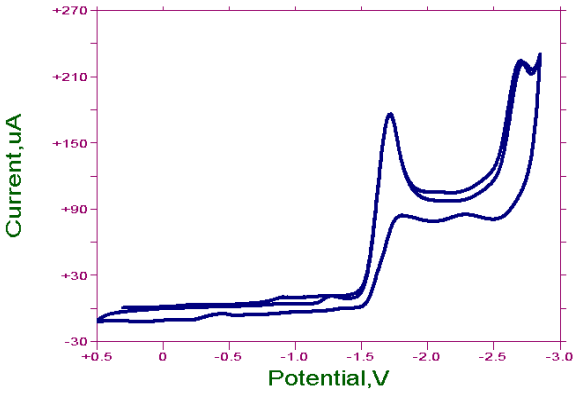

Cisoidal

E_{red} = -1.73 & -2.72 V

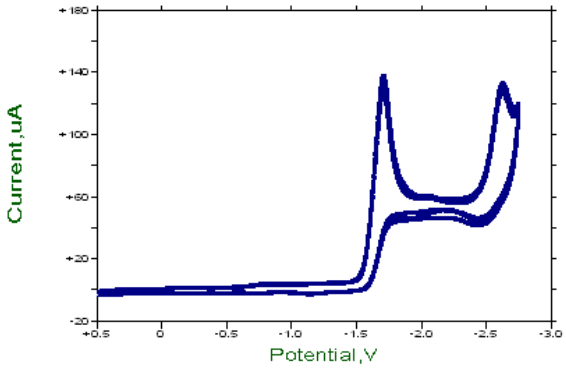

Transoidal

E_{pc1} = -1.71; E_{pc2} = -2.62 V

$^{Mes}DAB^{Me}$

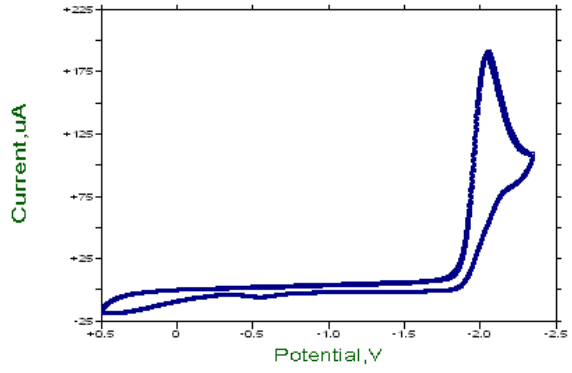

Cisoidal

E_{pc1} = -2.04 V

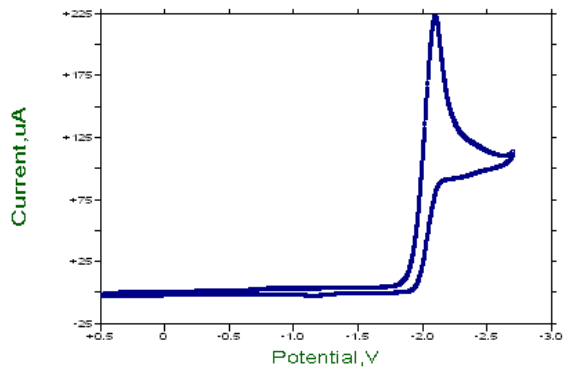

Transoidal

E_{pc1} = -2.10 V

InOTf

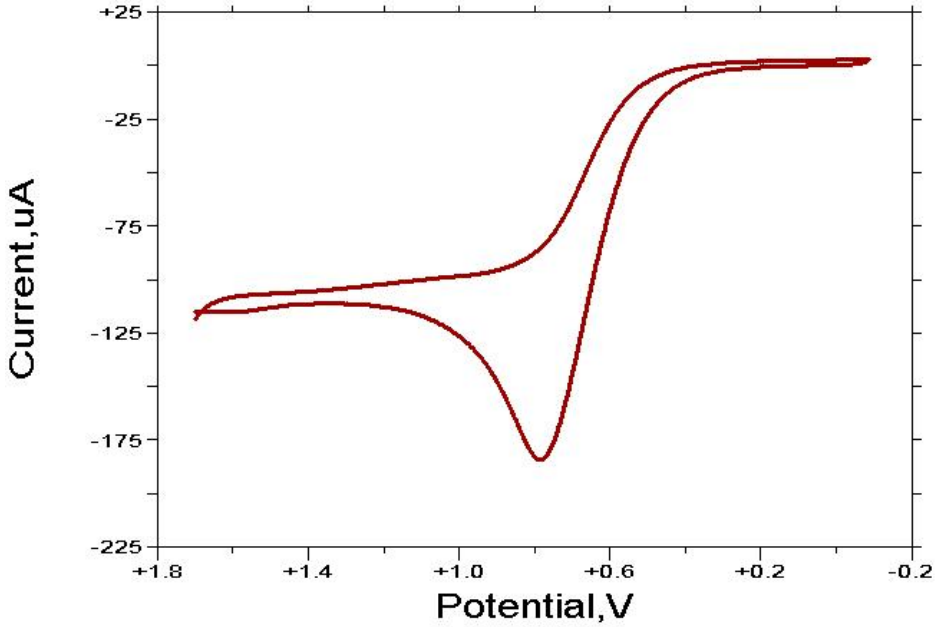

E_{pa1} = +0.79 V

4.8 References

[1] Jorgensen, C. K., *Coord. Chem. Rev.* **1966,** *1*, 164.
[2] Chirik, P. J., *Inorg. Chem.* **2011,** *50* (20), 9737.
[3] Kaim, W., *Inorg. Chem.* **2011,** *50* (20), 9752.
[4] Kaim, W.; Schwederski, B., *Coord. Chem. Rev.* **2010,** *254* (13-14), 1580.
[5] Kaim, W., *Coord. Chem. Rev.* **2011,** *255*, 2503.
[6] Praneeth, V. K. K.; Ringenberg, M. R.; Ward, T. R., *Angew. Chem. Int. Ed.* **2012,** *51*, 10228.
[7] Kraft, S. J.; Williams, U. J.; Daly, S. R.; Schelter, E. J.; Kozimor, S. A.; Boland, K. S.; Kikkawa, J. M.; Forrest, W. P.; Christensen, C. N.; Schwarz, D. E.; Fanwick, P. E.; Clark, D. L.; Conradson, S. D.; Bart, S. C., *Inorg. Chem.* **2011,** *50*, 9838.
[8] ^{R}DAB$^{R'}$ indicates a 1,3-diazabutadiene ligand where R represents the substituents on the nitrogen atoms and R' represents the substituents on the carbon atoms. e.g. ^{Dipp}DAB^{H} has 2,6-diisopropyl phenyl groups on the nitrogens with hydrogen atoms on the carbon backbone.
[9] The "non-innocent" behavior associated with DAB ligands is not limited to redox chemistry; tautomerization of certain DAB ligands can result in C,N rather than N,N' ligation.
[10] Tuononen, H. M.; Roesler, R.; Dutton, J. L.; Ragogna, P. J., *Inorg. Chem.* **2007,** *46* (25), 10693.
[11] Asay, M.; Jones, C.; Driess, M., *Chem. Rev.* **2011,** *111* (2), 354.
[12] Gudat, D., *Acc. Chem. Res.* **2010,** *43* (10), 1307.
[13] Reeske, G.; Cowley, A. H., *Inorg. Chem.* **2007,** *46*, 1426.
[14] Dube, J. W.; Farrar, G. J.; Norton, E. L.; Szekely, K. L. S.; Cooper, B. F. T.; Macdonald, C. L. B., *Organometallics* **2009,** *28*, 4377.
[15] Cowley, A. H.; Gorden, J. D.; Abernethy, C. D.; Clyburne, J. A. C.; McBurnett, B. G., *Dalton Trans.* **1998,** (12), 1937.
[16] Pott, T.; Jutzi, P.; Neumann, B.; Stammler, H. G., *Organometallics* **2001,** *20* (10), 1965.
[17] Brown, D. S.; Decken, A.; Cowley, A. H., *J. Am. Chem. Soc.* **1995,** *117*, 5421.
[18] Baker, R. J.; Farley, R. D.; Jones, C.; Kloth, M.; Murphy, D. M., *J. Chem. Soc., Dalton Trans.* **2002,** (20), 3844.
[19] Pott, T.; Jutzi, P.; Kaim, W.; Schoeller, W. W.; Neumann, B.; Stammler, A.; Stammler, H. G.; Wanner, M., *Organometallics* **2002,** *21* (15), 3169.
[20] Baker, R. J.; Farley, R. D.; Jones, C.; Kloth, M.; Murphy, D. M., *Chem. Commun.* **2002,** (11), 1196.
[21] Baker, R. J.; Farley, R. D.; Jones, C.; Mills, D. P.; Kloth, M.; Murphy, D. M., *Chem. Eur. J.* **2005,** *11*, 2972.
[22] Tuck, D. G., *Chem. Soc. Rev.* **1993,** *22*, 269.
[23] Jones, C.; Stasch, A., The Chemistry of the Group 13 Metals in the +1 Oxidation State. In *The Group 13 Metals Aluminium, Gallium, Indium and Thallium: Chemical Patterns and Peculiarities.*, Aldridge, S.; Downs, A. J., Eds. John Wiley and Sons Ltd.: 2011; p 285.
[24] Pardoe, J. A. J.; Downs, A. J., *Chem. Rev.* **2007,** *107* (1), 2.

[25] Green, S. P.; Jones, C.; Stasch, A., *Angew. Chem. Int. Ed.* **2007,** *46* (45), 8618.
[26] Cole, M. L.; Jones, C.; Kloth, M., *Inorg. Chem.* **2005,** *44*, 4909.
[27] Khan, M. A.; Peppe, C.; Tuck, D. G., *Can. J. Chem.* **1984,** *62*, 601.
[28] Uhl, W., *Naturwissenschaften* **2004,** *91* (7), 305.
[29] Cooper, B. F. T.; Hamaed, H.; Friedl, W. W.; Stinchcombe, M.; Schurko, R. W.; Macdonald, C. L. B., *Chem. Eur. J.* **2011,** *17*, 6148.
[30] Macdonald, C. L. B.; Corrente, A. M.; Andrews, C. G.; Taylor, A.; Ellis, B. D., *Chem. Commun.* **2004,** (2), 250.
[31] Cooper, B. F. T.; Macdonald, C. L. B., *New J. Chem.* **2010**.
[32] Andrews, C. G.; Macdonald, C. L. B., *Angew. Chem. Int. Ed.* **2005,** *44* (45), 7453.
[33] Cooper, B. F. T.; Macdonald, C. L. B., *J. Organomet. Chem.* **2008,** *693* (8-9), 1707.
[34] Jurca, T.; Lummiss, J.; Burchell, T. J.; Gorelsky, S. I.; Richeson, D. S., *J. Am. Chem. Soc.* **2009,** *131* (13), 4608.
[35] Jurca, T.; Korobkov, I.; Yap, G. P. A.; Gorelsky, S. I.; Richeson, D. S., *Inorg. Chem.* **2010,** *49* (22), 10635.
[36] Higelin, A.; Sachs, U.; Keller, S.; Krossing, I., *Chem. Eur. J.* **2012,** *18* (32), 10029.
[37] Higelin, A.; Haber, C.; Meier, S.; Krossing, I., *Dalton Trans.* **2012,** *41* (39), 12011.
[38] Higelin, A.; Keller, S.; Gohringer, C.; Jones, C.; Krossing, I., *Angew. Chem. Int. Ed.* **2013,** *52*, 4941.
[39] Martin, C. D.; Ragogna, P. J., *Inorg. Chem.* **2012,** *51*, 2947.
[40] Reeske, G.; Cowley, A. H., *Chem. Commun.* **2006**, 4856.
[41] Baker, R. J.; Jones, C.; Kloth, M.; Mills, D. P., *New J. Chem.* **2004,** *28*, 207.
[42] Hill, N. J.; Vargas-Baca, I.; Cowley, A. H., *Dalton Trans.* **2009,** (2), 240.
[43] Uhl, W.; Layh, M., Formal Oxidation State +2: Metal-Metal Bonded Versus Mononuclear Derivatives. In *The Group 13 Metals Aluminium, Gallium, Indium and Thallium. Chemical Patterns and Peculiarities*, Aldridge, S.; Downs, A. J., Eds. John Wiley and Sons: Chichester, UK, 2011; pp 246.
[44] Stender, M.; Power, P. P., *Polyhedron* **2002,** *21*, 525.
[45] Hill, M. S.; Hitchcock, P. B.; Pongtavornpinyo, R., *Science* **2006,** *311*, 1904.
[46] Hasan, K.; Zysman-Colman, E., *J. Phys. Org. Chem.* **2013,** *26* (3), 274.
[47] Li, L. D.; Lopes, P. S.; Rosa, V.; Figueira, C. A.; Lemos, M.; Duarte, M. T.; Aviles, T.; Gomes, P. T., *Dalton Trans.* **2012,** *41* (17), 5144.
[48] Klein, R. A.; Elsevier, C. J.; Hartl, F., *Organometallics* **1997,** *16* (6), 1284.
[49] Macdonald, C. L. B.; Bandyopadhyay, R.; Cooper, B. F. T.; Friedl, W. W.; Rossini, A. J.; Schurko, R. W.; Eichhorn, S. H.; Herber, R. H., *J. Am. Chem. Soc.* **2012,** *134* (9), 4332.
[50] Blundell, S., *Magnetism in Condensed Matter*. OUP: 2001.
[51] Morton, J. R.; Preseton, K. F., *J. Magn. Reson.* **1978,** *30*, 577.
[52] Rieger, P. H., *Electron Spin Resonance: Analysis and Interpretation*. RSC: 2007.
[53] Shuvaev, K.; Decken, A.; Grein, F.; Abedin, T. S. M.; Thompson, L. K.; Passmore, J., *Dalton Trans.* **2008**, 4029.
[54] Cameron, T. S.; Decken, A.; Kowalczyk, R. M.; McInnes, E. J. L.; Passmore, J.; Rawson, J. M.; Shuvaev, K.; Thompson, L. K., *Chem. Commun.* **2006**, 2277.

[55] Alberola, A.; Carter, E.; Constantinides, C. P.; Eisler, D. J.; Murphy, D. M.; Rawson, J. M., *Chem. Commun.* **2011,** *47*, 2532.
[56] Genoud, F.; Decorps, M., *Mol. Phys.* **1977,** *34*, 1583.
[57] Hatfield, W. E.; Hoffmann, S. K.; Corvan, P. J.; Singh, P.; Sethulekshmi, C. N.; Metzger, R. M., *Le Journal de Physique Colloques* **1983,** *44*, C3.
[58] Kozo, F.; Takashi, A.; Tasushi, M.; Shigeaki, N.; Koichi, T.; Kagetoshi, Y.; Kazunobu, S.; Akira, N.; Kazuhiro, N., *Bunshi Kozo Sogo Toronkai Koen Yoshishu* **2000,** *559*.
[59] Bond distances obtained from judicious selection of crystal structures featuring In(II)-In(II) bonds reported in the CCSD.
[60] Allen, F. H., *Acta Crystallogr., Sect. B: Struct. Sci.* **2002,** *58*, 380.
[61] Mantina, M.; Chamberlin, A. C.; Valero, R.; Cramer, C. J.; Truhlar, D. G., *The Journal of Physical Chemistry A* **2009,** *113*, 5806.
[62] Uhl, W., *Adv. Organomet. Chem.* **2004,** *51*, 53.
[63] Hinchliffe, A.; Mair, F. S.; McInnes, E. J. L.; Pritchard, R. G.; Warren, J. E., *Dalton Trans.* **2008,** (2), 222.
[64] Metzler-Nolte, N., *New J. Chem.* **1998,** *22* (8), 793.
[65] Schoeller, W. W.; Grigoleit, S., *J. Chem. Soc., Dalton Trans.* **2002,** (3), 405.
[66] Sundermann, A.; Reiher, M.; Schoeller, W. W., *Eur. J. Inorg. Chem.* **1998,** (3), 305.
[67] Schmidt, E. S.; Jockisch, A.; Schmidbaur, H., *J. Am. Chem. Soc.* **1999,** *121* (41), 9758.
[68] Tuononen, H. M.; Armstrong, A. F., *Dalton Trans.* **2006,** (15), 1885.
[69] Uhl, W.; Melle, S.; Prott, M., *Z. Anorg. Allg. Chem.* **2005,** *631* (8), 1377.
[70] Green, S. P.; Jones, C.; Lippert, K. A.; Mills, D. P.; Stasch, A., *Inorg. Chem.* **2006,** *45* (18), 7242.
[71] Snapping energies were calculated by taking the complexed InOTf•DAB complex and running single point calculations on the ligand and InOTf fragment separately.
[72] Relax energies are the completely optimized InOTf and DAB ligand (fragments calculated separately).
[73] Folga, E.; Ziegler, T., *J. Am. Chem. Soc.* **1993,** *115*, 5169.
[74] In(I) halides are clearly much more reactive as they do not appear to be capable of being stabilized as acid-free entities by crown ethers or dimpy ligands
[75] Slattery, J. M.; Higelin, A.; Bayer, T.; Krossing, I., *Angew. Chem. Int. Ed.* **2010,** *49* (18), 3228.
[76] Welsch, S.; Bodensteiner, M.; Dusek, M.; Sierka, M.; Scheer, M., *Chem. Eur. J.* **2010,** *16*, 13041
[77] Pangborn, A. B.; Giardello, M. A.; Grubbs, R. H.; Rosen, R. K.; Timmers, F. J., *Organometallics* **1996,** *15* (5), 1518.
[78] *SAINTPlus*, Bruker AXS Inc.: Madison, WI, 2008.
[79] *SADABS*, Bruker AXS Inc.: Madison, WI, 2008.
[80] Sheldrick, G. M., *Acta Crystallogr., Sect. A: Found. Crystallogr.* **2008,** *A64*, 112.
[81] Farrugia, L. J., *J. Appl. Crystallogr.* **1999,** *32*, 837.
[82] Spek, A. L., *J. Appl. Crystallogr.* **2003,** *36*, 7.

[83] Perdew, J. P.; Chevary, J. A.; Vosko, S. H.; Jackson, K. A.; Pederson, M. R.; Singh, D. J.; Fiolhais, C., *Phys. Rev. B* **1992,** *46*, 6671.
[84] Perdew, J. P.; Burke, K.; Wang, Y., *Phys. Rev. B* **1996,** *54*, 16533.
[85] Becke, A. D., *J. Chem. Phys.* **1993,** *98* (7), 5648.
[86] Frisch, M. J.; Trucks, G. W.; Schlegel, H. B.; Scuseria, G. E.; Robb, M. A.; Cheeseman, J. R.; Montgomery, J., J. A.; Vreven, T.; Kudin, K. N.; Burant, J. C.; Millam, J. M.; Iyengar, S. S.; Tomasi, J.; Barone, V.; Mennucci, B.; Cossi, M.; Scalmani, G.; Rega, N.; Petersson, G. A.; Nakatsuji, H.; Hada, M.; Ehara, M.; Toyota, K.; Fukuda, R.; Hasegawa, J.; Ishida, M.; Nakajima, T.; Honda, Y.; Kitao, O.; Nakai, H.; Klene, M.; Li, X.; Knox, J. E.; Hratchian, H. P.; Cross, J. B.; Bakken, V.; Adamo, C.; Jaramillo, J.; Gomperts, R.; Stratmann, R. E.; Yazyev, O.; Austin, A. J.; Cammi, R.; Pomelli, C.; Ochterski, J. W.; Ayala, P. Y.; Morokuma, K.; Voth, G. A.; Salvador, P.; Dannenberg, J. J.; Zakrzewski, V. G.; Dapprich, S.; Daniels, A. D.; Strain, M. C.; Farkas, O.; Malick, D. K.; Rabuck, A. D.; Raghavachari, K.; Foresman, J. B.; Ortiz, J. V.; Cui, Q.; Baboul, A. G.; Clifford, S.; Cioslowski, J.; Stefanov, B. B.; Liu, G.; Liashenko, A.; Piskorz, P.; Komaromi, I.; Martin, R. L.; Fox, D. J.; Keith, T.; Al-Laham, M. A.; Peng, C. Y.; Nanayakkara, A.; Challacombe, M.; Gill, P. M. W.; Johnson, B.; Chen, W.; Wong, M. W.; Gonzalez, C.; Pople, J. A. *Gaussian 03*, C.02; Gaussian Inc.: Wallingford, CT, 2004.
[87] Frisch, M. J.; Trucks, G. W.; Schlegel, H. B.; Scuseria, G. E.; Robb, M. A.; Cheeseman, J. R.; Scalmani, G.; Barone, V.; Mennucci, B.; Petersson, G. A.; Nakatsuji, H.; Caricato, M.; Li, X.; Hratchian, H. P.; Izmaylov, A. F.; Bloino, J.; Zheng, G.; Sonnenberg, J. L.; Hada, M.; Ehara, M.; Toyota, K.; Fukuda, R.; Hasegawa, J.; Ishida, M.; Nakajima, T.; Honda, Y.; Kitao, O.; Nakai, H.; Vreven, T.; Montgomery, J., J. A.; Peralta, J. E.; Ogliaro, F.; Bearpark, M.; Heyd, J. J.; Brothers, E.; Kudin, K. N.; Staroverov, V. N.; Kobayashi, R.; Normand, J.; Raghavachari, K.; Rendell, A.; Burant, J. C.; Iyengar, S. S.; Tomasi, J.; Cossi, M.; Rega, N.; Millam, N. J.; Klene, M.; Knox, J. E.; Cross, J. B.; Bakken, V.; Adamo, C.; Jaramillo, J.; Gomperts, R.; Stratmann, R. E.; Yazyev, O.; Austin, A. J.; Cammi, R.; Pomelli, C.; Ochterski, J. W.; Martin, R. L.; Morokuma, K.; Zakrzewski, V. G.; Voth, G. A.; Salvador, P.; Dannenberg, J. J.; Dapprich, S.; Daniels, A. D.; Farkas, Ö.; Foresman, J. B.; Ortiz, J. V.; Cioslowski, J.; Fox, D. J. *Gaussian 09*, A.1; Gaussian Inc.: Wallingford, CT, 2009.
[88] Reed, A. E.; Curtiss, L. A.; Weinhold, F., *Chem. Rev.* **1988,** *88* (6), 899.
[89] Glendening, E. D.; Reed, A. E.; Carpenter, J. E.; Weinhold, F. *NBO Version 3.1*, Madison, Wisconsin.
[90] O'Brien, D. A.; Duling, D. R.; Fann, Y. C. EPR spectral simulation for MS-Windows, Public EPR Software Tools NIEHS.
[91] PIP: A program for simulation of anisotroptic EPR spectra; Nilges, M.; Rawson, J. M. *Illinois EPR Research Centre*, 2.1; PIP4WIN, Rawson, J. M., University of Windsor, PIP for Windsows: **2011**.

Chapter 5: Conclusions and Future Work

The primary focus of this dissertation has been on the stabilization of InX (X=Cl, Br, I, OTf) through weak interactions, as well as exploration of the chemistry that can be done with the use of destabilizing ligands. Despite the indium(I) halides' poor solubility in most organic solvents, they still remain the primary starting material for many In(I) compounds. The use of acyclic polyether ligands (glymes) was shown to greatly increase the solubility of the indium(I) halides as well as InOTf and may prove useful for future synthesis that involve these salts. Reactions that, previously, have not proceeded or have given poor yields may benefit from the increase in salt in solution. Future work for the InX•glyme systems consists of attempting to synthesize well established reactions that begin with an indium(I) halide in the presence of glyme and compare the yields and kinetics of the reaction (e.g. synthesis of InCp*: InCl + "glyme" + LiCp* →). Reactions that require activation of a Lewis acid may not benefit from the addition of glyme due to competing complexation.

Through the use of destabilizing ligands it was demonstrated that the "lone pair" of electrons on indium can be controlled through judicious ligand selection. In particular, softer Lewis bases destabilize the metal centre more than the lighter atom analogues. This should prove useful for fine tuning and controlling the reactivity of low oxidation state indium complexes. Though computational investigations it was shown that the insertion of InX in R-X (X=Cl, Br, I) is most likely through a radical pathway as the proposed intermediates are the lowest in energy compared to anionic or cationic pathways, which is consistent with what is presented in the literature.

Investigation into the addition of InOTf to α-diimine ligands showed that the redox potential for the ligand is dependent on the electronics of the backbone, rather than substitution patterns present on the aryl rings. The more electron-rich methyl backbone DAB ligand was found to be difficult to reduce than the electron-poor, hydrogen backbone. The addition of InOTf to MesDABMe was the first example where there was no formal charge transfer to the ligand and existed as a donor-acceptor complex. To date there has yet to be an example of a full 2 electron charge transfer to the ligand from an indium centre. However, similar to how AlCp* and GaCp* fully reduced the DAB ligand, it is possible that the more electron rich InCp* ligand may do the same. It will depend on not only the oxidation potential for the In(I) source, but also how effectively the DAB ligand destabilizes the 5s electrons.

Vita Auctoris

Name: Christopher John Allan

Education: Oakridge Secondary School, London, Ontario, 2001-2005
The University *of* Western Ontario, London, Ontario, 2005-2009, B.Sc.
University of Windsor, Windsor, Ontario, 2009-2013, Ph.D.

Publications:

C.J. Allan; B.F.T. Cooper; H.J. Cowley; J.M. Rawson; C.L.B. Macdonald. *Chemistry - a European Journal*. **2013**, Accepted.

R.R. San Juan, **C.J. Allan**, M. Iqbal, S.H. Eichhorn, C.L.B. Macdonald* and T.B. Carmichael. *Journal of the American Chemical Society*. **2013**, Accepted.

C.J. Allan; C.L.B. Macdonald. *Low Coordinate Group 13 Compounds* in *Comprehensive Inorganic Chemistry*. **2013**, Accepted.

C.J. Allan; C.R.W. Reinhold; L.C. Pavelka; K.M. Baines. *Organometallics*, **2011**, *30*, 2010.

A.J. Ruddy, P.A. Rupar, K.J. Bladek, **C.J. Allan**, J.C. Avery, K.M. Baines, *Organometallics*, **2010**, *29*, 1362-1367.